JOURNAL OF APPLIED PHYSICS

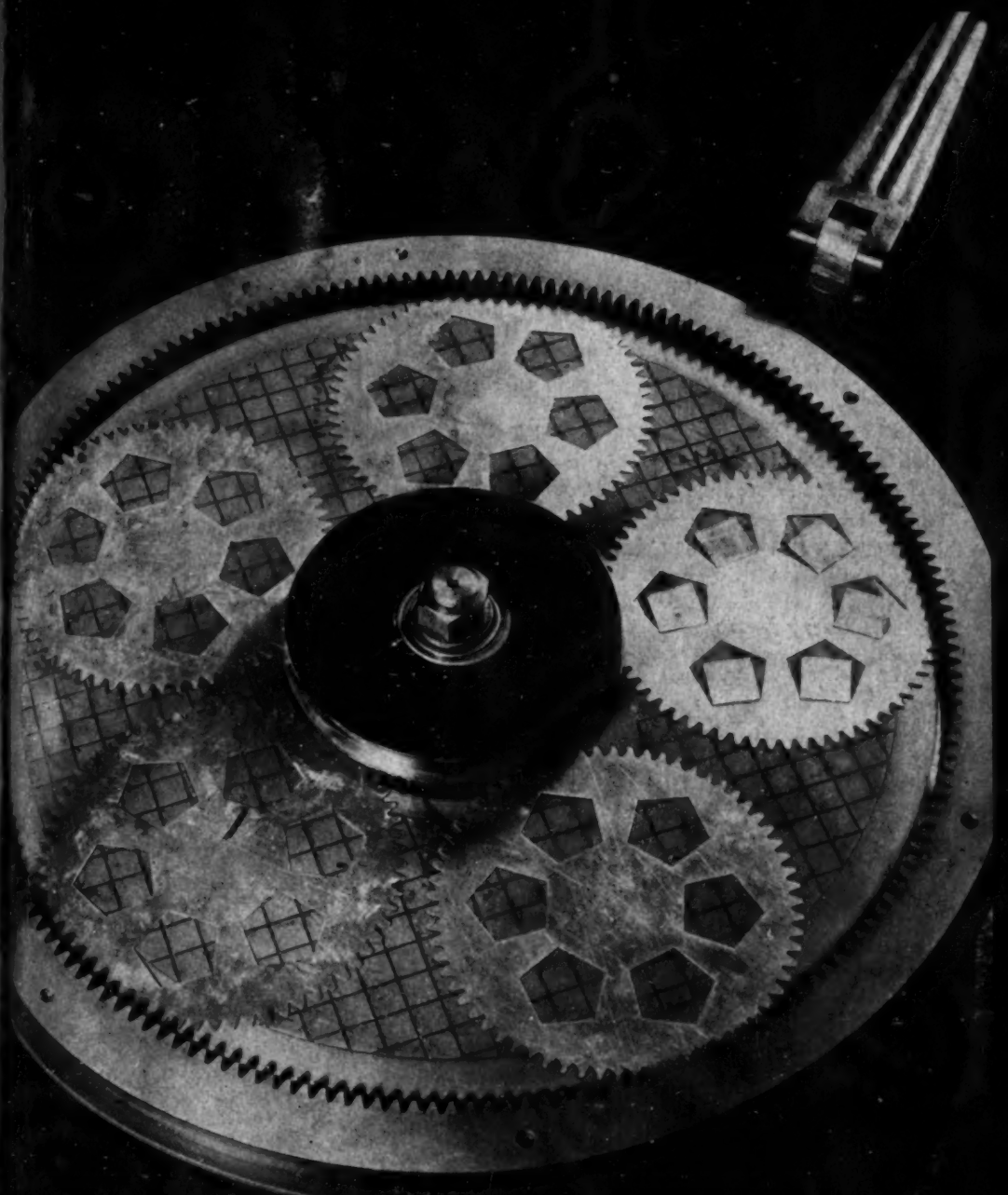

JOURNAL OF APPLIED PHYSICS

Vol. 15, No. 8 AUGUST, 1944

In This Issue

Page

Contributed Original Research

Bibliography of Electron Microscopy. II
CLAIRE MARTON AND SAMUEL SASS 575

Further Studies of the Infra-Red Absorption of Rubber
DUDLEY WILLIAMS AND BROCK DALE 585

Poisson's Ratio at High Temperatures
F. L. EVERETT AND JULIUS MIKLOWITZ 592

Numerical Method in the Theory of Vibrating Bodies
ANDREW VAZSONYI 598

Closed Cell for Electron Microscopy
I. M. ABRAMS AND J. W. MCBAIN 607

Simple Vector Method for the Determination of Orientations of Cubic Single Crystals from Back Reflection X-Ray Photographs BEULAH FIELD DECKER 610

On the Representation of Rigid Rotations
ELLIOT T. BENEDIKT 613

Single- and Double-Stub Impedance Matching
ALEXANDER H. WING AND JULIAN EISENSTEIN 615

Letters to the Editor

Rate of Rise of Water in Capillary Tubes GERALD PICKETT 623

Dark Field Illumination in Electron Microscopy GABOR B. LEVY 623

Viscosity of Water J. R. COE, JR., AND T. B. GODFREY 625

Etymology of the Word Microradiograph S. E. MADDIGAN 626

Rapid Determinations of Elastic Constants of Glass and Other Transparent Substances W. T. SZYMANOWSKI 627

In Every Issue

New Books 579

Here and There 583

Calendar of Meetings 584

Recent Applications of Physics 627

Index to Advertisers xxii

BOARD OF EDITORS

ELMER HUTCHISSON, *Editor*

Associate Editors

R. B. BARNES
OTTO BEECK
W. F. BUSSE
S. H. CALDWELL
CLARK GOODMAN
SELIG HECHT
W. J. LYONS
MORRIS MUSKAT
THOMAS H. OSGOOD
PAUL E. SABINE
FREDERICK SEITZ
J. R TOWNSEND

Publication of the American Institute of Physics

ADMINISTRATIVE STAFF

HENRY A. BARTON, *Director*

MADELINE M. MITCHELL, *Publications Manager*

JOHN T. TATE, *Adviser on Publications*

GOVERNING BOARD

PAUL E. KLOPSTEG, *Chairman*

GEORGE B. PEGRAM, *Secretary*

T. D. COPE
R. B. DOW
L. A. DUBRIDGE
FLOYD A. FIRESTONE
HARVEY FLETCHER
R. C. GIBBS
K. S. GIBSON
HERMANN MARK
A. G. WORTHING
JOHN T. TATE
L. W. TAYLOR
N. W. TAYLOR
WALLACE WATERFALL

The JOURNAL OF APPLIED PHYSICS, published monthly at Prince and Lemon Sts., Lancaster, Pa., is devoted to physics in its role as the science basic to other natural sciences and to the arts and industries. Previous to 1937 this publication was known as PHYSICS. The JOURNAL OF APPLIED PHYSICS publishes editorials, news of physicists, and reviews, as well as technical papers of applied physics.

Manuscripts should be submitted to Elmer Hutchisson, Editor, 50th floor, 350 Fifth Avenue, New York 1, New York.

Subscriptions and orders for back numbers should be addressed to Prince and Lemon Streets, Lancaster, Pa. or to the American Institute of Physics, 57 East 55 Street, New York 22, N. Y.

Subscription Price

	U. S. AND CANADA	ELSEWHERE
To members of scientific societies	$5.00	$5.70
To all others	7.00	7.70

Back Number Prices

Complete set: Vol. 1, July, 1931–Vol. 14, 1943—**$87.50**
Yearly back number rate: **$7.70**
Single copies: **$0.70** each.

Changes of address and proofs should be addressed to the Publications Manager.

Advertising rates supplied on request. Orders, advertising copy, and cuts should be sent to the American Institute of Physics.

Entered as second class matter January 22, 1937, at the Post Office at Lancaster, Pennsylvania, under the Act of March 3, 1879.
Accepted for mailing at the special rate of postage provided for in the Act of February 28, 1925, authorized May 2, 1932.

Copyright 1944, by the American Institute of Physics.

Journal
of
Applied Physics

Volume 15, Number 8 August, 1944

A Bibliography of Electron Microscopy. II

COMPILED BY

CLAIRE MARTON, *Division of Electron Optics, Stanford University, Stanford University, California*

AND

SAMUEL SASS, *In Charge of Physics and Observatory Libraries, University of Michigan, Ann Arbor, Michigan*

SINCE the closing date of our bibliography published in this journal,[1] a number of papers on electron microscopy appeared in this country and a large number of foreign papers came to our knowledge. This supplement is an attempt, therefore, to bring the bibliography up to date. Due to wartime conditions it may not be as complete as we would wish, but we hope that these additions will help the research workers in this new field.

As previously, the material is arranged in eight groups; within each group the arrangement is chronological and within each year alphabetical by author and title.

We again wish to acknowledge the assistance of Professor L. Marton, of the Division of Electron Optics, Stanford University.

March 1, 1944.

I. BOOKS

Ramsauer, C., editor. *Das freie Elektron in Physik und Technik.* J. Springer, Berlin, 1940.

Ramsauer, C. *Elektronenmikroskopie. Bericht über Arbeiten der AEG-Forschungs-Instituts 1930 bis 1941.* Second edition. J. Springer, Berlin, 1942.

II. EMISSION MICROSCOPY

Boersch, H. Increase of resolution of the emission electron microscope. *Naturwiss.* **30**, 120 (1942).

Boersch, H. Improvement of the resolving power of the emission electron microscope. *Zeits. f. techn. Physik* **23**, 129–130 (1942).

Brüche, E. The limit of resolution of the emission electron microscope. *Kolloid Zeits.* **100**, 192–206 (1942).

Dosse, J. and Müller, H. O. The resolving power of the emission electron microscope. *Zeits. f. Physik* **119**, 415–422 (1942).

Huber, H. and Wagener, S. X-ray and electron optical study of crystal structure of alkali earth oxide mixtures. *Zeits. f. techn. Physik* **23**, 1–12 (1942).

Mahl, H. An experiment in emission microscopy with electrostatic lenses. *Zeits. f. techn. Physik* **23**, 117–119 (1942).

Mecklenburg, W. Electrostatic emission electron microscope. *Zeits. f. Physik* **120**, 21–30 (1942).

Recknagel, A. Resolving power of the emission electron microscope. *Zeits. f. Physik* **120**, 331–362 (1943).

III. TRANSMISSION TYPE MICROSCOPE

Ardenne, M. von. The resolving power of photographic emulsions for electron beams. *Zeits. f. Physik* **114**, 379 (1939).

Borries, B. von and Ruska, E. Technique of the Siemens electron microscope. *Siemens Zeits.* **20**, 217–227 (1940).

[1] J. App. Phys. **14**. 522–531 (1943).

Ardenne, M. von. Electron microscopy at elevated temperatures with the universal electron microscope. *Kolloid Zeits.* **97**, 257–272 (1941).

Brüche, E. The development of the electron microscope with electrostatic lenses. *V.D.I.* **85**, 221–229 (1941).

Lundgren, E. H. The electron microscope. *Tek. Tid. Uppl. A-c, Kemi* **71**, 20–35 (1941).

Boersch, H. Construction and possibilities of application of an electron microscopical arrangement. *Phys. Zeits.* **43**, 515–520 (1942).

Frey, F. Orientation marks on sample holders for the electron microscope. *Zeits. f. techn. Physik* **23**, 82 (1942).

Frey, F. Application and construction of a plateholder for two exposures with the Siemens electron microscope in its normal construction. *Zeits. f. techn. Physik* **23**, 176–177 (1942).

Matthias, A. Remark on the origin of the electron microscope. *Phys. Zeits.* **43**, 129–130 (1942).

Prebus, A. The electron microscope. *Ohio State Univ. Eng. Exp. Sta. News* **14**, 3 (1942).

Ruska, E. Taking of photographs with the electron microscope at high pressures. *Kolloid Zeits.* **100**, 212–219 (1942).

Ardenne, M. von. Electron microcinematography with the universal electron microscope. *Zeits. f. Physik* **120**, 397–412 (1943).

Brüche, E. The development of the electron microscope. *Phys. Zeits.* **44**, 176–180 (1943).

Mahl, H. and Pendzich, A. Electron-mirror microscope: a new electron microscope. *Zeits. f. techn. Physik* **24**, 38–42 (1943).

Rüdenberg, R. The early history of the electron microscope. *J. Appl. Phys.* **14**, 434–436 (1943).

Zworykin, V. K. and Hillier, J. A compact high resolving power electron microscope. *J. Appl. Phys.* **14**, 658–673 (1943).

IV. OPTICS OF THE TRANSMISSION TYPE ELECTRON MICROSCOPE

Savchenko, F. The dependence of certain optical parameters on the electric and geometric parameters of electric immersion lens. *Zhurnal Tekhnicheskoi Fiziki, Moscow*, **9**, 2211–2219 (1939).

Borries, B. von and Ruska, E. The influence of electron interferences on the image formation of crystals in the electron microscope. *Naturwiss.* **28**, 366–367 (1940).

Dosse, J. Theoretical and experimental investigation of electron emitters. *Zeits. f. Physik* **115**, 530–556 (1940).

Ardenne, M. von. Supplement to the papers: "The testing of electron lenses of short focal length" and "A 200-kv universal electron microscope with an object screen." *Zeits. f. Physik* **118**, 384–388 (1941).

Glaser, W. and Lammel, E. For which electromagnetic fields is Newton's image equation valid? *Ann. d. Physik* **40**, 367–384 (1941).

Glaser, W. On the distribution of the ampere-turn density of a given magnetic field produced by a cylindrical coil. *Zeits. f. Physik* **118**, 264–268 (1941).

Ardenne, M. von. The faithful representation of the structures close to the limit of resolution with the light microscope and the electron microscope. *Kolloid Zeits.* **100**, 206–211 (1942).

Bertram, S. J. Calculation of axially symmetric fields. *J. Appl. Phys.* **13**, 496–502 (1942).

Boersch, H. The influence of crystal lattice interferences on the imaging in the electron microscope. *Zeits. f. Physik* **118**, 706–713 (1942).

Copeland, P. L. Thin electrostatic lenses for electrons. *Am. J. Phys.* **10**, 236–246 (1942).

Craggs, J. D. The electrostatic focusing of high speed ion and electron beams. *J. Appl. Phys.* **13**, 772–786 (1942).

Glaser, W. Electron-optical imaging with distorted rotational symmetry. *Zeits. f. Physik* **120**, 1–15 (1942).

Boersch, H. Edge diffraction of electrons. *Phys. Zeits.* **44**, 32–38 (1943).

Boersch, H. Fresnel diffraction in the electron microscope. *Phys. Zeits.* **44**, 202–211 (1943).

Glaser, W. Image formation and resolving power of the electron microscope from the point of view of wave mechanics. *Zeits. f. Physik* **121**, 647–667 (1943).

Wendt, G. The dioptrics of electron optical instruments with arbitrarily curved optical axis. *Zeits. f. Physik* **120**, 720–741 (1943).

Marton, L. and Hutter, R. G. E. The transmission type of electron microscope and its optics. *Proc. I.R.E.* **32**, 3–12 (1944).

Marton, L. and Hutter, R. G. E. On apertures of transmission type electron microscopes using magnetic lens. *Phys. Rev.* **65**, 161–167 (1944).

Opatowski, I. Refractive index in electron optics. *Phys. Rev.* **65**, 54–55 (1944).

V. IMAGE DEFECTS

Ardenne, M. von. On the magnitude of the aperture defect in the electron microscope. *Zeits. f. techn. Physik* **20**, 289–290 (1939).

Dosse, J. Supplement to the paper: "Optical characteristics of strong electron lenses." *Zeits. f. Physik* **118**, 375–383 (1941).

Gobrecht, R. Experimental investigations of spherical aberration in electrostatic lenses. *Arch. f. Elektrotechn.* **35**, 672–685 (1941).

Scherzer, O. The lower limits of focal distance and of chromatic defect of magnetic electron lenses. *Zeits. f. Physik* **118**, 461–466 (1941).

Plass, G. N. Errata: Electrostatic electron lenses with a minimum of spherical aberration. *J. Appl. Phys.* **13**, 524 (1942).

Boersch, H. Secondary images in electron microscopy. *Zeits. f. Physik* **121**, 746–754 (1943).

VI. ELECTRON SPEEDS ABOVE 100 KV

Ardenne, M. von. Supplement to the papers: "The testing of electron lenses of short focal length" and "A 200-kv universal electron microscope with an object screen." *Zeits. f. Physik* **118**, 384–388 (1941).

VII. DIFFERENT RELATED INSTRUMENTS

Ruthemann, G. Discrete energy losses of fast electrons in solids. *Naturwiss.* **29**, 648 (1941).

Haefer, R. Field electron microscopic observations on tungsten points. *Zeits. Krist.* **104**, 1–10 (1942).

Ruthemann, G. Electron retardation at x-ray levels. *Naturwiss.* **30**, 145 (1942).

Hillier, J. On microanalysis by electrons. *Phys. Rev.* **64**, 318–319 (1943).

Müller, E. W. Resolving power of the field electron microscope. *Zeits. f. Physik* **120**, 270–282 (1943).

Müller, E. W. Velocity distribution of electrons for field emission. *Zeits. f. Physik* **120**, 261–269 (1943).

VIII. APPLICATIONS OF THE TRANSMISSION TYPE MICROSCOPE

Ardenne, M. von. The wedge sectioning method for producing microtome cuts of less than 10^{-3} mm thickness for purposes of electron microscopy. *Ztschr. f. wissensch. Mikr.* **56**, 8–23 (1939).

Ardenne, M. von. Experiments in photographing the virus of the hoof and mouth disease by means of the universal electron microscope. *Naturwiss.* **28**, 531–532 (1940).

Mahl, H. Electron microscope images of objects by transmitted radiation and of metal surfaces. *Zeits. angew. Photogr.* **2**, 58–63 (1940).

Radczewski, O. E., Müller, H. O., and Eitel, W. Electron microscopic investigations of the hydration of lime. *Veröffentl. Kaiser Wilhelm-Inst. Silikatforsch.* **10**, 139–142 (1940).

Ruska, H. Significance and results of the electron microscope. *Siemens Zeits.* **20**, 228–234 (1940).

Ardenne, M. von. Experiments on making visible molecular roughness of crystal edges inclined to the lattice planes in the universal electron microscope. *Naturwiss.* **29**, 780–781 (1941).

Ardenne, M. von and Weber, H. H. Electron microscopic investigations of the muscle protein "myosin." *Kolloid Zeits.* **97**, 322–325 (1941).

Endell, J. Significance of the electron microscope for identifying the microstructure of clays. *Tonind. Ztg.* **65**, 69–72 (1941).

Henneberg, W. Electron microscope, supermicroscope and metallography. *Stahl u. Eisen* **41**, 769–777 (1941).

Koch, L. and Lehmann, A. Electron microscope investigation of smooth aluminum surfaces. *Aluminium* **23**, 304–309 (1941).

Mahl, H. The electrostatic electron microscope and some results from the metallurgical field. *Zeits. f. Metallk.* **33**, 68–73 (1941).

Mahl, H. Electron microscopic detection of metallic precipitation by the replica method. *Metallwirtschaft* **20**, 983–986 (1941).

Mahl, H. The damaging of cellulose fibers by radiation in the electron microscope. *Kolloid Zeits.* **96**, 7–10 (1941).

Meldau, R. and Teichmüller, M. The morphology of finest lead-oxide sublimates. III. *Zeits. f. Elektrochem.* **47**, 630–634 (1941).

Meldau, R. and Teichmüller, M. The morphology of finest lead-oxide sublimates. IV. *Zeits. f. Elektrochem.* **47**, 634–636 (1941).

Ruska, H. Technique and research results of electron microscopy. *Vierteljrsch. d. Naturf. Ges. Zürich* **86**, 20–21 (1941).

Ardenne, M. von. Recent research on the universal electron microscope. *Forschng. u. Fortschr.* **18**, 32–35 (1942).

Ardenne, M. von. On an electron microscopic investigation of the structure of reflection reducing layers and on the determination of the dimensions of such layers. *Zeits. angew. Photogr.* **4**, 15–16 (1942).

Borries, B. von. On the intensity relations in the electron microscope. I. The blackening of photographic plates by electron beams. *Phys. Zeits.* **43**, 190–204 (1942).

Borries, B. von. On the intensity relations in the electron microscope. II. Magnification, graininess, and resolving power of electron exposed photographic plates. *Zeits. angew. Photogr.* **4**, 3–4 (1942).

Borries, B. von. On the intensity relations in the electron microscope. III. Suitability and limits of sensitivity of photographic plates for electron microscope pictures. *Zeits. f. Physik* **119**, 498–521 (1942).

Duffek, V. and Mahl, H. The electron microscope representation of metallic surfaces by the replica process without injury to the surface of the sample. *Arch. Eisenhüttenw.* **16**, 73–76 (1942).

Fischer, H. and Kurz, F. Electron microscope images of anodic oxide films on aluminum and their growth. *Korros. und Metallschutz* **18**, 42–50 (1942).

Gotthardt, E. Stereoscopic measurements of objects with the electron microscope. *Zeits. f. Physik* **118**, 714–717 (1942).

Gundermann, J. and Külz, H. Observations on zinc black by means of the electron microscope. *Kolloid Zeits.* **98**, 287–289 (1942).

Haam, E. von and Schuh, M. Cytologic studies with the electron microscope. *J. Tech. Methods* **22**, 75–80 (1942).

Heidenreich, R. D. and Peck, V. G. Electron microscope study of surface structure. *Phys. Rev.* **62**, 291–293 (1942).

Mahl, H. The electron microscopic representation of surfaces with the replica method. *Naturwiss.* **30**, 207–217 (1942).

Mahl, H. and Pawlek, F. Electron microscopic structural investigations of non-alloyed steels. *Arch. Eisenhüttenw.* **16**, 219–222 (1942).

Mahl, H. and Pawlek, F. Electron microscopic investigations of Al alloys. *Zeits. f. Metallk.* **34**, 232–236 (1942).

Müller, H. O. Measurement of the depth of electron microscopic objects. *Kolloid Zeits.* **99**, 6–28 (1942).

Müller, H. O. and Pasewaldt, C. W. Observations on the fine structure of the test diatom *Pleurosigma angulatum* W.Sm. and stereoscopic pictures with the electron microscope. *Naturwiss.* **30**, 55–60 (1942).

Rawlins, T. E. Recent evidence regarding the nature of viruses. *Science* **96**, 425–426 (1942).

Roberts, E. A. The structure of chloroplasts, chromoplasts, leucoplasts, and carotin "crystals" and their relationship to cellulose "particles" and colloidal carbon. *Am. J. of Botany* **29**, Suppl. p. 16 (1942).

Rüdiger, O. Use of beryllium for electron microscopic replica foil. *Naturwiss.* **30**, 279 (1942).

Semmler-Alter, E. Electron microscope investigation of martensite in different tempering stages in steel with 0.24 percent carbon. *Arch. Eisenhüttenw.* **16**, 223–225 (1942).

Smakula, A. Remark on the paper of M. von Ardenne, "On an electron-microscopic investigation of the structure of reflection reducing layers and the determination of such layers." *Zeits. angew. Photogr.* **4**, 15–16 (1942).

Tiselius, A. and Gard, S. Electron microscopic observations on poliomyelitis virus preparations. *Naturwiss.* **30**, 728–731 (1942).

Winterfeld, E. von. The universal electron microscope. Recent results of electron microscopy. *Messtechn.* **18**, 98–102 (1942).

Ardenne, M. von. Suitability of gelatine-free photographic film for electron microscopy. *Zeits. f. Physik* **121**, 1–6 (1943).

Ardenne, M. von and Beischer, D. Electron microscope photographs of fine reaction layers on crystals of metal oxide smokes. *Kolloid Zeits.* **102**, 127–131 (1943).

Baker, R. F., Ramberg, E. G., and Hillier, J. Erratum: The photographic action of electrons in the range between 40 and 212 kilovolts. *J. Appl. Phys.* **14**, 39 (1943).

Barrett, C. S. Metallography with the electron microscope. *Metals Technology* **10**, 1–19 (1943).

Bole, G. A. and Loomis, G. A. Some physical procedures used in ceramic research. *J. Appl. Phys.* **14**, 443–450 (1943).

Bragg, L. Seeing ever-smaller worlds. *Nature* **151**, 545–547 (1943).

Burton, E. F. Electron microscope studies of the capture of airborne particles by single fibers. *Nature* **152**, 540 (1943).

Fullam, E. F. Magnification calibration of the electron microscope. *J. Appl. Phys.* **14**, 677–683 (1943).

Gard, S. Purification of poliomyelitis viruses. Experiments on murine and human strains. *Acta Med. Scandinavica, Supplementum* 143 (1943).

Gard, S. Electron microscope observations on purified poliomyelitis virus preparations. II. A contribution to the question of the epidemiology of infantile paralysis. *Klin. Wochenschr.* **22**, 315–318 (1943).

Gard, S. Electron microscope observations on purified poliomyelitis virus preparations. III. A comparison with the results of physico-chemical experiments. *Arch. Ges. Virusforschung* (1943). An abstract of this article was published in *Arkiv för Kemi*, Stockholm, 17/B. I. (1943).

Glaser, R. W. and Stanley, W. M. Biochemical studies on the virus and the inclusion bodies of silkworm jaundice. *J. Exp. Med.* **77**, 451–466 (1943).

Gölz, E. Electron microscopic fine structure of fractured glass surfaces. *Zeits. f. Physik* **120**, 773–777 (1943).

Gölz, E. Surface electron microscopy of glass and ceramics by the replica method. *Zeits. f. techn. Physik* **24**, 8–11 (1943).

Green, H. and Fullam, E. F. Some applications of the high resolving power of the electron microscope. *J. Appl. Phys.* **14**, 332–340 (1943).

Harker, D. and Schaefer, V. J. Metallography by electron microscope. *Metal Prog.* **43**, 68–69 (1943).

Heidenreich, R. D. Interpretation of electron micrographs of silicon surface replicas. *J. Appl. Phys.* **14**, 312–320 (1943).

Henle, W. and Henle, G. Interference of inactive virus with the propagation of virus of influenza. *Science* **98**, 87–89 (1943).

Hock, C. W. and McMurdie, H. F. Structure of the wool fiber as revealed by the electron microscope. *J. Res. Nat. Bur. Stand., Wash.*, **31**, 229–236 (1943).

Johnson, F. H., Zworykin, N., and Warren, G. A study of luminous bacterial cells and cytolysates with the electron microscope. *J. Bact.* **46**, 167–185 (1943).

Jungeblut, C. W. and Bourdillon, J. Electronmicrography of murine poliomyelitis virus preparations. *J. Am. Med. Ass.* **123**, 399–402 (1943).

Kinder, E. Magnesium oxide crystals in the electron microscope. *Naturwiss.* **31**, 149 (1943).

Knaysi, G. and Mudd, S. The internal structure of certain bacteria as revealed by the electron microscope. A contribution to the study of the bacterial nucleus. *J. Bact.* **45**, 349–359 (1943).

Linke, F. Condensation nuclei made visible in the electron microscope. *Naturwiss.* **31**, 230–231 (1943).

Luria, S. E., Delbruck, M. and Anderson, T. F. Electron microscope studies of bacterial viruses. *J. Bact.* **46**, 57–77 (1943).

Marx, T., Klemm, W., and Smekal, A. Electron microscope studies of scratches. *Naturwiss.* **31**, 143–144 (1943).

Morton, H. E. and Anderson, T. F. The morphology of *Leptospira icterohemorragiae* and *L. canicola* as revealed by the electron microscope. *J. Bact.* **45**, 143–146 (1943).

Mudd, S. Changes in the bacterial cell brought about by the action of germicides and antibacterial substances as demonstrated by the electron microscope. *Am. J. Public Health* **33**, 167–168 (1943).

Mudd, S., Heinmets, F., and Anderson, T. F. The pneumococcal capsular swelling reaction studied with the aid of the electron microscope. *J. Exp. Med.* **78**, 327–332 (1943).

Mudd, S., Polevitzky, K., and Anderson, T. F. Bacterial morphology as shown by the electron microscope. V. *Treponema pallidum, T. macrodentium, and T. microdentium. J. Bact.* **46**, 15–24 (1943).

Mudd, S., Heinmets, F., and Anderson, T. F. Bacterial morphology as shown by the electron microscope. VI. Capsule, cell-wall, and inner protoplasm of pneumococcus, type III. *J. Bact.* **46**, 205–211 (1943).

O'Brien, H. C. and McKinley, G. M. New microtome and sectioning method for electron microscopy. *Science* **98**, 455–456 (1943).

Picard, R. G. and Duffendack, O. S. Studies on the structure of thin metallic films by means of the electron microscope. *J. Appl. Phys.* **14**, 291–305 (1943).

Preckshot, G. W., DeLisle, N. G., Cottrell, C. E., and Katz, D. L. Asphaltic substances in crude oils. *Am. Inst. of Mining and Metal. Engrs. Petroleum Division Section, Transactions* **151**, 188–205 (1943).

Quarrell, A. G. Electron microscope and its application to engineering problems. *Engineer* **176**, 499–502; 526–528 (1943).

Schmidt, R. W. Oxidation of metal powders in electron microscopic investigations. *Kolloid Zeits.* **102**, 15–17 (1943).

Seeman, H. Migratory schlieren in electron optical pictures of single crystals, especially molybdenum oxide. *Naturwiss.* **31**, 415–416 (1943).

Seymour, F. J. Electron microscope, fertility, and gynecology. *M. Woman's J.* **50**, 151 (1943).

Sharp, D. G., Taylor, A. R., Beard, D., and Beard, J. W. Morphology of the Eastern and Western strains of the virus of equine encephalomyelitis. *Arch. Path.* **36**, 167–176 (1943).

Sjöstrand, F. Electron-microscopic examination of tissues. *Nature* **151**, 725–726 (1943).

Sliepcevich, C. M., Gildart, L., and Katz, D. M. Crystals from Portland cement hydration; an electron microscope study. *Industr. and Engr. Chem., Ind. ed.*, **35**, 1178–1187 (1943).

Taylor, A. R., Sharp, D. G., McLean, I. W., Jr., Beard, D., Beard, J. W., Dingle, J. H., and Feller, A. E. Purification and character of the swine influenza virus. *Science* **98**, 587–589 (1943).

Taylor, A. R., Sharp, D. G., Beard, D., Beard, J. W., Dingle, J. H., and Feller, A. E. Isolation and characterization of influenza virus A (PR 8 Strain). *J. Immun.* **47**, 261–282 (1943).

Weiss, L. J. Electron micrographs of bacteria medicated with penicillin. *Proc. Indiana Acad. Sci.* **52**, 27–29 (1943).

Weiss, L. J. Electron micrographs of Rickettsiae of typhus fever. *J. Immun.* **47**, 353–357 (1943).

Wile, W. J. and Kearney, E. B. The morphology of *Treponema pallidum* in the electron microscope; demonstration of flagella. *J. Am. Med. Ass.* **122**, 167–168 (1943).

Zworykin, V. K. Applications of the electron microscope in metallurgy. *Trans. Am. Inst. Mining Met. Engrs., Inst. Metals Div.*, Tech. Pub. No. 1594, 1–25 (1943).

Fuller, M. L., Brubaker, D. G., and Berger, R. W. Mounting of pigments for electron microscopy. *J. Appl. Phys.* **15**, 201 (1944).

Martin, D., Baylor, M. R. B., and Clark, G. L. A preliminary electron microscope study of the active deposit from radiothorium. *Science* **99**, 185 (1944).

Melnick, J. L. Detection with the electron microscope of rod-shaped particles in stools of normal and poliomyelitic individuals. *J. Immun.* **48**, 25–28 (1944).

Sharp, D. G., Taylor, A. R., McLean, I. W., Jr., Beard, D., Beard, J. W., Feller, A. E., and Dingle, J. H. Isolation and characterization of influenza virus B (Lee Strain). *J. Immun.* **48**, 129–153 (1944).

New Books

The Physical Chemistry of Electrolytic Solutions. A.C.S. Monograph Series, No. 95

By Herbert S. Harned and Benton B. Owen. Pp. 611+xxxvi, Figs. 165, 15×23½ cm. Reinhold Publishing Corporation, New York, 1943. Price $10.00.

The purpose of this treatise, as stated by the authors in their preface, is to present the well-established interionic attraction theory in a logical rather than a historical order and to discuss the numerical treatment of the data and the various properties of electrolytes in terms of the fundamental equations of theory.

The fifteen chapters of the monograph are divided into three general parts. Chapters one to five contain a thermodynamic introduction, a general statement of the interionic attraction theory, the theory of ionic solutions in equilibrium and in perturbed states, and a very useful numerical summary of the theoretical results in which the theoretical equations are reduced to their simplest forms. Chapters six to ten contain discussions of experimental methods, with emphasis on the numerical treatment of data rather than experimental techniques, employed to study the properties of electrolytic solutions. These include conductance in aqueous and non-aqueous solutions, freezing point, boiling point, vapor pressure, and the electromotive force method. The last section, chapters eleven to fifteen, deals with the properties of electrolytes, beginning with hydrochloric acid and proceeding to other 1–1 electrolytes, polyvalent electrolytes, mixtures of strong electrolytes and weak electrolytes. These chapters and the appendix contain a large amount of useful information, much of it critically evaluated, in the form of figures and tables.

In general the purpose of the authors is well achieved. Their extensive experience in the experimental study of electrolytes is well known and gives authority to their

treatment and judgment. An apparent overemphasis on the electromotive force method is probably justified by the unequaled contributions in this field from the Yale laboratories. This reviewer regrets that the scope of the monograph does not quite match the promise of the title. A less promising title would confirm the statement of the authors that little or no attention has been paid to electrode processes, ionic entropies, Raman spectra, refractive indices, and other optical properties. No doubt limitations of size and the interruptions of the war are responsible.

The reviewer is a little puzzled by the bibliography. It is extensive but not complete. The authors state that they have tried to incorporate the most accurate results in their discussions. No reference could be found to several papers, selected at random, which the reviewer considers important. And, although the monograph was published on the last day of 1943, no references to original papers published in that year were met. A few references to 1942 publications seem to have been inserted during the proof-reading. A statement by authors about the extent and period of literature coverage would in general be welcome.

These remarks are minor matters. The monograph is highly recommended to all workers in the field of electrolytes and to others who are interested in a logical presentation of the interionic theory and its use and limitations in interpreting the properties of electrolytic solutions.

A. L. Robinson
University of Pittsburgh

The Chemical Background for Engine Research. Volume II

Edited by R. E. Burk and Oliver Grummitt. Pp. 297+vii, Figs. 89, 16×23½ cm. Interscience Publishers, Inc., New York, 1943. Price $3.50.

This presents an edited collection of a two-hour lecture by each of six noted experts in the field of combustion and engine research. The choice of general subject matter is excellent and the editors are to be congratulated on the typography and layout; some few duplications of figures and tables may be excused on the grounds of providing continuity in each section. Although the newer fields of engine research are of necessity cloaked in secrecy, it is regrettable that in the discussions of applied research, the lecturers have dealt with the Otto cycle almost to the exclusion of existing published material on Diesel and gas turbine applications. The bibliographies at the end of each section are well chosen and represent pertinent literature to 1941. It is felt that the able coverage of material on chemical reactions and reaction kinetics is too narrow an interpretation of "chemical background." Exposition is desirable on physical kinetics of mixing phenomena and "freezing" of reactions by dilution since these latter factors may be controlling in many cases. Little mention is made of the effect of chemical equilibria at high pressures and temperatures of engine performance.

The introductory section on combustion research is exceptionally lucid and interesting. The chapter on thermodynamics of hydrocarbons presents a condensed review of thermodynamic principles and a large amount of valuable data on heats and free energies of formation and isomerization of hydrocarbons. It is believed that the contents of this chapter might have been more pertinent to general interest had less emphasis been placed on detailed calculation of entropies and free energy changes of isomerization and more emphasis been put on thermodynamic calculations of combustion reactions, and cracking of hydrocarbons. This should in no way, however, be construed as detracting from the value of the material presented. The third chapter embodies a brief survey of the organic chemistry involved in laboratory and industrial preparations of synthetic hydrocarbons. Chapter IV is a summary of the kinetics of combustion, with a view toward predicting over-all reaction rates and igniting conditions from rates and effects of the elementary reactions; there is an excellent introduction to the reaction kinetics of gas-phase combustion, but no discussion of the attendant physical and chemical kinetics of the combustion of liquid or solid fuels. Chapter V contains much descriptive material of experimental equipment for following the progress of combustion in the actual engine. Not only is the apparatus described, but there is considerable critical discussion of the test results obtained, especially from the standpoint of evaluating knocking characteristics in the Otto cycle. More discussion of material methods of exhaust gas analysis would be desirable. This reviewer is entirely unfamiliar with the problems of lubrication which are the subject matter of the last chapter, but the material given was extremely interesting and is apparently a presentation in keeping with the high quality of the preceding chapters. It is believed that inclusion of more information on extreme pressure lubricants would be proper.

Many of the suggestions above undoubtedly would have been included in a book written expressly for engine research workers, and it is with this thought in mind that they are made. Viewed merely as a collection of lecture material stemming from various individuals, the contents are outstanding in pertinence to the general subject matter. The technical caliber of the lectures is such that the book might be more highly recommended to physicists, physical chemists, and chemical engineers rather than to unspecialized personnel, although it should prove a valuable reference to the latter as well as a rather well-rounded survey to serve as an introduction to engine research.

Glenn C. Williams
Massachusetts Institute of Technology

Empirical Equations and Nomography

By Dale S. Davis. Pp. 200+ix, Figs. 70, 15½×23½ cm. McGraw-Hill Book Company, Inc., New York, 1943. Price $2.50.

This book is recommended to those who wish an elementary introduction into the subjects of empirical equations and nomography. The various techniques which the author has included are very carefully and clearly explained. Each is illustrated by a detailed discussion of

well-chosen problems usually taken from chemical engineering practice. Only elementary mathematics is used throughout.

The scope of this book is, however, rather limited. For example, empirical formulas for periodic curves are not discussed. The method of least squares is applied only to the straight line equation, being dismissed even in this case as too laborious. In this connection, it may be noted that tables* exist which permit the easy application of this method to polynomial approximation.

HERMAN FESHBACH
Massachusetts Institute of Technology

The Total and Free Energies of Formation of the Oxides of Thirty-Two Metals

BY MAURICE DEKAY THOMPSON. Pp. 89. Electrochemical Society, Inc., New York, 1942. Price $1.00.

This publication presents a compilation in one booklet of the free energies and the heats of formation of the oxides of thirty-two metals of importance particularly in metallurgy.

The author has made a careful selection of the best data available for the computations, and, in the cases where there exists considerable variation in thermal values obtained by different investigators, appears to have justified his selection.

The author might with some advantage to readers have expanded his reasons for selecting a form of specific heat equation of the type $Cp=a+bT+cT^{-1}$ for water hydrogen and oxygen. This form of heat capacity equation appears to reproduce the spectroscopic values with only minor deviations, particularly at the higher temperatures.

The metallurgist will welcome this new publication in condensed form of the thermal values of practically all of the oxides of metallurgical significance. It contains many implied suggestions for the revision of certain data, and the need for more precise determinations is quite evident.

The educator will find here a wealth of data for use in the classroom to illustrate the fundamentals of thermal calculations.

GEBHARD STEGEMAN
The University of Pittsburgh

Astronomy, Maps, and Weather

BY C. C. WYLIE. Pp. 449+x, Figs. 196, 16×24 cm. Harper & Brothers, New York, 1942. Price $3.00.

The unprecedented combination of seemingly unrelated subjects attempted in this book is accomplished with considerable success. A specific need prompted its preparation and, while all the subjects are treated in an elementary fashion, the author has succeeded in producing a very useful and instructive textbook. The prospective airplane pilot or navigator, for whom the book was written, will find much useful and basic information.

The astronomy necessary for the understanding of navigation occupies a large portion of the book. The opening chapters deal with the concept of the celestial sphere, the constellations with a number of star maps, and good descriptions and explanations of the various types of astronomical telescopes. The earth itself is then discussed with special attention to its shape, position, and motion relative to the sun; this is followed by an explanation of the seasons and the calendar.

Since but three short chapters are devoted to weather, clouds, and weather forecasting, the treatment of the meteorology useful to the pilot and navigator is brief; this section of the book could have been enlarged and made more comprehensive. However, the information included is very useful and well chosen.

Although maps appear as a part of the title of the book, but a brief chapter is devoted to the subject; it would seem that a much more complete treatment should have been included. An excellent chapter on time and timekeepers is followed by an equally excellent chapter on celestial navigation. The principles of navigation and the use of instruments involved are set forth clearly and concisely.

The concluding chapters, about one-third of the book, are devoted to a further discussion of astronomy. It is largely descriptive and contains much interesting information, although of doubtful value to the pilot or navigator of airplanes.

The author has handled a difficult assignment in a very creditable manner; he has developed his topics in excellent style. One of the delightful features of the book is the frequent historical references contained in almost every chapter. The general reader will find much pleasure and profit in the book.

JOHN G. ALBRIGHT
Rhode Island State College

High Frequency Thermionic Tubes

BY A. F. HARVEY. Pp. 235+viii, Figs. 99, 14½×22½ cm. John Wiley & Sons, Inc., New York, 1943. Price $3.00.

As may be seen by a perusal of the chapter titles, this book gives an introduction to all the commonly known methods of producing high frequency oscillations. Thus the first chapter treats the low frequency properties of diodes, triodes, and more complex multi-element tubes; the second tells of the changes that occur as the frequency is raised; the third has to do with retarding field generators; the fourth and fifth with magnetrons; and the sixth with velocity modulation tubes and also wave guides and resonators.

Plainly it is impossible to treat all these subjects thoroughly in a book of 235 pages.

The author has chosen to treat the static magnetron and the "dynatron" type of magnetron oscillator in considerable detail, while to the various other subjects he devotes enough space to give at least a good introduction.

It seems to the reviewer that this was a wise choice on the author's part, for: (a) he has been personally interested

* *Tables of Higher Mathematical Functions* (Principia Press, Bloomington, Indiana, 1935), Vol. 2.

in magnetrons of this sort and is able to give a convincing and connected account of a very interesting group of phenomena, and (b) most of the other subjects are either like the triode, which is quite well understood, but for which the information is already collected in other places, or like velocity modulation tubes, for which a really detailed treatment is not available. Moreover, such deficiencies as exist are at least partially remedied by liberal bibliographies at the end of each chapter.

It must be said, however, that some of the topics are treated so briefly that the choice of subject matter becomes difficult and there arise some curious omissions and commissions. For example, when the first chapter covers diodes, triodes, pentodes, secondary emission, noise, class *A*, *B*, and *C* amplifiers, and positive and negative feedback in twenty-one pages, one is a little surprised to find about one page given to core dimensions in audio transformers. Again, although considerable space is devoted to the description of magnetron oscillators of the resonance and electronic types there never is a clear and concise statement of the supposed mechanism of operation of either.

Thus this book may perhaps be regarded as a monograph on the static and "dynatron" types of magnetron, with useful additional information on related topics. Both phases of the book should prove useful and interesting. To many readers the book will be useful as a good introduction to the field and its literature. But to the present reviewer the part of greatest interest is that relating to the static magnetron. For the author shows that experiment and theory usually disagree by considerable amounts. This is astounding for one is accustomed to regard this as one of the simplest of classical problems. Yet the disagreement is there and very considerable experimental work on the author's part has given no hint as to cause for the discrepancy.

WILLIAM W. HANSEN
Stanford University

Radio Receiver Design, Part I

BY K. R. STURLEY. Pp. 435+xii, Figs. 187, 14×22 cm. John Wiley & Sons, Inc., New York, 1943. Price $4.50.

As the author states, "An attempt has been made in this book to bring together the fundamentals of receiver design." After reading the book, one feels that the attempt has been fairly successful. Theory and design are taken up in logical order from the far end of the antenna to the input of the first audio amplifier. The audio end of the receiver, measurements, and testing are to be presented in a second volume.

In the preface, the author says that his sequence of presentation may not be the most desirable and that therefore the student should plan his own order of topics. The text is then so interspersed with cross references that if one just begins and follows instructions, a good sequence will result. However, if the student is sufficiently advanced to derive much information from the presentation, the course of study is not at all important. The material is presented at a fairly high mathematical level. A knowledge of network theory, transmission lines, and electronics and radio in general is necessary for complete understanding.

Written in England, the book has many expressions with which American students and engineers are not familiar, such as pulsance, Swegger oscillator, reaction, Miller effect, and mains driven, etc. Many of the sentences are so long and involved that the reader loses track of the original thought before reaching the end. The terms "former" and "latter" are used so freely that there results considerable confusion; whereas, merely repeating one word or phrase would clarify the meaning completely. Many of the equations have insufficient explanation as to notation and interpretation. A test case was made of one such shortcoming.

About twenty pages of rather involved theory were read carefully. The book was put aside for several days after which time an attempt was made to use an equation which appeared at the conclusion of the development. In spite of the fact that the reader had understood the material on the first reading, it required 45 minutes of careful search to discover what was meant by the various letters and symbols used in the equation. Substitutions of letters for whole quantities are not placed conspicuously but are hidden at the ends of the equations in which they first appear and are not repeated.

There should be, it is felt, an introductory section to explain terms and notation so that the student will be able to find what is meant by r-f amplifier, detection, modulation, selectivity, sensitivity, etc. Then there are numerous examples of poor wording such as "higher frequency wave ranges" and "the oscillator reradiated." The impression was left that were the author to give a series of lectures to supplement the book, the results would be completely satisfactory. On one page, ideas are presented with clearness and simplicity while on the next, the student is apt to find himself floundering among j operators, Bessel functions, Fourier series, hyperbolic functions, and network equations. The use of the word "it" instead of repeating the real subject of the sentence tends to keep the reader searching for the subject to which "it" refers. Some topics are developed rather completely while other equally important topics are treated lightly.

The desirable features of the book far outweigh the undesirable ones mentioned. There are many fine sections and after the student becomes used to the style and manner of presentation, he can learn a great deal in the field of receiver design. A few more examples would be in order, but this might necessitate reducing the theoretical content to keep the volume to convenient size. The section on frequency modulation is about the best summary the writer has yet found. The material on input admittance of vacuum tubes is quite complete, lacking only a clinching summary of facts and effects. The section on antennae (aerials) is complete enough for design purposes under ordinary circumstances. There is an excellent summary of coils at radiofrequencies, and r-f amplifiers are considered in detail. The often confusing problem of superheterodyne oscillator-mixer circuits is given especially good attention

in two chapters. The principle of oscillators is explained simply and clearly. The chief problems met in the design of i-f amplifier and detector circuits are treated with equal clarity. A brief but interesting summary of the use of the *j* operator and of Fourier series is made in the appendix.

The book can be recommended to students and even design engineers as it brings together many important graphs and tables used in design procedure in addition to the discussion of fundamental principles.

T. A. BENHAM
Haverford College

Man's Physical Universe

BY A. T. BAWDEN. Pp. 832+xv, Figs. 321, 16×25 cm. The Macmillan Company, New York, 1943. Price $4.00.

Professor Bawden's physical science survey text has earned a well-deserved success. It is an easily readable, interesting, and highly discussive treatment of a multitude of topics ranging from scientific method through astronomy, geology, physics, aviation, biology, to the social implications of science. The review questions are aptly chosen and should be of great help to the student.

Despite its many excellent features, the book, in some respects, is disappointing. Far too many physics topics are introduced and too little emphasis is given to basic physics. The author devotes one and one-half pages to giant telescopes, but not even a single line to image formation of extended objects. He gives one and one-quarter pages to the gyroscope and precession yet scarcely more space to a discussion of Newton's laws of (rectilinear) motion. Far too many technical terms such as spherical and chromatic aberration, infra-red, and ultraviolet (pp. 64 and 66) are employed without definition. A glossary of such terms is badly needed. In summary, this book teaches much about physics but too little about fundamental physics. It will do little to convert students to the belief that physics is not only a marvelous science but also understandable by the intelligent citizen.

O. H. BLACKWOOD
University of Pittsburgh

Basic Physics for Pilots and Flight Crews

BY E. J. KNAPP. Pp. 118+v, Figs. 91, 13×19 cm. Prentice-Hall, Inc., New York, 1943. Price $1.65.

This 118-page book will help intelligent preflight students to learn a little essential physics in a short time. It might well have been titled "Selected topics in mechanics, heat, and meteorology for the aircrew." The subject matter is well chosen and adequately presented. Admirable use of line drawings is made, but they have no descriptive legends. The numerous worked problems and those for the student to solve deal mostly with the operation of the airplane, with the determination of bomb trajectories, parachute jumps, and other anticipated experiences of the prospective airman. Professor Knapp is to be congratulated for a good job, neatly done.

O. H. BLACKWOOD
University of Pittsburgh

Here and There

Paul E. Klopsteg, Chairman of the Governing Board of the American Institute of Physics and former president of Central Scientific Company of Chicago, has been appointed Director of Research and Professor of Applied Science in the Technological Institute of Northwestern University, it was announced today by President Franklyn B. Snyder. The appointment takes effect at once. Dr. Klopsteg was a member of a committee of prominent industrialists and educators, of which Charles F. Kettering was chairman, to advise the Institute on postwar development. In his new duties he will undertake the development of advanced studies and the coordination of research for the postwar period.

Nelson Doubleday, President and Chairman of the Board of Doubleday, Doran & Company, Inc., announces that the company has acquired, through a wholly-owned subsidiary company, the assets and business of The Blakiston Company, Philadelphia, as a going concern. Under the name of The Blakiston Company, this firm will continue its present business of publishing medical and scientific books and the performance of existing contracts, substantially as carried on at this time. The offices will continue at 1012 Walnut Street, Philadelphia 5, Pennsylvania.

The annual meeting of the Optical Society of America will be held at the Hotel Pennsylvania, in New York City, on October 20 and 21, 1944.

Appointment of Garet W. Denise to be General Manager of Littelfuse Chicago Plant Operations has just been announced by Littelfuse Incorporated, manufacturer of aircraft fuses and a wide range of instrument fuses and accessories at El Monte, California.

Mr. Denise comes to Littelfuse from Republic Aviation Corporation, Farmingdale, New York. Prior to this connection, he was engaged for ten years as an industrial consulting engineer—five years as Plant Production Engineer with Ditto, Inc., and five years as Operations Manager with the Temple Radio Corporation.

Industrial Research Institute

Eighty-five industrial research executives and their guests attended the sixth annual meeting of the Industrial Research Institute held on May 19 and 20, at the Roosevelt Hotel, Pittsburgh, Pennsylvania. Harold K. Work, Manager, Research and Development, Jones and Laughlin Steel Corporation, Pittsburgh, was elected Chairman of the Institute for the ensuing year, and John M. McIlvain, Administrative Supervisor, Research and Development Department, The Atlantic Refining Company, Philadelphia, was elected Vice Chairman. Charles S. Venable, Director of Chemical Research, American Viscose Corporation, Marcus Hook, Pennsylvania, and Harry M. Williams, Vice President, The National Cash Register

Company, Dayton, Ohio, were elected to the Executive Committee.

The Industrial Research Institute, an affiliate of the National Research Council, undertakes to promote improvement of methods and more economical and effective management in industrial research through the cooperative efforts of its members. The sixty-six member companies are represented by their key executives in charge of research.

University of Missouri Benefits

The Department of Physics at the University of Missouri is the chief benefactor under the will of Oscar M. Stewart, Professor Emeritus of Physics, who died last week. It provides at least $1000 a year for the department. It is estimated the total estate may be valued at about $100,000.

The net income from the estate will go to the Board of Curators of the University for some educational or scientific purpose connected with the Department of Physics. The president of the University, with the aid and advice of two physics department members, will select the purpose for the use of the fund. The income is not to be used for the maintenance of the department or to assume any of the burden of legislature, but as a trust fund for undergraduate or graduate scholarships or fellowships for students majoring or minoring in physics, for payment of famous physicists to give special lectures, or in extraordinary cases for the purchase of research apparatus.

Biological Photographic Association

The Biological Photographic Association will hold its Fourteenth Annual Meeting September 7–9, 1944, in Binghamton, New York. Papers will be presented by experts in the fields of still and motion picture photography, photomicrography, etc. A salon of pictures made by leading biological photographers from all over the country will be an important feature of the meeting and representatives from firms specializing in precision equipment will demonstrate their products.

The Association is a non-profit organization for the study of photography as applied to medicine, dentistry, and the biological and natural sciences. The B.P.A. Journal is published quarterly and is furnished free to members. Further information about the Association and the convention program may be obtained by writing to: The Secretary of the Biological Photographic Association, University Office, Magee Hospital, Pittsburgh, Pennsylvania.

Pan American Institute of Mining Engineering and Geology

The first Pan American Congress of Mining Engineering and Geology, organized and directed by the Institute of Mining Engineering of Chile and officially authorized by the government of Chile and the South American Union of Engineering Associations, was held in Santiago, Chile, January 15 to 23, 1942. The A.I.M.E. appointed several delegates to this Congress including Edward Steidle and Will Wright. Mr. Wright was selected to head the group and prepared the report on the meetings which was published in *Mining and Metallurgy* of March, 1942. Our government appointed D. F. Hewett to represent the Geological Survey, Elmer Pehrson the Bureau of Mines, and Will Wright the State Department. Edward Steidle represented the Commonwealth of Pennsylvania. At this Congress it was decided to organize a Pan American Institute of Mining Engineering and Geology with headquarters in Santiago, Chile. National sections have been organized in Argentina, Bolivia, Brazil, Chile, Peru, and Uruguay.

PAIMEG desires to cooperate with all the mineral industries societies of the Americas, support all activities that will benefit the mineral industries, and expand fundamental knowledge of geological conditions and encourage the standardization of technical terminology. The Institute will also facilitate the interchange of publications, students, professional men, and industrialists connected with the mineral industries. Members of any mineral industries society in the United States and Canada are eligible to join the National Section. Further information can be obtained from Edward Steidle, Chairman, National Directorate, PAIMEG, State College, Pennsylvania.

Bulletin of Mathematical Biophysics

The September, 1944 issue of the *Bulletin of Mathematical Biophysics*, Vol. 6, No. 3, which is edited by N. Rashevsky will have the following table of contents:

A theory of membrane permeability—INGRAM BLOCH.
Outline of a mathematical theory of the removal of malarial parasites from the blood stream—H. D. LANDAHL.
Simplified equations for the distribution of chloride in body water—WALTER S. WILDE.
On the form and strength of trees: Part I. The trunk—I. OPATOWSKI.
A contribution to the mathematical biophysics of visual perception and aesthetics—N. RASHEVSKY AND VIRGINIA BROWN.
On the theory of blood-tissue exchanges: I. Fundamental equations—R. E. SMITH AND M. F. MORALES.

Calendar of Meetings

August

29–Sept. 1 American Institute of Electrical Engineers, Los Angeles, California

September

11–16 American Association for the Advancement of Science, Cleveland, Ohio
13–15 Society of Automotive Engineers, Milwaukee, Wisconsin

October

5– 6 American Institute of Mining and Metallurgical Engineers, Pittsburgh, Pennsylvania
5– 7 National Electronics Conference, Chicago, Illinois
5– 7 Society of Automotive Engineers, Los Angeles, California
6– 9 Electronic Parts and Equipment Industry Conference, Chicago, Illinois
9–14 American Society of Civil Engineers, Cleveland, Ohio
16–18 American Institute of Mining and Metallurgical Engineers, Cleveland, Ohio
16–20 American Society for Metals, Cleveland, Ohio
16–21 American Welding Society, Cleveland, Ohio
20–21 Optical Society of America, Hotel Pennsylvania, New York, New York
28 American Mathematical Society, New York, New York

November

2– 3 Society of Automotive Engineers, Tulsa, Oklahoma
17–18 Society of Rheology, New York, New York

Contributed Original Research

Further Studies of the Infra-Red Absorption of Rubber

DUDLEY WILLIAMS AND BROCK DALE
University of Oklahoma, Norman, Oklahoma

(Received May 1, 1944)

The transmission spectrum of natural rubber has been studied in the region between 1μ and 15μ and the effects of linear and radial stretch have been observed. Linear extension greater than 400 percent of the original length produces an increase in the C—C vibrational frequency. Both linear and radial stretch produce an increase in absorption coefficient and a decrease in reflection coefficient. The changes in absorption and reflection coefficients are greatest at short wave-lengths.

INTRODUCTION

THE infra-red absorption of highly purified natural rubber has been studied by Stair and Coblentz,[1] who found that the spectra of the alpha- and beta-components are almost identical and that aging (oxidation) of rubber is accompanied by increased absorption near 3μ and 6μ and in the region between 7μ and 11μ. Other infra-red studies of rubber and related compounds have been made by Williams,[2] Sears,[3] Wells,[4] and Barnes.[5] The transmission curves obtained in these latter studies are in essential agreement with those published by Stair and Coblentz. Minor variations are to be expected in view of the wide variations of the physical properties exhibited by rubber obtained from different sources and processed in different ways.

Williams and Taschek[6] have studied the effects of elastic stretch on the absorption of rubber between 2μ and 8μ. The shapes of the absorption bands in this region were modified when the material was stretched, but the positions of the absorption maxima remained unchanged. Samples stretched radially to twelve times their original area exhibited minor transmission minima between 4μ and 5μ; however, these minima were possibly produced by interference effects in the thin absorbing layers. Absorption and reflection coefficients for rubber under various conditions of stretch were calculated from transmission data on samples of different thickness at similar elongations. Although there were inherent weaknesses in this method (for example, the assump-

[1] R. Stair and W. W. Coblentz, J. Research Nat. Bur. Stand. **15**, 295 (1935).
[2] D. Williams, Physics **7**, 399 (1936); Rubber Chem. Tech. **10**, 249 (1937).
[3] W. C. Sears, J. App. Phys. **12**, 35 (1941).
[4] A. J. Wells, J. App. Phys. **11**, 137 (1940).
[5] R. B. Barnes, Ind. Eng. Chem. **15**, 83 (1943).
[6] D. Williams and R. Taschek, J. App. Phys. **8**, 497 (1937); Rubber Chem. Tech. **10**, 697 (1939).

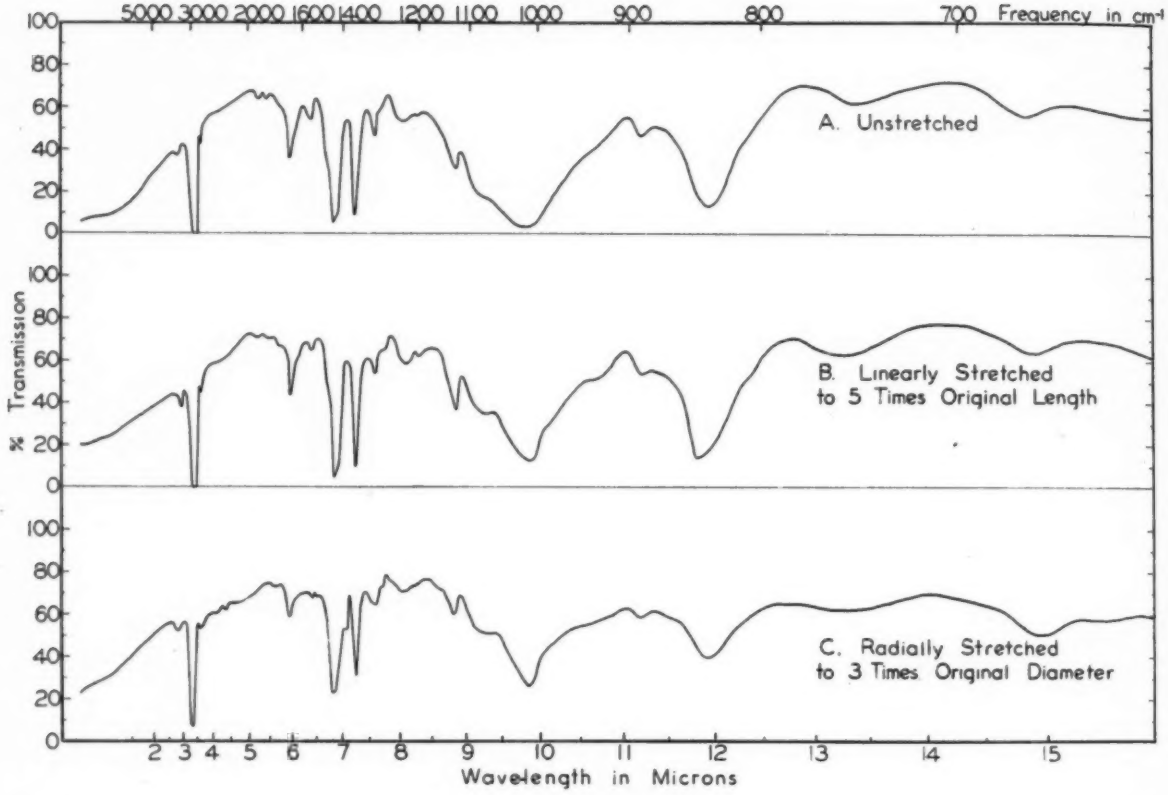
5000 3000 2000 1600 1400 1200 1100 1000 900 800 700 Frequency in cm⁻¹
A. Unstretched
B. Linearly Stretched to 5 Times Original Length
C. Radially Stretched to 3 Times Original Diameter
% Transmission
Wavelength in Microns

FIG. 1. The transmission spectrum of rubber: curve *A*, unstretched rubber; curve *B*, rubber stretched unilaterally to five times its original length; and curve *C*, rubber stretched radially to three times its original diameter.

tion that the surface conditions of the samples were the same), the results indicated that stretching produced an increase in the absorption coefficient and a decrease in the reflection coefficient. The absorption coefficients as computed were a measure of the combined effects of true absorption and scattering within the sample; the reflection coefficients were a measure of all surface effects producing decreases in transmission.

The purpose of the present study has been to extend the range of the earlier measurements to 15μ in the hope of detecting any changes in the lower vibrational frequencies produced by stretch and to obtain more accurate data at various wave-lengths on the changes in absorption and reflection coefficients accompanying stretch. In the case of a material like rubber in which there is considerable variation even in samples cut from a single sheet, it is possible to obtain only semi-quantitative data, but it is felt that even data of this type might be useful in the development of adequate theories of the structure of rubber.

EXPERIMENTAL WORK AND RESULTS

The rubber samples used were cut from sheets of vulcanized rubber of low sulphur content.* The range of thickness of the unstretched samples was 0.03—0.07 mm. The thicknesses were measured by means of a micrometer screw equipped with a ratchet. Comparison revealed that the thicknesses of the unstretched material as measured with the micrometer were consistently 12 percent less than the gauge equipped with a 3-oz. counter weight which is widely used in industrial work on rubber.

The samples being studied were mounted on metallic supporting frames placed in such a way that the radiation passed through parts of the

* Note: Comparison of the observed spectra with transmission curves published by Stair and Coblentz revealed no bands other than those present in the pure hydrocarbon except for weak bands in the regions where oxidation products produce absorption. The maximum linear extension obtainable was 6.5 times the original length as compared with 9 to 10 times the original length for unvulcanized material. The maximum radial extension was 3.5 times the original diameter.

sample remote from the points of support. The spectrometer used was a rocksalt prism instrument of the Littrow type and has been described by Nielsen and Smith.[7]

The results obtained are indicated in Fig. 1. Curve *A* represents the percent transmission of a single layer of unstretched rubber. This curve is similar to the transmission curves published by Stair and Coblentz except for a strong band near 9.5μ and weak bands at 6μ and 3μ produced by oxidation. It should be noted that the transmission is low at short wave-lengths even in regions where there are no strong characteristic absorption bands. Curve *B* shows the transmission of a sample stretched linearly to five times its original length. It will be observed that the positions of the major absorption bands remain unchanged except in the case of the strong band near 11.9μ, which has shifted to shorter wave-lengths and has become asymmetrical in shape. Curve *C* gives the transmission of a sample stretched radially to three times its original diameter. In order to obtain measurable absorption in the minor bands, it was necessary to place two sheets in the light beam. Hence, in curve *C* the decreases in transmission due to reflection are exaggerated. The positions of the absorption bands in curve *C* are the same as in curve *A* within the limits of ex-

[7] J. Rud Nielsen and D. Smith, Ind. Eng. Chem. **15**, 609 (1943).

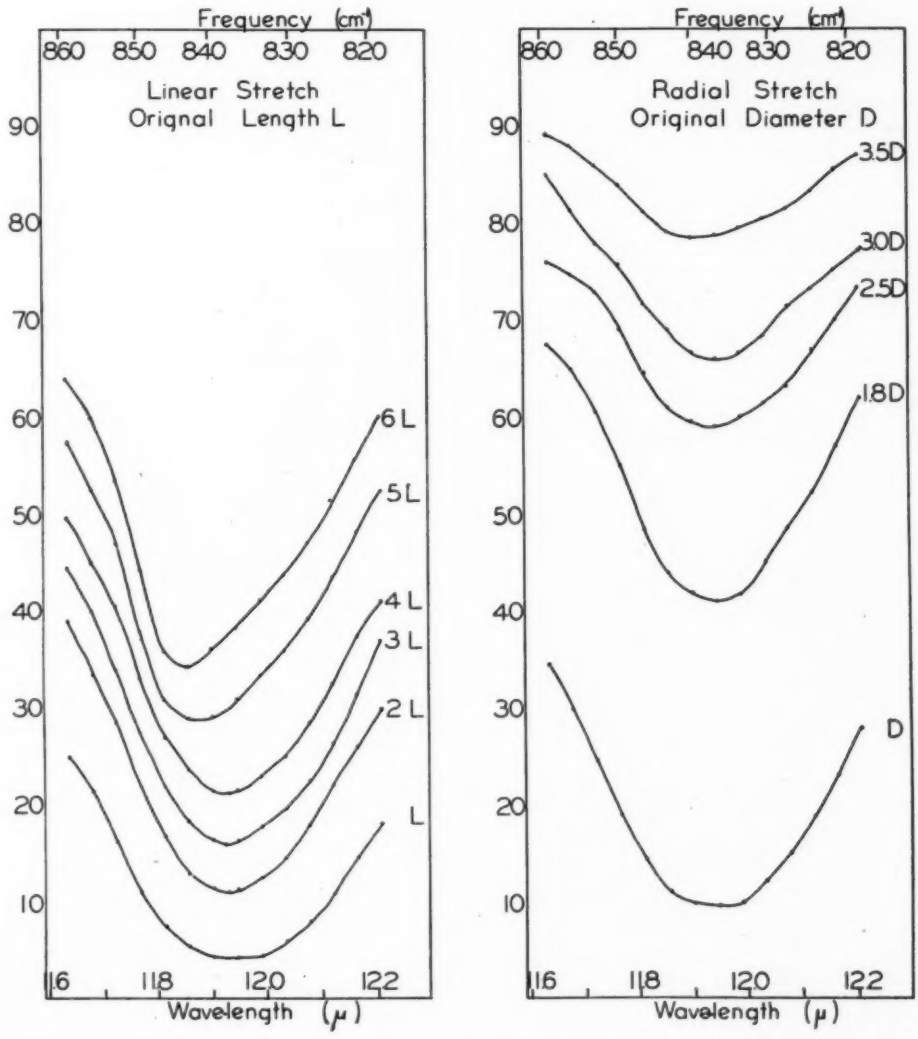

FIG. 2. The transmission of rubber in the region of 11.9μ under various conditions of stretch.

perimental error. Although the band near 11.9μ is slightly asymmetrical, the magnitude of the shift to shorter wave-lengths is not appreciably greater than the experimental error encountered in locating absorption maxima.

In order to determine the position of the 11.9μ band as a function of stretch, this region was carefully studied for samples stretched linearly by various amounts up to 6 times the original length and radially up to 3.5 times the original diameter. Typical results are shown in Fig. 2. It will be noted that in the case of linear stretch the position of the band is not changed appreciably until the sample has been stretched to 4 times its original length but changes position rapidly as greater elongations are attained. As linear stretch of the sample increases, the band becomes more and more asymmetrical. The curves for radial stretch indicate changes in band shape but very little shift in the position of maximum absorption.

In order to determine the changes in absorption coefficient with changing conditions of stretch, transmission measurements were made at the positions of maximum absorption in the 3.3-μ, 6.9-μ, 7.3-μ, and 11.9-μ bands. These percent transmission measurements were then plotted on a semilogarithmic scale as a function of thickness. These plots may be interpreted from Lambert's Law:

$$I=(1-R)I_0 10^{-\alpha t}, \qquad (1)$$

where I_0 and I are the intensities of the incident and transmitted radiation, respectively, R is the reflection coefficient, and α is the absorption coefficient, which includes true absorption and body scattering. This relation can also be written in the following logarithmic form:

$$\log (I/I_0)=\log T=\log (1-R)-\alpha t, \qquad (2)$$

where T is the transmission. From Eq. (2) it can be seen that a semilogarithmic plot of transmission as a function of thickness should be a

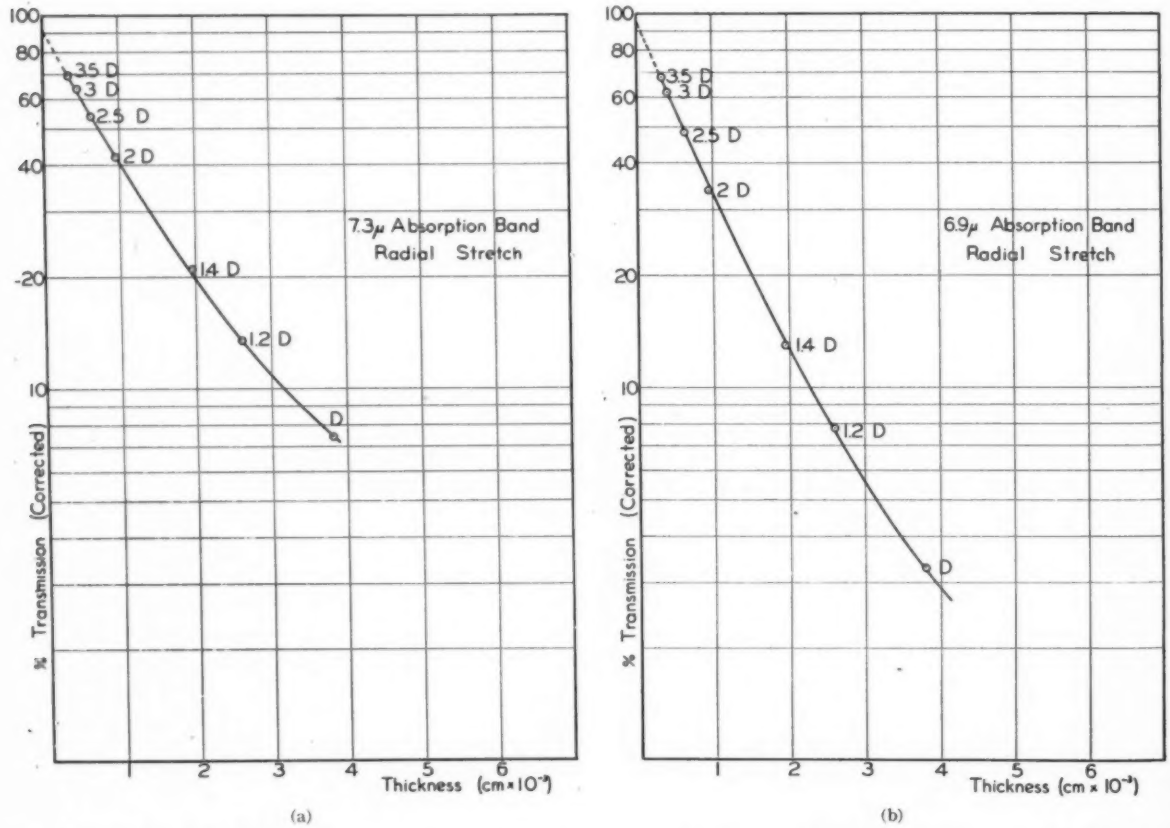

FIG. 3. The effects of radial stretch on the transmission of rubber in the 6.9-μ and 7.3-μ regions. Transmission is plotted as a function of thickness; the conditions of stretch are indicated at the points on the curve.

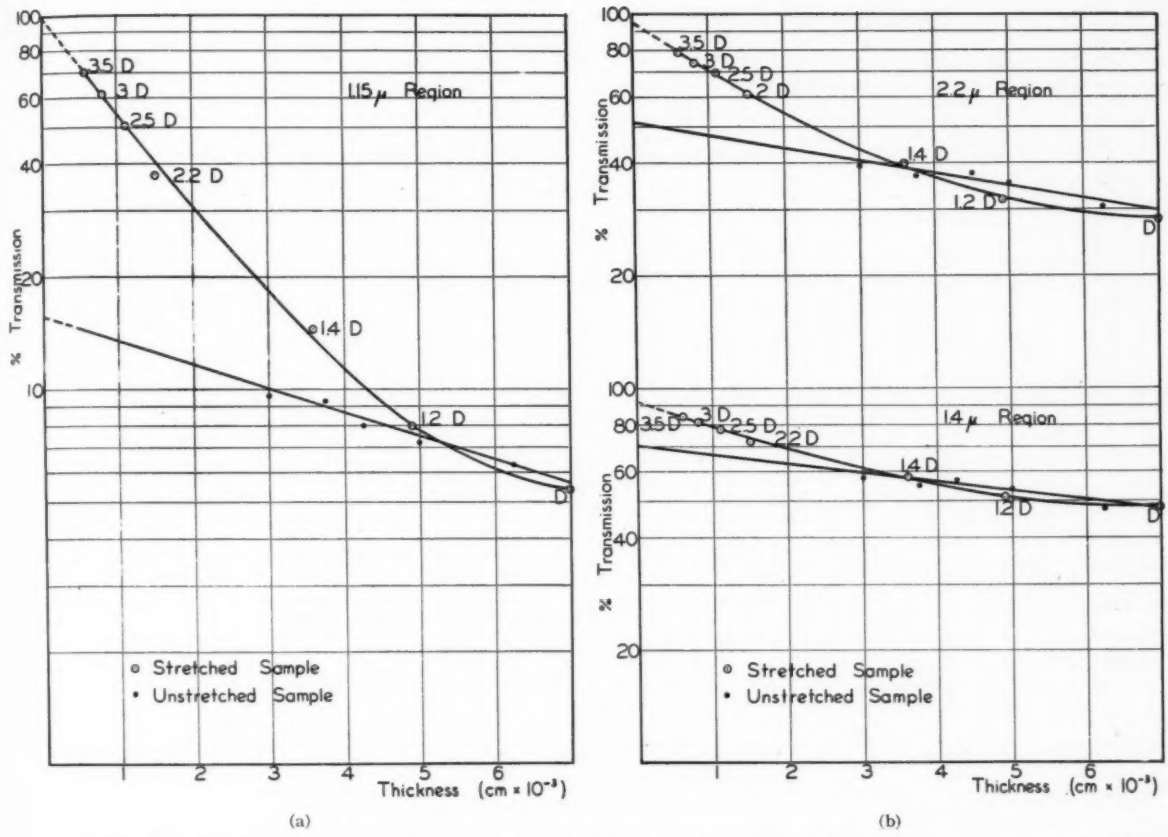

FIG. 4. The effects of radial stretch on the transmission of rubber in regions remote from strong absorption bands. Transmission is plotted as a function of thickness; the conditions of stretch are indicated at the points on curve. The region indicated as 1.4μ at the center of part (b) should be 4.1μ instead.

straight line if Lambert's law is obeyed; the negative slope is equal to the absorption coefficient and the intercept on the log T axis gives a measure of the reflection coefficient.

It was found that the plots actually obtained were not straight lines even after the data had been corrected for stray radiation.* Typical plots for two bands are shown in Fig. 3. The observed curvature can be explained if the absorption coefficient increases and the reflection coefficient decreases as the sample is stretched. The absorption coefficient at a given elongation can be obtained graphically by finding the slope of the tangent drawn at the appropriate point; the reflection coefficient can be determined from the intercept of the tangent. Whether the observed increase in the absorption coefficient is caused by an increase in true absorption or by an increase in body scattering cannot be determined, but the indications are that the increase is due to increased body scattering, since the plots for all bands studied show the same type of curvature.

Unfortunately the accuracy with which percentage transmission can be determined is only about 1 percent. In the graphical determination of absorption coefficients this inaccuracy introduces large errors when the transmission is low. Hence, the measured values of the absorption and reflection coefficients given in Table I for the strong absorption bands are not very accurate. It

* Note: The corrected percent transmission T was obtained from the observed percent transmission T' by means of the following relation: $T=T'-(C_1-C_0T')$ where C_1 is the percent of stray radiation transmitted by the rubber and C_0 the percent of stray radiation in the incident beam. The relation holds for small values of C_1 and C_0. The magnitudes of the corrections were obtained by measuring the percent transmission at the flat bottoms of absorption bands produced by samples so thick that true transmission was negligible. Thick rubber samples were used to find C_1 and thick cells containing hydrocarbons were used to determine C_0. This value of C_0 is not an exact measure of the total stray radiation, but the values are applicable since rubber is a hydrocarbon.

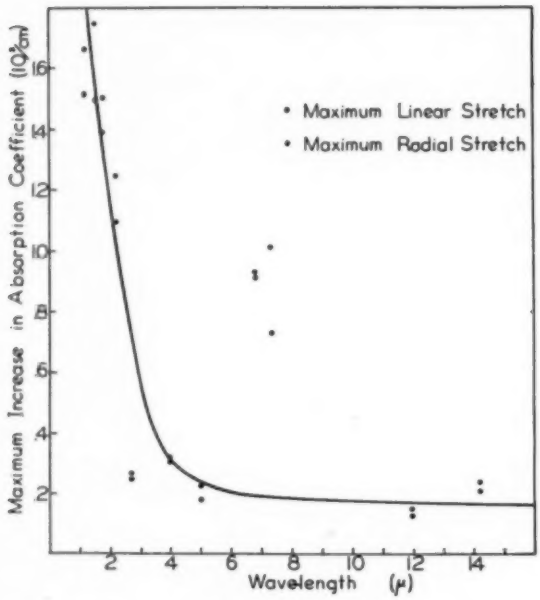

FIG. 5. The increase in the absorption coefficient of rubber produced by stretching. The increases are plotted as a function of wave-length.

will be noted that for all bands studied the absorption coefficients increase and the reflection coefficients decrease with increasing stretch.

In order to estimate the part of the increased absorption arising from body scattering, measurements were made at various wave-lengths far from strong absorption bands. Typical results are shown in Fig. 4. Since the transmission is high in these regions, the errors in the absorption coefficient produced by errors in transmission measurement are small. It will be seen from Fig. 4 that the changes in both α and R are greatest at short wave-lengths and become extremely small at long wave-lengths.

Figure 5 gives a graphical presentation of the observed changes in α as a function of wave-length, and Fig. 6 shows the changes in R as a function of wave-length. It will be noted that most of the points on these graphs fall near the smooth curves except the changes in α for the bands at 6.9μ and 7.3μ. It is difficult to say whether the great changes observed at these wave-lengths are due to actual increases in true absorption or to experimental errors in determining the low transmissions at the center of these bands.

TABLE I. Absorption and reflection coefficients for characteristic absorption bands.

Band	Absorption coefficient			Reflection coefficient		
	Unstretched	Max. linear extension	Max. radial extension	Unstretched	Max. linear stretch	Max. radial stretch
3.3μ	—*	7.7×10^3 cm^{-1}	9.2×10^3 cm^{-1}	—*	10%	10%
6.9	3.6×10^3 cm^{-1}	4.6	4.6	30%	9	6
7.3	2.6	3.6	3.3	34	9	12
11.9	2.4	2.6	2.8	20	5	6

* The sample was too thick for the determination of these coefficients.

DISCUSSION OF RESULTS

A qualitative interpretation of the results of this study can be made in terms of the recent theories of rubber structure advanced by Wall[8] and by James and Guth.[9] From a consideration of the familiar properties of rubber these authors conclude that in the lightly vulcanized state it consists of a coherent network of flexible hydrocarbon chains composed of independent C−C and C=C links of fixed length together with other molecules not actively involved in the network but acting like a fluid through which the network extends and in which the chains move

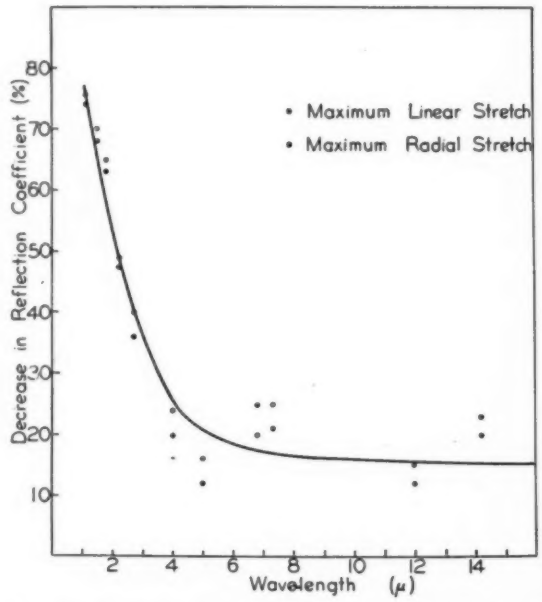

FIG. 6. The decrease in the reflection coefficient of rubber produced by stretching. The decreases are plotted as a function of wave-length.

[8] F. T. Wall, J. Chem. Phys. **10**, 132 (1942); *ibid.* **10**, 485 (1942); *ibid.* **11**, 527 (1943).

[9] H. M. James and E. Guth, Ind. Eng. Chem. **33**, 624 (1941); *ibid.* **10**, 485 (1943); J. Chem. Phys. **11**, 455 (1943).

with Brownian motion. It is estimated that approximately one-fourth of the molecules are involved in the network.

According to James and Guth, the structural elements of rubber must be different from those of normal solids in which bonds of electrostatic, chemical, or van der Waals type connect atoms and molecules into a definite, rigid three-dimensional structure. The large extensibility suggests a more open type of structure. The small forces required to produce large extension in the early stages of stretch suggest that the elastic restoring forces cannot be of the types listed above but may be explained in terms of flexible chains. Extensions to as much as four times the original length do not appreciably alter interatomic distances in the chains. Only for large extensions at which rubber begins to crystallize or approaches the breaking point do the chemical bonds between carbon atoms come into play. However, at maximum extension these chemical bonds do appear to contribute to the tensile strength of rubber, which (if computed with respect to the cross section at the breaking point) is almost equal to that of copper.

Upward curvature of the stress-strain curve for the rubber used in the present work sets in when the length of the sample is approximately four times the original length. This curvature is explained according to James' theory as due to the gradual approach of the molecular network to its maximum extension, which for the material used was six and one-half times its length in the unstretched state. It will be recalled that for extensions above four times the original length the band near 11.9μ began to shift toward shorter wave-lengths. This band has been observed in the spectra of many hydrocarbons and has been attributed to the fundamental vibration of the C$-$C group. Hence, the observed changes can be interpreted as arising from changes in the characteristic frequency of this group. These changes set in at the stage of extension where strains would be expected to begin in the individual links in the hydrocarbon chain. The asymmetrical shape of the band may possibly be caused by the fact that the C$-$C groups in molecules not involved in the network are subjected to stresses of a different type from that experienced by the C$-$C groups in the network; hence their vibrational frequencies would probably be different. The existence of slightly different C$-$C frequencies would generally produce an asymmetrical absorption band. As no changes were observed in the 6-μ region where the C$=$C group has an absorption band, it is concluded that the effects of strains on this group are not as great as in the case of the C$-$C group.

The observed increases in the absorption coefficient can be explained as arising from scattering by the crystalline lattices formed when maximum elongation is approached. The observed relationship between change in absorption coefficient and wave-length would tend to support this interpretation. Scattering by these crystal lattices would be of the type treated by Einstein[10] in his theory of scattering in dense media. From this relation the average crystal size could be calculated from the data obtained if the refractive indices of the crystal and matrix material were known. It would be interesting to test the hypothesis of scattering by crystals by measuring the transmission of stretched samples of synthetic rubber substitutes. Some of these show evidence of crystallization and others do not. The only indications of a change in true absorption were in the 6.9- and 7.3-μ bands. It is felt that this observed effect is probably due to experimental error in determining transmissions at the bottom of these strong bands or in an error in the correction for stray radiation.

The decreases in reflection coefficient are readily explained as being due to decreases in surface irregularities accompanying stretch. The variation of this change with wave-length is in agreement with this explanation and observation of the reflection of visible light at various angles of incidence affords additional confirmation.

The writers wish to express their appreciation to Professor J. Rud Nielsen for his criticism of the manuscript and to Miss Annette Herald for the preparation of the figures.

[10] A. Einstein, Ann. d. Physik **33**, 1275 (1910).

Poisson's Ratio at High Temperatures

By

F. L. Everett
University of Michigan, Ann Arbor, Michigan

and

Julius Miklowitz
Westinghouse Research Laboratories, East Pittsburgh, Pennsylvania

(Received June 5, 1944)

A method is presented whereby both the modulus of elasticity in tension and compression E and the modulus of elasticity in shear G may be obtained simultaneously from a simple test on a cantilever specimen subjected to combined bending and twist. By means of the relation $\nu=(E/2G)-1$, values of Poisson's ratio at various temperatures from ambient to 1000°F were obtained for five common steels.

I. INTRODUCTION

In recent years, the need for more information on the elastic properties of the ordinary steels at temperatures above ambient conditions has been pointed out. Unfortunately, statically obtained information along these lines exists in only a limited amount. The available data are confined to several references in the technical literature.[1]

In this investigation* an attempt was made to devise a simple test on one specimen which would yield simultaneously both the modulus of elasticity in tension and compression E and the modulus of elasticity in shear G. The moduli were obtained by subjecting a small cantilever rod of uniform circular cross section to combined bending and torsion, and measuring separately the deformations due to each. From the relation $\nu=(E/2G)-1$, a true value of Poisson's ratio would follow. The ultimate objective of the investigation was to determine the variations of Poisson's ratio values of five common steels in the range of temperatures from ambient to 1000°F. The variables of temperature, non-uniformity of the test specimen, manipulation, and others were minimized.

II. SPECIMEN, APPARATUS, AND METHOD

The five S.A.E. steel specimens were rods $\frac{5}{16}$ of an inch in diameter. The composition of each specimen is given in Table I.

The cantilever specimen was both bent and twisted by a single force applied as a dead weight at the end of a 6-inch torque arm which was connected to the free end of the cantilever specimen. A diagrammatic sketch is shown in Fig. 1.

The entire specimen was subjected to combined bending and torsion. The application of a load to

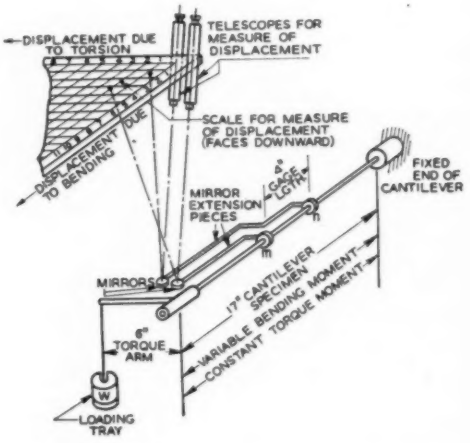

Fig. 1. Diagrammatic sketch of apparatus.

[1] (*a*) F. C. Lea and O. H. Crowther, Engineering **98**, 487 (1914).
(*b*) C. Bach and R. Baumann, *Festigkeit seigenschaften und Gefügebilder der konstruktionsmaterialien* (Springer, Berlin, 1921).
(*c*) F. C. Lea, Engineering **43**, 829 (1922).
(*d*) F. L. Everett, Trans. A.S.M.E. **53**, 117 (1931).
(*e*) E. Honegger, The Brown Boveri Review **19**, 143 (1923).
(*f*) G. L. Verse, Trans. A.S.M.E. **57**, 1 (1935).

* The work of this investigation was carried out at the University of Michigan in the year of 1942.

TABLE I. Composition of steels tested.

Type of steel	Composition (%) C	Mn	Si	P	S	Ni	Cr
S.A.E. 1095	0.9 –1.05	0.25–0.50	0.1–0.5	0.04	0.04	—	—
S.A.E. 5140	0.35–0.45	0.6–0.9	—	0.04	0.05	—	0.8 –1.1
S.A.E. 3340	0.35–0.45	0.3–0.6	—	0.04	0.05	3.25–3.75	1.25–1.75
S.A.E. 1020 (hot rolled)	0.15–0.25	0.3–0.6	—	0.045	0.05	—	—
S.A.E. 1020 (cold rolled)	0.15–0.25	0.3–0.6	—	0.045	0.05	—	—

the end of the torque arm caused relative displacement of two kinds to any two cross sections, m and n. The constant torque moment caused relative rotation around the axis of the specimen and the variable bending moment produced relative rotation about a locus of points[2] outside of the specimen in a plane containing the axis. The object of these experiments was to determine these two relative rotations under various conditions of temperature and amount of loading.

Loading and unloading was accomplished by means of a loading tray which hung from the end of the torque arm. Loads in amounts of 100 and 200 grams were placed on the tray. The maximum total load in any case did not exceed 2400 grams.

The measurements of angular rotations were made by mirrors connected to the end points of the gauge length mn. Extensions were necessary to bring the mirrors outside of the electric furnace

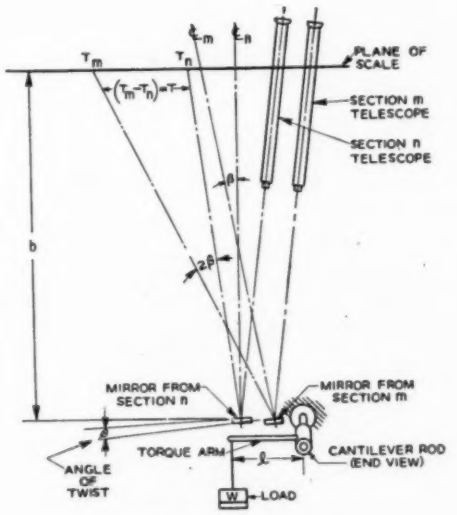

FIG. 2. Torsion problem.

[2] The points are the centers of curvature corresponding to the bending moments within the gauge length mn.

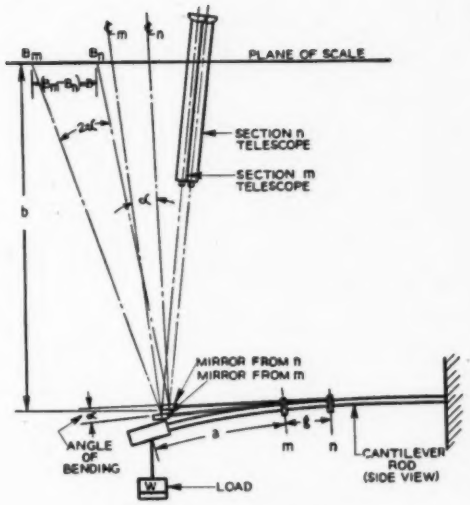

FIG. 3. Bending problem.

which surrounded the specimen and supplied the heat. The temperature was automatically controlled and held constant within $\pm 2°F$ for one hour before as well as during each experiment. A telescope was focused on each mirror and back on to a special two-dimensional scale consisting of graph paper which was suspended in a horizontal plane approximately $4\frac{1}{2}$ feet above the mirrors. Torsion of the rod caused readings on the graph paper in a direction perpendicular to the axis of the specimen, and bending produced readings in the direction parallel to the axis of the specimen. The torsion permitted the determination of the modulus of elasticity in shear G; and the bending, the modulus of elasticity in tension and compression E.

Dividing the problem into its elementary parts, torsion and bending, a simple sketch may be shown for each, as in Figs. 2 and 3.

The value of the modulus of elasticity in shear is found by use of the principles of the strength of materials. Referring to Fig. 2,

$$\beta = Wlg/GI_p, \qquad (1)$$

where β is the angle of twist for gauge length g, l is the torque arm, W the load, I_p the polar moment of inertia of a circular rod, and G the modulus of elasticity in shear. Since l, g, and I_p are all constants, we may write (1) as

$$G = K_1(W/\beta). \qquad (2)$$

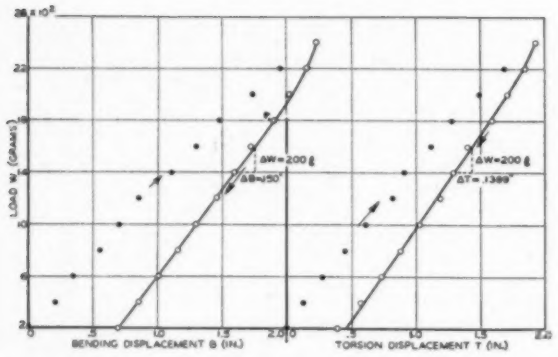

FIG. 4. Load-displacement curves for S.A.E. 1095 steel at 800°F.

We may also write as a close approximation

$$\beta = T/2b, \tag{3}$$

where T is the torsion scale reading corresponding to an angle of twist β, and b is the average vertical distance from the mirrors to the graphic scale.

The small change in b due to the deflection of the mirrors may be neglected. Therefore, considering b a constant and substituting (3) in (2), we have

$$G = K_2(W/T), \tag{4}$$

which may be written as

$$G = K_2(\Delta W/\Delta T). \tag{5}$$

From the load-torsion displacement curves a value for the modulus of elasticity in shear can be obtained with the use of Eq. (5).

The modulus of elasticity in tension and compression is found similarly (see Fig. 3). We have

$$\alpha = \frac{W(a+g)^2}{2EI} - \frac{Wa^2}{2EI} = \frac{Wg(g+2a)}{2EI}, \tag{6}$$

where α is the angle of bending for gauge length g, a the forelength of rod, W the load, I the moment of inertia about the neutral axis of the cantilever specimen, and E the modulus of elasticity in tension and compression. Since a, g, and I are all constants, we may write (6) as

$$E = K_3(W/\alpha). \tag{7}$$

By former reasoning we arrive at the following:

$$E = K_4(\Delta W/\Delta B), \tag{8}$$

where B is the bending scale reading corresponding to an angle of rotation due to bending, α. From the load-bending displacement curves a value for the modulus of elasticity in tension and compression can be obtained with the use of Eq. (8).

At constant temperatures of ambient, 200, 400, 600, 800, and 1000 degrees Fahrenheit, tests were run on each of the five different steels to obtain moduli values. The 800° and 1000°F tests were made by increasing the load on the specimen by equal increments and observing the readings of the rotation due to twist and that due to bending until noticeable creep occurred. The rod was then unloaded using the same small increments as before. Upon unloading, creep persisted for several readings only, and then became negligible, as evidenced by the fact that, upon plotting the data, a straight line resulted. This method of utilizing the data on unloading rather than on loading so as to eliminate the serious effect of

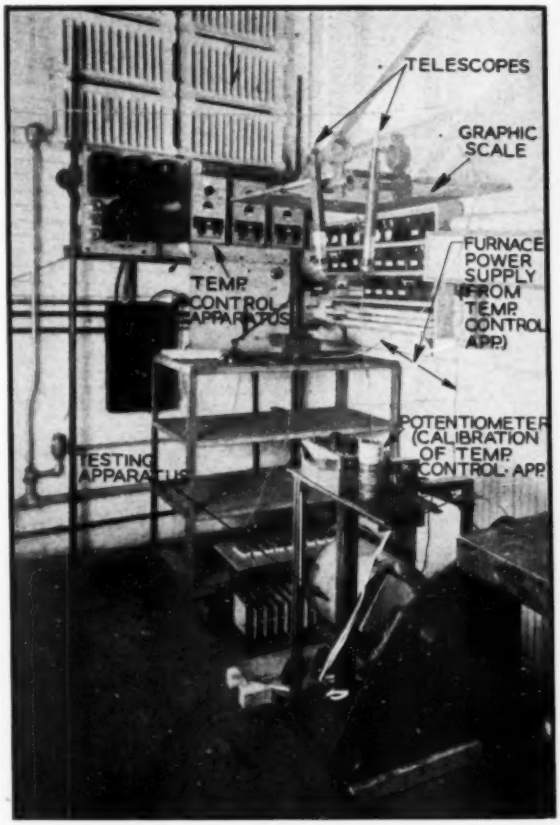

FIG. 5. Entire apparatus.

creep in obtaining the true values of the moduli was originally reported by one of the authors in an earlier paper[3] and was utilized in further experiments by G. L. Verse.[4]

In the 600°, 400°, 200°F and ambient temperature tests a similar procedure was used. Considerably less creep was evidenced; however, data on unloading only were considered to be reliable for establishing the values of the moduli. At each temperature the data for both moduli of a specific steel were plotted. Figure 4 shows a plot of load-displacement data of the 800°F test made on the S.A.E. 1095 steel. These curves are typical plots of the load-displacement data of this investigation. The slopes of the unloading curves in all cases, multiplied by the appropriate constants as given by Eqs. (5) and (8) above, gave the values of the two moduli.

From the values of the moduli a value for Poisson's ratio at each temperature was derived from the equation $\nu=(E/2G)-1$.

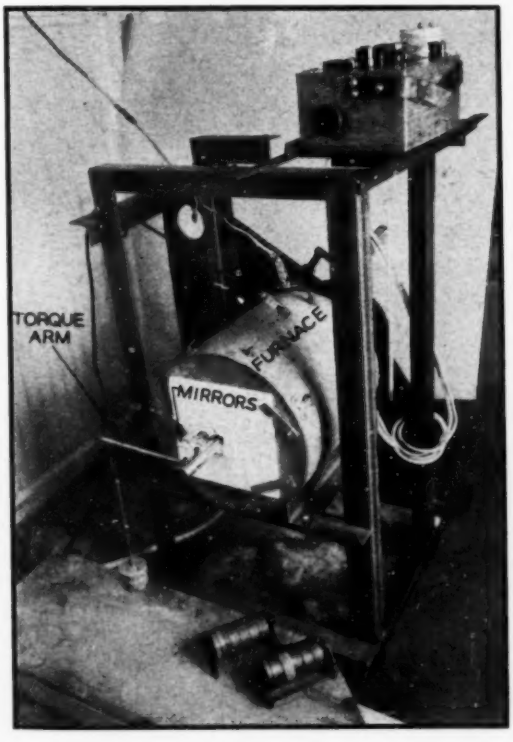

FIG. 6. Testing apparatus.

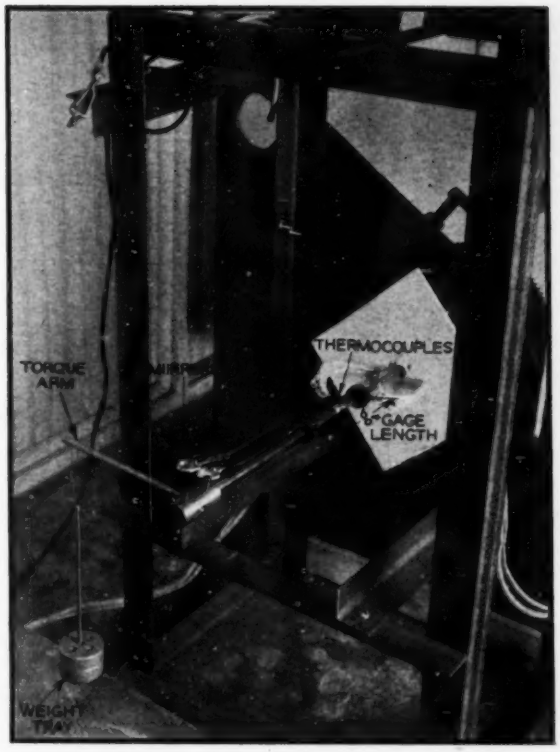

FIG. 7. The cantilever specimen.

The accuracy of obtaining Poisson's ratio by this method has been considered. When the relation

$$\nu=(E/2G)-1=(E-2G)/2G \tag{9}$$

is differentiated we have

$$d\nu=(dE/2G)-(EdG/2G^2). \tag{10}$$

Dividing (10) by (9) we have

$$\frac{d\nu}{\nu}=\frac{E}{E-2G}\left[\frac{dE}{E}-\frac{dG}{G}\right]. \tag{11}$$

From relation (11) it is seen that errors of like sign in measuring both E and G tend to cancel each other, while errors of unlike sign add, and when multiplied by the factor $E/(E-2G)$ might make an appreciable error in ν. There is no reason to believe that errors in measuring E and G were of unlike sign. The large magnification of the rotations due to bending and twist helps to make the readings accurate; the distance of the mirrors from the graphic scale was approximately 53 inches. The authors believe that the values for

[3] See reference 1(*d*).
[4] See reference 1(*f*).

Poisson's ratio found in this investigation are reliable within a fair degree of accuracy.

Figures 5–7 are pictures of the apparatus.

III. TEST RESULTS

Table II presents the final results of the moduli of tension and compression and of shear, and the derived values of Poisson's ratio. As stated previously, only data on unloading were used in calculating the moduli since creep may be considered negligible over the major portion of the unloading curve.

TABLE II. Tabulated results.

Temperature °F	Steel	E	G	P.R.(ν)
	S.A.E. 5140	30.35*	11.20*	0.355
	3340	29.75	11.30	.315
Ambient	1020 h.r.	29.80	11.33	.313
	1020 c.r.	29.20	11.35	.286
	1095	29.90	11.55	.295
	5140	29.90	11.06	.353
	3340	29.40	11.12	.320
200	1020 h.r.	29.40	10.90	.348
	1020 c.r.	29.18	11.00	.326
	1095	29.65	11.45	.297
	5140	30.40	10.50	.447
	3340	28.75	10.07	.425
400	1020 h.r.	28.95	10.45	.384
	1020 c.r.	28.60	10.36	.380
	1095	29.90	10.97	.362
	5140	29.40	9.72	.510**
	3340	28.35	9.65	.470
600	1020 h.r.	26.85	9.89	.358
	1020 c.r.	27.87	9.97	.398
	1095	28.20	10.11	.394
	5140	28.80	9.46	.520**
	3340	24.97	9.07	.376
800	1020 h.r.	26.15	9.33	.400
	1020 c.r.	26.30	9.53	.380
	1095	23.95	8.62	.389
	5140	24.90	8.23	.513**
	3340	23.30	8.34	.397
1000	1020 h.r.	22.90	7.90	.450
	1020 c.r.	18.76	6.50	.440
	1095	17.95	5.98	.500

* $\times 10^6$ lb./in.^{2}

** Slightly above maximum value for Poisson's ratio.

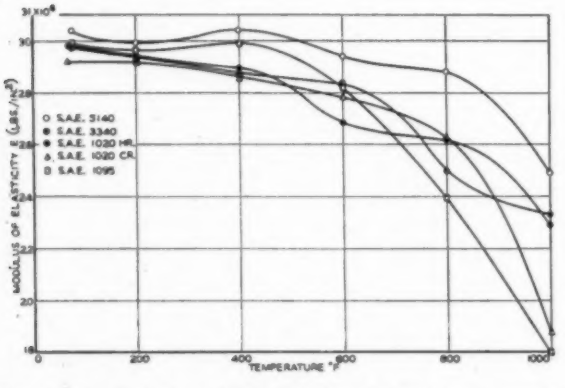

FIG. 8. The variation of the modulus of elasticity in tension and compression E with temperature.

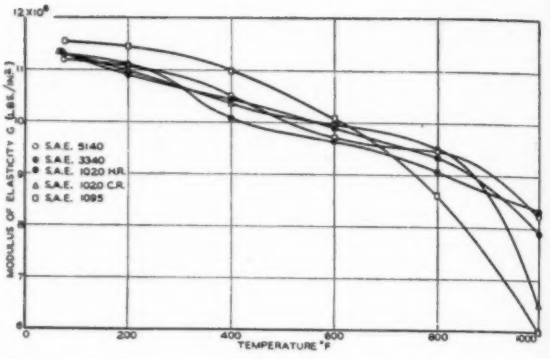

FIG. 9. The variation of the modulus of elasticity in shear G with temperature.

The values of the modulus of elasticity in tension and compression are plotted against their respective temperatures in Fig. 8. The major changes in E values occur after 400°F, the S.A.E. 1095 steel showing an 18×10^6 lb./in.^{2} modulus at 1000°F. The S.A.E. 5140 steel maintains its rigidity better than the other steels throughout the temperature range. This may be expected since the 5140 steel is commonly known as a high temperature alloy. The S.A.E. 1020 hot-rolled steel maintains its rigidity surprisingly well at the higher temperatures; its modulus drops to 22.9 $\times10^6$ lb./in.^{2} at 1000°F. The modulus of the S.A.E. 3340 steel drops suddenly at 600°F, but the drop is cut at 800°F; the final value (at 1000°F) being 23.3×10^6 lb./in.^{2}.

The values of the modulus of elasticity in shear are plotted against their respective temperatures in Fig. 9. The curves exhibit many similar trends. Immediate drop of the modulus G occurs with an increase of temperature. The S.A.E. 1095 and cold-rolled steel again show the lowest values at 1000°F. The hot-rolled steel again demonstrates its ability to keep its rigidity at high temperatures. The high temperature steels (S.A.E. 3340 and S.A.E. 5140) have the highest values of G at 1000°F: 8.3 and 8.2×10^6 lb./in.^{2}, respectively.

Figure 10 shows the variation of the derived Poisson's ratio with temperature of each steel

TABLE III. Comparison of modulus E values.

Temp.	S.A.E. 1020 hot-rolled	Bach & Baumann[a] mild steel	Lea[b] mild steel	Verse[c] 0.43% carbon steel	S.A.E. 1095	Bach & Baumann[a] carbon steel	Lea[b] high (0.95%) carbon steel
20 °C	29.8*	29.9	29.3	29.9	29.9	29.5	28.4
100	29.4	29.4	—	29.0	29.6	29.0	26.3
200	29.0	28.0	28.2	28.0	29.9	28.3	23.4
300	27.1	27.2	27.2	26.5	28.6	27.2	21.6
400	26.2	26.5	—	24.6	25.0	26.1	17.8
500	24.6	(20.1)	18.7	21.8	20.1	(21.8)	

[a] See reference 1(*b*).
[b] See reference 1(*c*).
[c] See reference 1(*f*).
* $\times 10^6$ lb./in.^{2}.

TABLE IV. Comparison of modulus G values.

Temp.	S.A.E. 1020 hot-rolled	S.A.E. 1020 cold-rolled	Everett[a] 0.34% C steel	Verse[b] 0.34% C steel	Lea[c] mild steel
70°F	11.3*	11.4	11.5	11.5	12.4
200	10.9	11.0	11.5	11.4	12.1
400	10.5	10.4	11.4	11.3	11.8
600	9.9	10.0	11.0	10.8	11.3
800	9.3	9.5	9.7	9.6	10.5
1000	7.9	6.5	6.2**	6.6**	9.0**

[a] See reference 1(*d*).
[b] See reference 1(*f*).
[c] See reference 1(*c*).
* $\times 10^6$ lb./in.^{2}.
** Extrapolated from curves.

tested. The resulting curves are irregular but show many similar trends. There is a definite increase of Poisson's ratio at the higher temperatures in all cases: This means that as the temperature rises the percentage decrease of the modulus in shear is greater than that of the modulus in tension and compression. There is no appreciable change in Poisson's ratio between ambient temperature and 200°F, for the S.A.E. 5140, S.A.E. 3340, and S.A.E. 1095 steels. The two S.A.E. 1020 specimens show a slight increase in Poisson's ratio over the same range. From 200° to 400°F there is a large increase for all steels; and, with the exception of the S.A.E. 1020 hot-rolled steel, Poisson's ratio continues to increase up to 600°F. From 600° to 800°F, the S.A.E. 3340, S.A.E. 1020 cold-rolled, and S.A.E. 1095 steels show a decrease in Poisson's ratio; the same steels show an increase from 800° to 1000°F. In the case of the two S.A.E. 1020 specimens and the S.A.E. 1095, Poisson's ratio reaches a maximum value at 1000°F; for the S.A.E. 3340 and S.A.E. 5140 steels, the maximum values are at 600° and 800°F, respectively.

From the strength of materials it can be shown that 0.5 is the maximum value of Poisson's ratio for isotropic materials. The dotted portion of the S.A.E. 5140 steel curve has been so designated since it lies above the limiting value of Poisson's ratio.

From 800°F on, the curves approach the limiting value which seems logical since in the plastic state Poisson's ratio is 0.5.

For the purpose of comparison, values taken from some of the works quoted in an earlier part of this paper[5] have been collected and are presented in Tables III and IV. With the exception of the results shown in the last columns

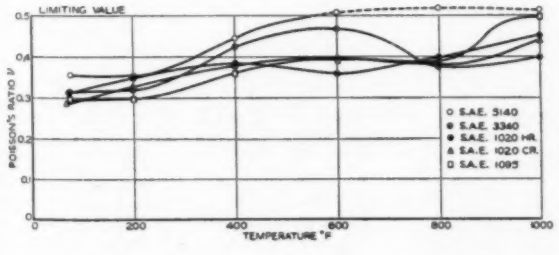

FIG. 10. The variation of Poisson's ratio ν with temperature.

[5] See reference 1.

of Tables III and IV, reasonably good agreement between the values given by the various experimenters is evidenced.

The encouragement given by Dr. A. Nadai of the Westinghouse Research Laboratories and by the Horace A. Rackham School for Graduate Studies, University of Michigan, is duly acknowledged. The authors also appreciate the help received at the Westinghouse Research Laboratories in the preparation of this paper.

A Numerical Method in the Theory of Vibrating Bodies

ANDREW VAZSONYI
Graduate School of Engineering, Harvard University, Cambridge, Massachusetts

(Received May 25, 1944)

In this paper a numerical method is presented for the determination of the characteristic numbers and modes of vibrating (conservative) systems. The method for continuous bodies is based on a finite difference approximation and is a "relaxation method" in the same sense as the term is used by R. V. Southwell. No claim is made of theoretical advancement in the subject; the paper purports to present a thoroughly practical method of obtaining numerical answers speedily. Detailed computations are carried out for the transverse vibrations of a quadrangular elastic membrane. The nature of the method is such that it can be easily extended to other vibrating systems of finite or infinite number of degrees of freedom. It is to be emphasized that the quadrangular shape is just a simple example; the real strength of the method lies in the fact that numerical results can be obtained for bodies with more complicated and irregular boundaries.

INTRODUCTION

THE two most successful procedures for obtaining numerical results in the study of vibrating bodies are the variational methods and the perturbation methods. These widely used "analytical" computational procedures are very powerful indeed so long as the bodies are simple in their shape, but fail in the case of complicated shapes because of the prohibitive amount of numerical work involved. To meet these circumstances the method of finite differences was developed by several authors.[1–4] The practical value of these attractive "non-analytical" computational procedures was strongly limited by the amount of numerical work involved in the solution of the difference equations. Recently this situation was remedied by the entirely new outlook of R. V. Southwell,[5] whose relaxation technique transforms the method of finite differences into a very powerful and thoroughly practical numerical procedure. Among other problems, Southwell has successfully attacked the equations of vibrating bodies with finite number of degrees of freedom, and also of one-dimensional continuous bodies.

Southwell's method could be easily extended to two-dimensional bodies also, but we prefer to present an entirely different technique which seems superior to that of Southwell's, both for systems of finite or of infinite number of degrees of freedom. It should not be at all surprising that such alternatives exist within the frame of the relaxation method, and a comparison is made between the two procedures when treating forced vibrations (see Section 8).

[1] R. von Mises and H. P. Geiringer, Zeits. f. angew. Math. u. Mech. **9**, 58–77, 152–164 (1929).
[2] F. Bleich and E. Melan, *Die Gewöhnlichen und Partiellen Differenzengleichungen der Baustatik* (Julius Springer, Berlin and Wien, 1927).
[3] G. E. Kimball and G. H. Shortley, Phys. Rev. **45**, 815–820 (1934).
[4] R. H. Bolt, Phys. Rev. **57**, 1057A (1940).
[5] R. V. Southwell, *Relaxation Methods in Engineering Science* (The Clarendon Press, Oxford, 1940).

It is aside from our purpose to give a general evaluation of the relaxation method;[6] we wish only to emphasize its extraordinary speed. In the case of the transverse vibration of a square membrane, the analytical solution is known and can be compared with the one obtained by our method (see Fig. 10), whereby 5 percent accuracy was obtained in 12 minutes, 1.2 percent accuracy required $2\frac{1}{2}$ hours.

It would be foolish to believe that any method exists which is best suited for every problem and undoubtedly there are many problems where the analytical procedure is the attractive one. However, the reader who takes pains and works out an actual numerical example will readily see where the superiority of the non-analytical approach lies.

1. RECAPITULATION OF THE THEORY OF THE VIBRATING MEMBRANE[7]

The equation of motion of the free vibrations of an elastic membrane is given by

$$S\left(\frac{\partial^2 U}{\partial X^2}+\frac{\partial^2 U}{\partial Y^2}\right)-m\frac{\partial^2 U}{\partial t^2}\equiv S\Delta U-m\frac{\partial^2 U}{\partial t^2}=0. \quad (1)$$

With respect to the boundary conditions, let us assume that

$$U=0 \text{ on } C. \quad (2)$$

The theory of vibrations is based on the study of the natural modes, i.e., solutions of Eq. (1) for which

$$U=V\sin(\omega t+\alpha), \quad (3)$$

where V is independent of time, i.e., V is a space variable. These solutions are synchronized in the sense that the whole membrane vibrates without changing its shape. Putting Eq. (3) into the equation of motion (1), we get the differential equation of the natural modes:

$$S\Delta V-m\omega^2 V=0. \quad (4)$$

Now we introduce the dimensionless variables

$$x=X/l, \quad y=Y/l, \quad a=A/l^2,$$
$$\lambda=A\omega^2(m/S), \quad v=V/D,$$

and get

$$\Delta v+(\lambda/a)v=0. \quad (5)$$

The advantage of the dimensionless Eq. (5) is that the numerical value of λ depends only on the shape of the membrane and not on the size, tension, etc.

The theory of vibrations tells us that Eq. (5) together with the boundary condition (2) cannot be satisfied for any arbitrary value of λ, but that on the contrary there exists an infinite sequence $\lambda_1\leqslant\lambda_2\leqslant\lambda_3\cdots$ of values of λ for which the equation can be solved. These λ's are called the characteristic values, the corresponding solutions $v_1, v_2, v_3, \cdots$ are called the characteristic functions or natural modes.

The natural modes have interesting properties:

(a) They are orthogonal, i.e.,

$$\int\int_B v_i v_k dxdy=0 \quad \text{when} \quad i\neq k. \quad (6)$$

(b) They form a complete set of functions, i.e., any "reasonably good" function satisfying the boundary condition (2) can be expanded into the series

$$\bar{v}=\varphi_1 v_1+\varphi_2 v_2+\varphi_3 v_3+\cdots. \quad (7)$$

The coefficients $\varphi_1, \varphi_2, \varphi_3, \cdots$ (the normal components of the function $\bar{v}$) can be easily computed from the following expression:

$$\int\int_B \bar{v}v_n dxdy=\varphi_n\int\int_B v_n^2 dxdy \qquad n=1, 2, 3, \cdots. \quad (8)$$

Finally, we mention briefly Rayleigh's principle: Consider the expression

$$\frac{\int\int_B (v_x^2+v_y^2)dxdy}{\int\int_B v^2 dxdy} \quad (9)$$

(the ratio of the "potential and kinetic energies");

---

[6] H. W. Emmons, "Numerical methods of solving partial differential equation," Quart. App. Math., to appear in October, 1944.

[7] This material can be found in any good book on mathematical physics. For instance, see R. Courant, *Advanced Methods in Applied Mathematics* (New York University Press, 1941); or Th. v. Kárman and M. A. Biot, *Mathematical Method in Engineering* (McGraw-Hill Book Company, Inc., New York and London, 1940).

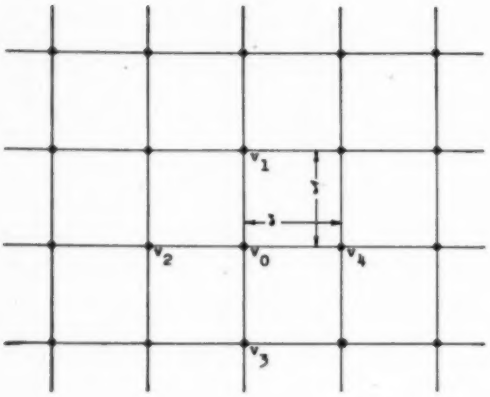

FIG. 1.

the nth natural mode λ_n is given by

$$\frac{\lambda_n}{a}=\frac{\int\int_B (v_{nx}^2+v_{ny}^2)dxdy}{\int\int_B v_n^2 dxdy}. \tag{10}$$

The importance of Eq. (10) lies in the fact that a small error made in the mode will entail an error of second order in the value of λ, or saying it otherwise: If we have a *moderately good approximation for the mode, expression (10) gives a good approximation for the characteristic number.*

Expression (10) can be easily transformed into the following

$$\frac{\lambda_n}{a}=\frac{-\int\int_B v_n \Delta v_n dxdy}{\int\int_B v_n^2 dxdy}. \tag{11}$$

Now this gives a simple interpretation of Rayleigh's principle. Namely, we can rewrite the right-hand side again and get

$$\frac{-\int\int_B v^2(\Delta v/v)dxdy}{\int\int_B v^2 dxdy}. \tag{12}$$

This expression is the *weighted (integral) mean* of the function $\Delta v/v$. (The weight function is v^2.) For the nth mode by the differential equation (5)

$$-\Delta v/v=\lambda_n/a. \tag{13}$$

Hence in this case the value of expression (12) must equal λ_n/a. If we make a small error in the mode, $-\Delta v/v$ will not be constant; however, the expression (12) being a mean value, the irregularities of $-\Delta v/v$ are ironed out and Eq. (10) still gives a good approximation for λ. Expression (11) will be very useful in our numerical work.

2. THE DIFFERENCE EQUATION OF THE VIBRATING MEMBRANE

Let us take a square net of points, with spacing δ. The derivatives can be approximated by difference quotients and we get

$$\Delta v \sim \frac{v_1+v_2+v_3+v_4-4v_0}{\delta^2}=\frac{\Delta_\delta v}{\delta^2} \tag{14}$$

which holds at every net point. (See Fig. 1.) Now we can write the system of difference equations corresponding to Eq. (5) as

$$\frac{\Delta_\delta v}{\delta^2}+\frac{\lambda}{a}v=0 \tag{15}$$

or

$$\Delta_\delta v+\lambda^* v=0 \tag{16}$$

for each net point. The physical interpretation of the difference equations is simple: Replace the original membrane by a system of discrete masses and springs, put equal masses at each net point, and connect adjoining masses with springs having the same spring constants (Fig. 2). *The natural modes of transverse vibrations of this system* (of finite degree of freedom) *are determined by the difference equations (16).* By solving

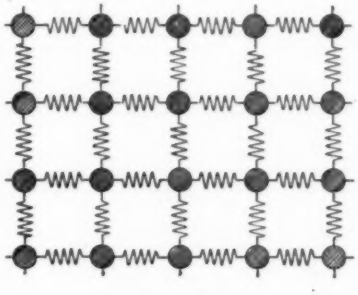

FIG. 2.

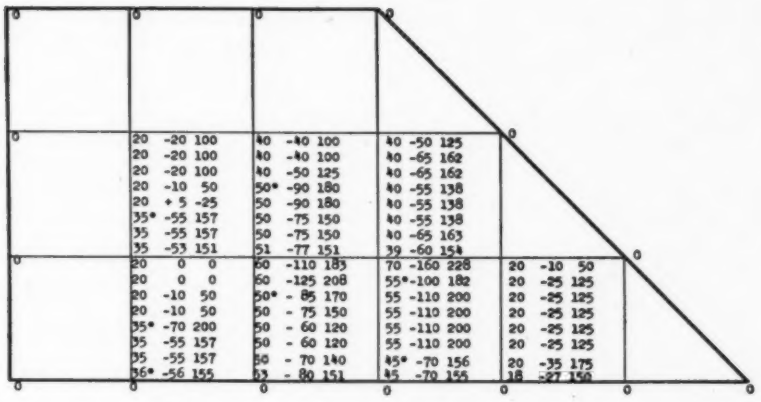

FIG. 3. Lowest natural frequency and mode of quadrangular membrane. First approximation. $\Delta v+(\lambda/a)v=0$, $v=0$ on edges, $\delta=1$, $a=13.5$, $\lambda_m^*=\Sigma v\Delta v/\Sigma v^2=0.8984$, $\lambda=(a/\delta^2)\lambda_m^*$. First characteristic value, $\lambda=20.61$. Order of relaxation: (31), (21), (22), (11), (12), (31), (21), (41), (22), (32), (21), (11). Recorded: v, Δv, $-100(\Delta v/v)(=100\lambda^*)$. The first 6 modifications and final result are shown. (Intermediate result based on the six modifications shown: $\lambda=20.65$.)

these difference equations, for finer and finer nets, the solution of the original differential equation (of natural modes of the membrane) can be approximated, to any desired accuracy.[8]

3. DETERMINATION OF THE LOWEST MODE

The relaxation method consists of assuming a "guess" solution for the difference equation (16) and then to improve the solution by successive modifications. Consider as an example the membrane shown in Fig. 3. As a first approximation we take 7 netpoints inside of the domain (i.e., the approximating system has seven degrees of freedom). The first number of the first row in each square shows our guess value for v. (No attempt was made to guess well.) The second number in each row is $\Delta_8 v$, the third row is $-100\Delta_8 v/v=100\lambda^*$. Let us write our original difference equations (16) in a little different way:

$$\Delta_8 v/v=-\lambda^*. \tag{17}$$

Then we can see what is wrong with our guess solution: The different λ^*'s (let us call them local λ^*'s) are not equal and we have to endeavor to change the v's so that all the λ^*'s become equal. All our efforts will be concentrated on attaining this equalization of the λ^*'s by some efficient procedure.

[8] R. Courant, K. Friedrichs, H. Levy, Math. Ann. **100**, 32–74 (1928).

It is useful to give a physical interpretation to our guess function v. Namely, consider a particle placed at each net point, with a mass proportional to the local λ^*. *The lowest mode of transverse vibration of this vibrating system is given exactly by our guess function v.* Hence we can say that at each stage of the relaxation process we have a solution to a certain vibration problem of non-homogeneous mass distribution. Our aim is to modify this system so that all the masses become equal.

From this physical picture it is to be expected (and will be proved shortly) that the correct value of λ^* is somewhere between the local λ^*'s. Rayleigh's principle gives important information on the value of λ^*. Namely, by replacing in Eq. (11) the integral sign by summation, we get

$$\lambda_{m1}^*=\frac{-\sum v\Delta v}{\sum v^2}$$

$$=\frac{20\times 20+40\times 40+40\times 50+\cdots}{20^2+40^2+40^2+\cdots}=1.71. \tag{18}$$

This is the first approximation to the correct λ^* value.

In order to have an efficient way to equalize the λ^*'s, we should start to modify our solution by improving the bad errors in it. Now obviously this is shown somehow by the deviations of the local λ^*'s from our first approximation $\lambda_{m1}^*=1.71$.

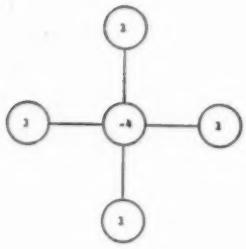

FIG. 4.

Looking at expression (12) we see that this deviation is more serious when v is large than when v is small: More accurately it is proportional to v^2. Looking now at our guess solution we judge that $\lambda^*_{31}=2.28$ is a "bad" error. (λ^*_{31} is the local λ^* at the third interior point to the right and first, upwards.) (There is no point in spending too much time in selecting the worst errors.) So we change v_{31} by -15 and put beneath 70 the new value 55. All the other v's are unchanged and we simply rewrote them at the second row. (We do this just to illustrate the method, otherwise of course we would not repeat the same numbers twice.) Now by changing v_{31} we have to correct the Δv's at the net point 31 and at the adjoining ones. This is done by using the relaxation pattern of Fig. 4, which shows the effect of a change of 1 in v_0. We changed v_{31} by -15; hence $\Delta_{31}v$ changes by $+60$, the adjoining ones by -15. We complete our new approximation by computing the new local λ^*'s. We observe that our new approximation (shown in the second row) is better because the range of λ^* is smaller.

At this point we make some observations. The nature of this relaxation method is such that the maximum value of the local λ^*'s *can* be steadily decreased or the minimum value increased. Hence we see that the relaxation process *can* be made convergent. However, the intelligent computer will *not* follow this procedure. We modified our solution such that λ^*_{31} decreased, and also we know (without carrying out the computations) that λ^*_{21} will increase. But we know also that our original value of λ^*_{21} was already too high. Hence by improving λ^*_{31} we will make λ^*_{21} worse. Now when in turn we decrease λ^*_{21} (by changing v_{21}) we will increase λ^*_{31}. One of the most important features of the relaxation process is that the computer makes allowance for this phenomenon. We should have "overshot" at point 31, i.e., *we should have made a change bigger than -15*. This is the point where the intelligence and experience of the computer enter.

Before continuing our solution we make another remark. From what we said above it follows that the correct value of λ^* is always between the local λ^*'s. Hence at each stage we know the range where λ^* lies and we should consider our solution completed when this range equals our desired accuracy.

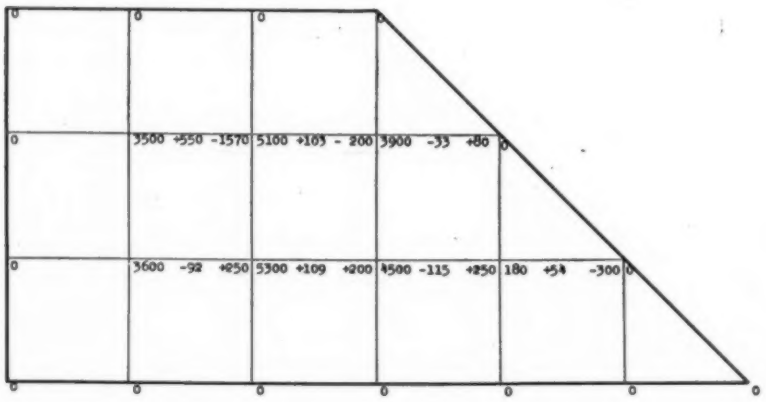

FIG. 5. Recorded:

$$100v,\ 100(\Delta v+1.53v),\ -\frac{\Delta v+1.53v}{v}10^5=10^5\lambda_1^*.$$

Let us continue our solution. $\lambda^*_{21}=2.08$ is a bad error so we make a change of -10 in v_{21}. (No overshooting is done as some of the adjoining λ^*'s are high, some low.) Then we change v_{22}, and so on. After completing 7 steps (there is no need for computing all the new local λ^*'s at each step) we observe that the λ^*'s are pretty well equalized. Now it is time to use Rayleigh's principle again and we get from Eq. (11) the second approximation for the characteristic value $\lambda^*_{m2}=1.529$. The last row on Fig. 3 shows the result of the twelfth modification. λ^* is determined again by Rayleigh's principle as $\lambda^*=1.527$.

It is troublesome to go to higher accuracy, since the λ^*'s cannot be computed with a slide rule. This difficulty can be avoided by a simple device. We *know* that $\lambda^*=1.53+\lambda_1^*$, where $\lambda_1^*<.01$, and we write the system of difference equations (17) in the form

$$\frac{\Delta_\delta v+1.53v}{v}=-\lambda_1^*. \tag{19}$$

In Fig. 5 we recorded at each net point $100v$, $100(\Delta v+1.53v)$, and $-10^5\lambda_1^*$ where the second number is computed on a machine but the λ^*'s are computed with a slide rule. The relaxation process can be started now using the slide rule, with the only difference that the pattern of Fig. 4 is replaced by the one shown in Fig. 6.

It should be noted, however, that in the example presented there is no point in going to too high accuracy, as the approximating system itself (of seven degrees of freedom) cannot approximate the continuous system but to a certain accuracy. One must therefore take a net with more points. Figure 7 shows the results of an approximation, where 15 interior points were used.

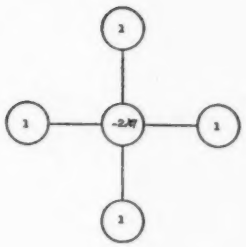

FIG. 6.

4. DETERMINATION OF THE SECOND MODE

The determination of the second mode can be reduced to first-mode computations by the following method: Take a nodal line across the membrane in some arbitrary fashion and imagine for the time being that the membrane is kept fixed along this line. We have now *two* different membranes and we can determine the lowest mode for each of them. The problem is to adjust the nodal line such that each of the membranes has the same characteristic number and that they can be considered as parts of one and the same membrane.

Our previous membrane will serve as illustration of our method. The values of our guess function v, Δv and $100\lambda^*$ are recorded in the first

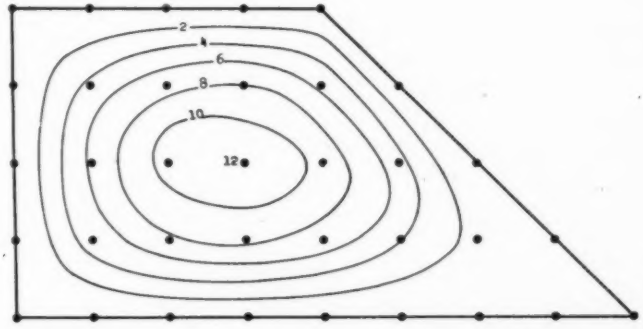

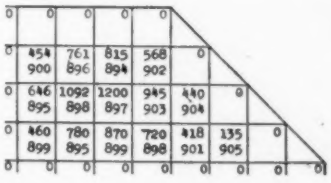

FIG. 7. Lowest frequency and natural mode of quadrangular membrane. Second approximation. $\Delta v+(\lambda/a)v=0$, $v=0$ on edges, $\delta=1$, $a=24$, $\lambda_m^*=\Sigma v\Delta v/\Sigma v^2=0.8984$, $\lambda=(a/\delta^2)\lambda_m^*$. First characteristic value, $\lambda=21.562$. Recorded:

$$\left\{\begin{array}{c} v \\ \hline -1000(\Delta v/v)(=1000\lambda^*) \end{array}\right\}.$$

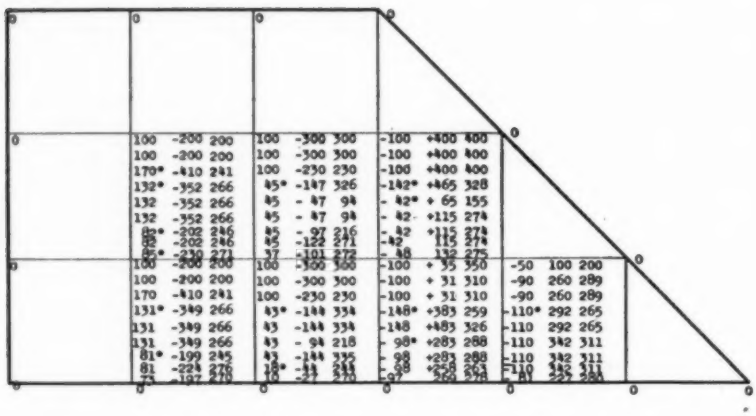

FIG. 8. Second natural frequency and mode of quadrangular membrane. First approximation. $\Delta v+(\lambda/a)v=0$, $v=0$ on edges, $\delta=1$, $a=13.5$, $\lambda_m{}^*=\sum v\Delta v/\sum v^2=2.748$. Second characteristic value, $\lambda=37.10$. Order of relaxation: (41), (12), and (11), Ort., (32), (31), (11), (12), (21), (41), (12), Ort., (31), (21), (41), (12), (21), (12). Recorded: v, Δv, $-100(\Delta v/v)(=100\lambda^*)$. The first 7 modifications and final result are shown. (Intermediate result based on the 7 modifications shown: $\lambda=37.54$.)

rows of Fig. 8. The nodal line goes between 21–31 and 22–32. Our "membrane" lying to the right of the nodal line (negative v's) consists of three particles and we notice that $\lambda^*_{41}=2.00$ is too low; hence our first step is to add -40 to v_{41}. Then we notice that for our left-hand "membrane" (consisting of four particles) λ^*_{11} and λ^*_{12} are too low. We change at once both of the v's (block relaxation). The new v's are recorded in the third row. Now the correct λ^* for the left-hand side membrane is smaller than 2.41; but for the right-hand side membrane λ^* is larger than 2.89; hence we see that the nodal line is at the wrong position. As the characteristic number is approximately inversely proportional to the area of a membrane, it is to be expected that the nodal line will shift to the left.

We could try to accomplish the shifting of the nodal line by changing individual v's properly. However, let us notice that if we make a change at 31 such that λ^*_{31} increases, then λ^*_{21} increases too in contradistinction to our experience with the lowest mode. Hence we see that λ^**'s separated by a nodal line change in the same direction* and thereby confusion might arise in the course of the relaxation process. Fortunately, however, this difficulty can be avoided since the orthogonal property of the natural modes gives a very efficient method for the location of the nodal line. Let us denote for the time being our present approximation by $\bar{v}$ and the first mode by v_1, tabulated in Fig. 5. Then Eq. (7) states that $\bar{v}$ can be written in the form

$$\bar{v}=\varphi_1 v_1+v, \tag{20}$$

where now v is *first-component free*, that is, v is orthogonal to v_1. The second mode *must* be orthogonal to v_1 and so it is reasonable to expect that v is a better approximation to the second mode than $\bar{v}$. So we compute φ_1 by formula 8 (integral signs are replaced by summation), and get

$$\varphi_1=\frac{\sum \bar{v}v_1}{\sum v_1{}^2}=\frac{35\times 170+51\times 100+39\times 100+\cdots}{35^2+51^2+39^2}. \tag{21}$$

Then we compute v from Eq. (20). Our new approximation is recorded in the fourth row of Fig. 8. The λ^*'s have a smaller scatter than before, i.e., our approximation has been really improved.

Further improvement is achieved by equalizing λ^*'s first for the right-hand side membrane, then for the left-hand side membrane. The result of the seventh modification (shown in the eighth row) shows a sufficiently small scatter in λ^* to

make it worth computing an approximation for the true λ^* from Rayleigh's principle. This is done exactly the same as for the first mode.

In the approximation just presented we used 7 interior points. Figures 8 and 9 show results to the same problem using 15 interior points.

Finally a few words on the first guess function. In the case presented the computer had some idea about the location of the nodal line and this was of course helpful. When the computer has absolutely no indication on the nodal line, he can start with an arbitrary function. The first step in this case should be to take out the first component.

5. HIGHER MODES

The foregoing can be applied obviously to determine the higher modes too, though it is to be expected that more time will be required to complete solutions. In particular for higher modes the shapes are more complicated and so finer nets are required to get a good approximation. It should be noted that the nth mode is orthogonal to all the lower ones.

6. ACCURACY OF THE METHOD

There are two questions with respect to accuracy: How accurate is the solution to the difference equation and how accurate is it to replace the differential equation by the difference equation. The first one is answered completely by our method of giving the range, where the characteristic value lies; the second one, however, cannot be answered readily. The computer should take finer and finer nets. See Fig. 10. When the characteristic values do not change any more in his significant figures, he can consider his solution completed.

7. CURVED BOUNDARIES

The example presented has a simple boundary and the net points fall on the boundary curve. If this is not the case, the best thing to do is to select net points in the neighborhood of the boundary curve and determine the v values on these points by interpolation or extrapolation from the first guess function (plotting curves might be very useful at this point). Then relax as if these net points formed the boundary. It will be necessary from time to time (in the course of the solution) to correct the v values on these "boundary" net points. *The computer will find that the inconvenience due to curved boundaries is insignificant.*

8. FORCED VIBRATIONS

The knowledge of the characteristic functions is all that is necessary for the determination of any free or forced vibration of the membrane. However, we want to spend a few lines on forced vibrations; in particular to compare our method with R. V. Southwell's.

Suppose that a periodic force of circular frequency ω acts upon the membrane. The equation of motion is now

$$S\Delta U - m(\partial^2 U/\partial t^2) = F(X, Y)\cos \omega t \qquad (22)$$

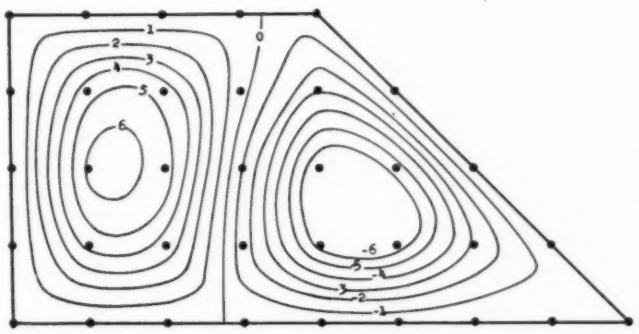

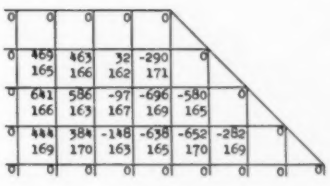

FIG. 9. Second frequency and natural mode of quadrangular membrane. Second approximation. $\Delta v + (\lambda/a)v = 0$, $v = 0$ on edges, $\delta = 1$, $a = 24$, $\lambda_m^* = \Sigma v\Delta v / \Sigma v^2 = 1.6716$, $\lambda = (a/\delta^2)\lambda_m^*$. Second characteristic value, $\lambda = 40.118$. Recorded:

$$\left\{\begin{array}{c} v \\ -100(\Delta v/v)\,(=100\lambda^*) \end{array}\right\}.$$

	□			1		2	
Order of Approximation	first	second	exact	first	second	first	second
Degrees of freedom of approximating system	9	49		7	15	7	15
Characteristic Value	18.75	19.508	$\pi^2 = 19.739$	29.61	21.562	37.10	40.118
Number of modifications used in solution	5	35		12	35	16	65
Accuracy	5%	1.2%					

□ Lowest Mode of the Square Membrane

1 Lowest Mode of a Quadrangular Membrane

2 Second Mode of a Quadrangular Membrane

FIG. 10. Characteristic values of membranes.

and we seek periodic solutions so that

$$U = V \cos \omega t, \tag{23}$$

where V is a space variable. V satisfies the following differential equation

$$S\Delta V + m\omega^2 V = F(X, Y) \tag{24}$$

(where now ω is given). To solve this equation by the relaxation method we start with an arbitrary V and get

$$S\Delta V + m\omega^2 V - F = R \tag{25}$$

where R is the "residual force." The relaxation method consists of the liquidation of R by successive improvements. This is the best method of treatment of forced vibration, when one is interested in the effect of one (particular) given periodic force.

Southwell uses the same method for the determination of the natural modes of the free vibration. Namely, one can guess an ω value by using Rayleigh's principle. Then one can start to liquidate the residue R by relaxing. However, since ω is not the correct natural frequency, the residual forces cannot be completely liquidated and it will be necessary, by using again Rayleigh's principle, to replace periodically ω by a new value. Southwell's method seems less well adapted to the important problem of computing the natural modes than the one presented in this paper.

NOMENCLATURE

$a = A/l^2$, projected dimensionless area of membrane.
A, projected area of membrane.
B, domain obtained as projection of membrane.
C, boundary of membrane.
D, characteristic length normal to membrane.
l, characteristic length along membrane.
m, mass density of membrane.
s, arc length along C.
S, tension in membrane.
t, time.
U, deflection of membrane.
V, deflection of natural mode.
$v = V/D$, dimensionless deflection of natural mode.
X, Y, coordinates.
x, y, dimensionless coordinates.
δ, net spacing.
φ_i, normal components.
λ, characteristic value (dimensionless) $= A\omega^2(m/S)$.
λ^*, $= \lambda\delta^2/a$.
Δ, Laplace (differential) operator.
Δ_δ, Laplace difference operator.

A Closed Cell for Electron Microscopy

I. M. Abrams and J. W. McBain
Department of Chemistry, Stanford University, Stanford University, California

(Received May 1, 1944)

ONE of the severest disabilities of the electron microscope has consisted in the fact that the specimen is exposed to high vacuum and consequently is completely desiccated and perhaps destroyed before observation. For many purposes it is desirable to study a specimen in its original medium without such desiccation and possible alteration. For this purpose an enclosed chamber is necessary, although none has yet been published.*

REQUIREMENTS FOR AN ENCLOSED CHAMBER

The essential requirements for windows in the cell are: (a) ready permeability to electrons, so that scattering is insufficient to obscure the image; (b) mechanical strength to withstand a vacuum; and (c) imperviousness to vapor of water or other solvent medium.

After trying and eliminating several types of polymeric materials, collodion was found to be the most suitable. The usual technique for preparing films for use in the electron microscope is to spread a drop of solution on water. However, such films were found to be far too weak to support the pressure of one atmosphere when covering a hole 0.1 millimeter in diameter; likewise they are permeable to water vapor.**

Taylor[1] in 1926 found that nitrocellulose films spread on mercury are stronger. We have found that even when they are so thin as to fulfill requirement (a) they are strong enough to fulfill requirement (b). Furthermore we have discovered that they are sufficiently impervious to vapors to fulfill requirement (c). They are able to hold a vacuum when wet with liquid water, dioxane, benzene, toluene, or petroleum ether. They rupture in contact with liquid ethyl alcohol or ethyl ether or any solvent for nitrocellulose.

PREPARATION OF COLLODION FILMS

Two drops of a 1 percent solution or one drop of a 2 percent solution of Baker U.S.P. collodion cotton in purified amyl acetate is allowed to spread on thoroughly cleaned mercury, nine centimeters square. The mercury is previously washed three or four times in a long column of 10 percent potassium hydroxide, followed by washings with 1*N* nitric acid, hot and cold water, and finally drying. Mercury and film are kept as free as possible from dust. The average thickness of films is less than six hundred angstroms. A rough indication of the film strength can be obtained by puncturing the film with a sharp point. If the point passes through without encountering any resistance, the film is weak; if it is stopped momentarily with wrinkles radiating out from the point of contact, then the film is relatively strong.

To place the films as a window covering a 0.1-mm hole, a centrally bored platinum disk is simply raised upward through the surface of the mercury. Scoring the film beforehand with a sharp needle facilitates its removal.

ELECTRON TRANSPARENCY OF THE FILM

We are indebted to Dr. L. Marton of Stanford University and Dr. Otto Beeck and Mr. A. E. Smith of the Shell Development Company,

---

* M. Von Ardenne, Zeits. f. physik. Chemie **B51**, 61 (1942), following a suggestion of L. Marton, Bull. Classe Sci. Acad. Roy. Belg. **21**, 553 (1935), constructed a reaction chamber in his universal electron microscope with open microscopic holes. A continuous gas supply enables a pressure of a few millimeters to be maintained within the chamber.

** K. Sollner, private communication, states that collodion swells 50 percent in water. Hence a film prepared on water would be considerably more porous than those prepared on non-swelling media.

[1] J. Taylor, J. Sci. Inst. **3**, 400 (1926).

Emeryville, for their very generous cooperation in operating the Stanford microscope and the Berkeley RCA microscope, respectively. Without this, our work could not have been carried out.

Visual and recorded images of the particles of an evaporated gold sol were very satisfactory in that both resolution and contrast were excellent, with scarcely noticeable scattering due to the films between which they were sandwiched.

MECHANICAL MOUNTING

We are indebted to Mr. J. Grebmeier, instrument maker, Menlo Park, California, for constructing our cells and the jig and supports used with them. They are made to fit both the RCA and the Stanford microscopes.

The cells may be of platinum or of platinum containing one or two percent iridium, and are machined with a jeweler's lathe. As shown in Fig. 1, the cell consists of two circular disks 3.125 mm (0.125 inch) in diameter. The lower disk is 1 mm, the upper 0.5 mm thick. A large annular groove made in the lower disk is about 0.5 mm deep and 1 mm wide. This is to hold adhesive wax and excess liquid from the specimen. The upper disk is turned down to leave a protruding annular ridge about 0.3 mm deep. When the two are pressed together, the wax forms a vacuum-tight seal.

In assembling the cell, the groove is first filled with plastic wax, such as Cenco "Tackiwax." The wax is trimmed with a sharp needle point so that only a narrow thread remains around the outer edges of the groove. The thin collodion films are then carefully deposited on each of the disks and a drop of the liquid to be examined is placed on the film of the lower disk. Excess liquid is carefully drawn off with small pieces of filter paper, and the disks are quickly stuck together.

A chartering jig aids in aligning the holes of the two disks. This consists simply of a circular brass holder with three prongs protruding upward placed so as to guide the two disks into a cylindrical hole the diameter of which is just 0.025 mm (0.001 inch) larger than that of the disks. The assembled cell is fitted into this hole and squeezed so that the ridge of the upper disk makes complete contact with the wax in the groove of the lower disk. This procedure automatically aligns the two holes so that the cell is then ready for examination in the electron microscope. It fits existing RCA microscopes and a special holder is used for the Stanford microscope.

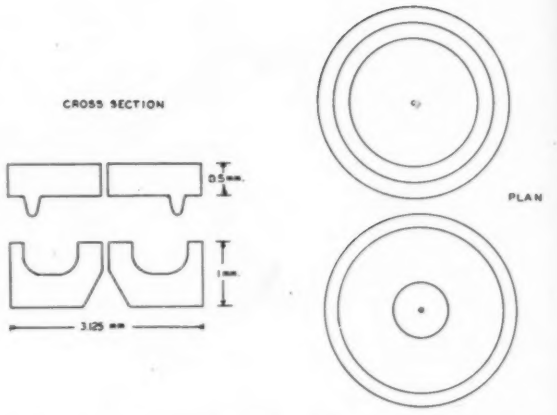

FIG. 1. Perforated platinum disks used to form enclosed electron microscope cell; cell and cover shown in cross section and in plan.

Cells have been tested for permeation by various liquids with a vacuum on the other side, but the most direct test is that of weighing the cell before and after putting in the liquid and after evacuation. The weight of liquid usually found is of the order of 0.020 mg. The cells were then tested by exposing them to vacuum for periods of from five minutes to an hour and reweighing them. A large part of the water usually remains in the cell.

The weighings were made with a Kuhlman microbalance. In three successive experiments, using the cell described above, the amount of fluid in the cell after wetting was 26, 23, and 25 micrograms; after evacuating for one ten-minute period the amounts remaining were 23, 0, and 18 micrograms. In another experiment using a somewhat different type of cell having a larger capacity, the original weight of liquid was 283 micrograms; after successive five-minute evacuations, the weights were 201, 189, 179, and 167 micrograms. The first evacuation, of course, removes any moisture or volatile material from the exterior of the cell.

In the electron microscope, movement of the liquid and bubbling have been observed. At Dr. Marton's suggestion, most of the cell is

shielded from the heating effects of the electron beam by covering it with a thin disk of mica on top of which is another disk of platinum, both with holes bored through the center. This precautionary measure is designed principally to prevent the wax from melting and flowing into the path of the electron beam.

Alternatively, the wax may be omitted, and the seal made mechanically by means of a hollow plunger screwed into the brass holder.

LIQUID SPECIMENS IN THE ELECTRON MICROSCOPE

The problem of examining liquid specimens in a closed chamber in the electron microscope is exactly analogous to that of examining the structure of the living brain by x-rays. The skull, like our membranes, must not obscure the result, and the liquid medium must not cause too much scattering. Water one micron thick is practically opaque to electrons of the usual voltage, so that its thickness must be kept to a minimum. Even for x-rays, considerably better contrast is obtained when air is substituted for the cephalic fluid.

With a sufficiently thin layer of liquid at least part of a highly intense beam will register on the fluorescent screen or photographic plate. In order to observe the presence of particles suspended in the liquid medium it is obvious that the advantage lies with particles of higher optical density. Thus a stationary gold particle, as for example one which is sorbed on the surface of a film, may be readily revealed, even though only a few hundred angstrom units in diameter. Focusing determines whether particles are attached to the upper or lower membrane.

BROWNIAN MOVEMENT AND THE ELECTRON MICROSCOPE

The problem of observing Brownian movement of ordinary colloidal particles such as gold in the electron microscope is similar to that of photographing a fly in a living room with a time exposure. This is because the ordinary electron microscope photograph requires many seconds of exposure whereas the particle makes a thousand billion erratic movements per second. Using the Einstein equation for average translation[2] it is seen that a particle 1000 angstroms in radius requires only 1/400 of one second for an excursion equal to its own radius and in one second it will have moved in various directions to a position two microns or twenty radii away. Even so large a particle that the radius is one micron will move irregularly to a position 0.6 radius in one second. Such a particle, if solid, is too thick to be contained by a layer of water transparent to the electrons. Hence such movement could only be observed with, for example, flattened emulsion droplets squeezed in the cell, or with loosely attached particles, or with a medium of extremely high viscosity such as a jelly, or with living cilia only near their base of attachment, unless their movement is rhythmically repetitious.

The ultramicroscope, using ordinary light, differs from transmission electron microscopes in that particles are visible in spite of Brownian movement because they are luminous points against a dark background; the points are sources of light even though they are too small to be resolved in the ultramicroscope. Instead, in the electron microscope they are dark constantly shifting particles on a bright background. Dark ground illumination for the electron microscope would be highly desirable.

SUMMARY

A very simple closed chamber for electron microscopy has been devised. The plastic windows interfere very little with electron examination and they are liquid and vapor tight and easily withstand a difference of one atmosphere pressure between the inside of the cell and the remainder of the electron microscope.

Some limitations of electron microscopy in examining specimens in liquid or attempting to observe ordinary Brownian movement have been emphasized. Particles in free Brownian movement necessarily elude observation.

---

[2] A. Einstein, Ann. d. Physik **17**, 549 (1905); **19**, 371 (1906).

A Simple Vector Method for the Determination of Orientations of Cubic Single Crystals from Back Reflection X-Ray Photographs

BEULAH FIELD DECKER
Research Laboratory, General Electric Company, Schenectady, New York

(Received May 22, 1944)

This paper describes a new and simpler method for the determination of orientations of cubic single crystals from back reflection x-ray photographs by use of vectors in the reciprocal lattice. An example is given to illustrate the usefulness of the method.

THE orientation of a single crystal is usually determined from a stereographic plot of the crystal. The data to be recorded on this plot are read from a back reflection x-ray photograph using a Greninger and a polar net. A back reflection photograph contains spots corresponding to a comparatively small portion of the total number of crystal directions. Thus it is necessary to employ some scheme, either graphical or analytical, to determine the orientations of directions not represented on the photograph. For the stereographic plot the reading and recording of data consume a comparatively large amount of time. Also, in order to change the direction from which the crystal is viewed, each spot on the stereographic projection must be rotated to its new position by using a stereographic net. This process is tedious and every rotation introduces additional error of location. A simpler and more accurate method for determining the orientation of a cubic single crystal has been developed and will be described in this paper. In addition, an example of its application will be given.

This method for the quantitative determination of the orientation of a cubic single crystal is based on certain relations among the reciprocal lattice vectors corresponding to principal crystal lattice planes.[1] The directions of two important reciprocal lattice vectors, determined in the usual way from the corresponding spots on the back reflection x-ray photograph, are sufficient to locate quantitatively any other vector. However, the vector operations required are less complicated if the directions of three vectors not contained in the same zone are known, and usually three such vectors are quite easily located.

In a cubic crystal structure, the reciprocal lattice vector of a crystal lattice plane is normal to the plane and, therefore, is directed along the crystal lattice row corresponding to the plane concerned; that is, the reciprocal lattice vector for the plane (111) is directed along [111]. Consequently, since only directions are of interest in an orientation determination, operations with reciprocal lattice vectors may replace operations with crystal lattice rows.

Consider a cube with edges of unit length along the X, Y, and Z axes of a Cartesian coordinate system. (See Fig. 1.) Let the vector from the origin to the point (1, 0, 0) be the reciprocal lattice vector $\mathbf{R}^*_{(100)}$, the vector to the point (0, 1, 0) the reciprocal lattice vector $\mathbf{R}^*_{(010)}$, and the vector to the point (0, 0, 1) the reciprocal lattice vector $\mathbf{R}^*_{(001)}$. It follows that the cube diagonal will be the vector $\mathbf{R}^*_{(111)}$ and the face

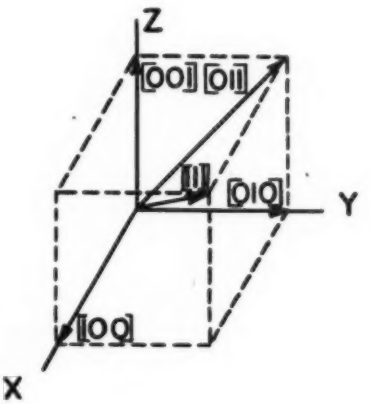

FIG. 1. A unit cube showing reciprocal lattice vectors along the principal crystallographic directions.

[1] Similar considerations were used in the author's paper "Vector formulas for identification of twinned lattices," Am. Mineral. (1944), in press.

diagonal in the plane YOZ the vector $\mathbf{R}^*_{(011)}$. Thus any reciprocal lattice vector $\mathbf{R}^*_{(hkl)}$ is the vector from the origin to the point (h, k, l). Each of these vectors may be represented as a combination of the unit vectors $\mathbf{i}$, $\mathbf{j}$, $\mathbf{k}$ along the coordinate axes. The vectors shown in the figure may be described as follows:

$$\mathbf{R}^*_{(111)} = \mathbf{i}+\mathbf{j}+\mathbf{k},$$
$$\mathbf{R}^*_{(011)} = \quad \mathbf{j}+\mathbf{k},$$
$$\mathbf{R}^*_{(001)} = \quad\quad \mathbf{k},$$
$$\mathbf{R}^*_{(010)} = \quad \mathbf{j},$$
$$\mathbf{R}^*_{(100)} = \mathbf{i}.$$

Consider now the following groups of vector equations which enable the remaining vectors to be determined from any two of the vectors $\mathbf{R}^*_{(111)}$, $\mathbf{R}^*_{(011)}$, and $\mathbf{R}^*_{(001)}$, or all three.

I. Given $\mathbf{R}^*_{(001)}$ and $\mathbf{R}^*_{(011)}$

$$\mathbf{R}^*_{(011)} - \mathbf{R}^*_{(001)} = \mathbf{j} = \mathbf{R}^*_{(010)},$$
$$\mathbf{R}^*_{(011)} \times \mathbf{R}^*_{(001)} = \mathbf{i} = \mathbf{R}^*_{(100)},$$
$$\mathbf{R}^*_{(011)} + \mathbf{R}^*_{(100)} = \mathbf{i}+\mathbf{j}+\mathbf{k} = \mathbf{R}^*_{(111)}.$$

II. Given $\mathbf{R}^*_{(001)}$ and $\mathbf{R}^*_{(111)}$

$$\mathbf{R}^*_{(111)} - \mathbf{R}^*_{(001)} = \mathbf{i}+\mathbf{j} = \mathbf{R}^*_{(110)},$$
$$\mathbf{R}^*_{(111)} \times \mathbf{R}^*_{(001)} = \mathbf{i}-\mathbf{j} = \mathbf{R}^*_{(1\bar{1}0)},$$
$$\frac{\mathbf{R}^*_{(110)} + \mathbf{R}^*_{(1\bar{1}0)}}{2} = \mathbf{i} = \mathbf{R}^*_{(100)},$$
$$\mathbf{R}^*_{(111)} - \mathbf{R}^*_{(100)} = \mathbf{j}+\mathbf{k} = \mathbf{R}^*_{(011)},$$
$$\mathbf{R}^*_{(011)} - \mathbf{R}^*_{(001)} = \mathbf{j} = \mathbf{R}^*_{(010)}.$$

III. Given $\mathbf{R}^*_{(011)}$ and $\mathbf{R}^*_{(111)}$

$$\mathbf{R}^*_{(111)} - \mathbf{R}^*_{(011)} = \mathbf{i} = \mathbf{R}^*_{(100)},$$
$$\mathbf{R}^*_{(111)} \times \mathbf{R}^*_{(011)} = \mathbf{j}+\mathbf{k} = \mathbf{R}^*_{(0\bar{1}1)},$$
$$\frac{\mathbf{R}^*_{(011)} + \mathbf{R}^*_{(0\bar{1}1)}}{2} = \mathbf{k} = \mathbf{R}^*_{(001)},$$
$$\mathbf{R}^*_{(011)} - \mathbf{R}^*_{(001)} = \mathbf{j} = \mathbf{R}^*_{(010)}.$$

IV. Given $\mathbf{R}^*_{(111)}$, $\mathbf{R}^*_{(011)}$ and $\mathbf{R}^*_{(001)}$

$$\mathbf{R}^*_{(111)} - \mathbf{R}^*_{(011)} = \mathbf{i} = \mathbf{R}^*_{(100)},$$
$$\mathbf{R}^*_{(011)} - \mathbf{R}^*_{(001)} = \mathbf{j} = \mathbf{R}^*_{(010)}.$$

In addition to the vectors considered, any other vector may be determined. For example:

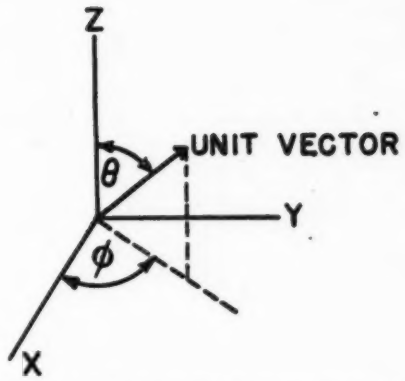

FIG. 2. The geometrical relation between Cartesian coordinates and the angular coordinates θ and φ.

$$\mathbf{R}^*_{(111)} + \mathbf{R}^*_{(001)} = \mathbf{R}^*_{(112)},$$
$$\mathbf{R}^*_{(011)} + \mathbf{R}^*_{(001)} + \mathbf{R}^*_{(001)} = \mathbf{R}^*_{(013)},$$
$$\mathbf{R}^*_{(100)} + \mathbf{R}^*_{(010)} + \mathbf{R}^*_{(111)} = \mathbf{R}^*_{(221)}.$$

It is necessary to use the vector product when only two vectors are known, but only addition and subtraction are needed when three or more vectors (along rows not in the same zone) are known, thus simplifying the procedure.

These same vector relations are true in any Cartesian coordinate system if the vector lengths remain the same. In considering a back reflection photograph it is convenient to choose the Z axis normal to the film, which puts the X and Y axes in the plane of the film. Each spot on the film represents a row in the crystal lattice. The inclination θ of this row to the Z direction in the chosen system of axes may be read from the film with a Greninger net. The angle φ between the X axis and the projection of the crystal lattice row on the XOY plane may be found with a polar net. These two angles describe the orientation of the row, as shown in Fig. 2. If the Miller indices of the spot in question are (hkl), then the components of the reciprocal lattice vector $\mathbf{R}^*_{(hkl)}$ along the axes of the chosen coordinate system are:

$$(R^*_{(hkl)})_x = (h^2+k^2+l^2)^{\frac{1}{2}} \sin\theta \cos\varphi,$$
$$(R^*_{(hkl)})_y = (h^2+k^2+l^2)^{\frac{1}{2}} \sin\theta \sin\varphi,$$
$$(R^*_{(hkl)})_z = (h^2+k^2+l^2)^{\frac{1}{2}} \cos\theta.$$

The vector operations indicated above may be carried out on the components of the vectors in

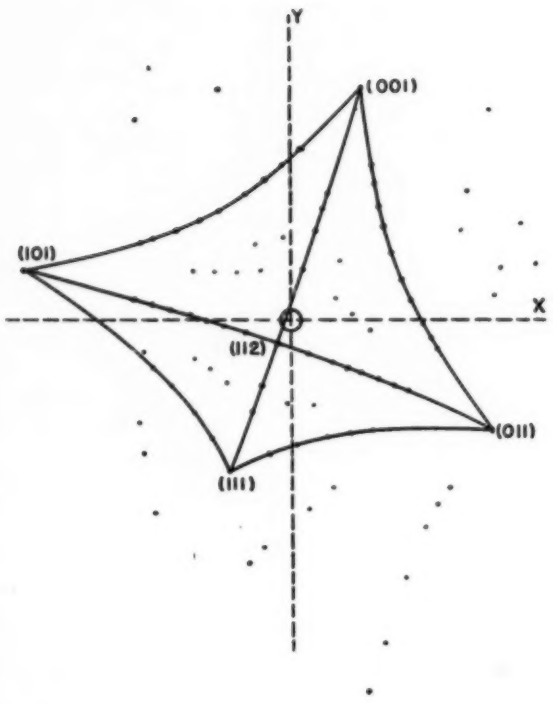

FIG. 3. A tracing of a back reflection x-ray photograph of a grain in a silicon steel strip, with principal spots indexed and common zones drawn.

this newly chosen Cartesian system. In this manner the orientation of any crystal lattice row may be determined if the orientations of two or more rows are known.

An example will make this clear.

Figure 3 shows a tracing of a back reflection x-ray photograph of a grain in a silicon steel strip. The principal spots are indexed. This has been done in the usual way with the aid of a Greninger net and tables of angular separations of principal planes. A set of Cartesian coordinate axes for reference has been chosen with X and Y axes as shown and Z axis directed vertically upwards; i.e., the X axis is in the rolling direction, the Y axis in the cross-rolling direction, and the Z axis normal to the plane of rolling. The three directions [111], [011], and [001] are used to determine the directions [010] and [100]. φ and θ are measured for each spot using a polar and a Greninger net, and from these values the Cartesian coordinates are determined by the formulas (1). These quantities are recorded in the first three rows of Table I. The coordinates

TABLE I. Observed and calculated data for principal spots shown in Fig. 3.

hkl	φ	θ	R_x^*	R_y^*	R_z^*
111	248°	24¾°	−0.272	−0.672	1.572
011	331½	29½	0.611	−0.332	1.230
001	72	30¼	0.156	0.479	0.864
010	299¼	68¾	0.455	−0.811	0.366
100	200¾	70	−0.883	−0.340	0.342

for $\mathbf{R}^*_{(010)}$ and $\mathbf{R}^*_{(100)}$ are found using the formulas IV; that is, $(R^*_{(100)})_x=(R^*_{(111)})_x-(R^*_{(011)})_x=-0.272-0.611=-0.883$, etc. After the coordinates for the unknown have been found, θ is determined from the z component and then φ from the x and y components, using formulas (1). To make this clear, consider the unknown vector $\mathbf{R}^*_{(100)}$. Its z component is 0.342. Therefore, $\cos\theta=0.342/(h^2+k^2+l^2)^{\frac{1}{2}}=0.342$, $\theta=70°$. The x component is -0.883, and $\cos\varphi=-0.883/\sin 70°$; $\varphi=200\frac{1}{4}°$. Or, using the y component, -0.340, $\sin\varphi=-0.340/\sin 70°$, $\varphi=201\frac{1}{4}°$. The average of these two values is $200\frac{3}{4}°$, the amount recorded in Table I.

The double determination of φ gives a check on the measurements and calculations. The two values should usually lie within a range of two degrees. Sometimes, if the direction of a vector chosen is too close to one of the axes, the results will be off by a large amount because of the slow change of sine or cosine with change of angle. Therefore, it is always best to choose vectors which make angles of at least 10° with the axes.

The precautions to be taken in the application of this method for the determination of orientations of cubic single crystals from back reflection x-ray photographs are:

(1) Choose vectors which make angles of at least 10° with the Cartesian coordinate axes.
(2) Make very careful measurements of θ and φ from the spots on the photograph.

If these precautions are followed, the calculations can be made with the slide rule. The entire process will require about 20 to 30 minutes and the inaccuracy of the angles obtained will usually be no greater than one degree.

The author wishes to express her appreciation to Dr. David Harker for helpful suggestions in this work.

On the Representation of Rigid Rotations

ELLIOT T. BENEDIKT
University of Florida, Gainesville, Florida
(Received April 20, 1944)

The group of formulae of Euler and Rodriguez describing the (finite) rotation of a rigid body is written under absolute (coordinate—free) tensor form. Formulae for the products and powers of certain tensors appearing in the transformation formulae are established. By their application, it is shown that the tensor which, operating on a radius vector defining the position of a point of a rigid body with respect to a point o defining the position of the same point after the body has been subjected to a rotation of amplitude θ around an axis containing o, and parallel to the unit vector $\mathbf{h}$, can be written under the form $e^{\theta\mathbf{h}\times}$. This representation is compared to the one obtained using quaternions.

THE problem of the representation of rigid rotations has been the subject of a considerable amount of research. It led to the introduction by W. R. Hamilton of the quaternions,[1] which were so extensively used for this and other purposes by the mathematical physicists in the second half of the last century. It is the purpose of the present paper to introduce a representation of rigid rotations which is more consistent with the operational methods used at present in other fields.

Consider a rotation of amplitude θ around an axis ξ. Let P and P' be the positions occupied by a generic point, respectively before and after the rotation, and x, y, z; x', y', z' their coordinates with respect to a Cartesian system having its origin at a point 0 of ξ. Let further α, β, γ be the angles formed by ξ with the axes. The coordinates of P' will then be given, as function of the coordinates of P and the elements defining the rotation by the group of formulae:[2]

$$\begin{aligned} x' &= x - 2\sin^2\tfrac{1}{2}\theta(x\sin^2\alpha \\ &\quad - y\cos\alpha\cos\beta - z\cos\alpha\cos\gamma) \\ &\quad + 2\sin\tfrac{1}{2}\theta\cos\tfrac{1}{2}\theta(z\cos\beta - y\cos\gamma), \\ y' &= y - 2\sin^2\tfrac{1}{2}\theta(y\sin^2\beta \\ &\quad - z\cos\beta\cos\gamma - x\cos\beta\cos\alpha) \qquad (1) \\ &\quad + 2\sin\tfrac{1}{2}\theta\cos\tfrac{1}{2}\theta(x\cos\gamma - z\cos\alpha), \\ z' &= z - 2\sin^2\tfrac{1}{2}\theta(2\sin^2\gamma \\ &\quad - x\cos\gamma\cos\alpha - y\cos\gamma\cos\beta) \\ &\quad + 2\sin\tfrac{1}{2}\theta\cos\tfrac{1}{2}\theta(y\cos\alpha - x\cos\beta). \end{aligned}$$

Let us indicate with $\mathbf{r}, \mathbf{r}'$ the radii-vectors defining the positions of P, P' with respect to 0, and with $\mathbf{h}$ a unit vector having the direction of ξ, and of sense such that an observer placed along it will see the rotation performed in the direction considered positive. Formulae (1) can then be written in vector notation under the form:

$$\begin{aligned} \mathbf{r}' &= \mathbf{r} + 2\sin^2\tfrac{1}{2}\theta[\mathbf{r} - \mathbf{r}\cdot\mathbf{hh}] \\ &\quad + 2\sin\tfrac{1}{2}\theta\cos\tfrac{1}{2}\theta\mathbf{h}\times\mathbf{r} \qquad (1') \end{aligned}$$

indicating with $(\mathbf{h}^2)$ the tensor-square[3] of $\mathbf{h}$ and since

$$-2\sin^2\tfrac{1}{2}\theta = \cos\theta - 1; \quad 2\sin\tfrac{1}{2}\theta\cos\tfrac{1}{2}\theta = \sin\theta,$$

we see that we can write the last formula under the form:

$$\mathbf{r}' = \mathbf{r} + (\cos\theta - 1)[\mathbf{r} + (\mathbf{h}^2)\mathbf{r}] + \sin\theta\mathbf{h}\times\mathbf{r} \qquad (2)$$

[1] W. R. Hamilton, *Elements of Quaternions* (Longmans, Green and Company, London, 1901), p. 359. See also: P. Kelland and P. G. Tait, *Introduction to Quaternions* (The Macmillan Company, London, 1904), pp. 55, 56.

[2] L. Euler, *Novi Comment. Petrop XX* (1776), p. 208. This formula has been wrongly attributed in a previous work by the author [E. T. Benedikt, Bol. Matemat. **14**, 67 (May, 1941)] to O. Rodriguez. For the derivation of formulae (1) see E. T. Whittaker, *Analytical Dynamics* (Cambridge University Press, 1937), pp. 6, 8. For derivation with vector methods see E. T. Benedikt, Bol. Matemat. **14**, 67 (May, 1941).

[3] The tensor product $(\mathbf{uv})$ of two vectors $\mathbf{u}$, $\mathbf{v}$ is defined by the relation $(\mathbf{uv})\mathbf{y} = [\mathbf{u}\cdot\mathbf{y}]\mathbf{v}$, where $\mathbf{y}$ is any vector. In a Cartesian system of coordinates, with respect to which u_i v_j are the components of $\mathbf{u}$, $\mathbf{v}$, the components of $(\mathbf{uv})$ will be u_iv_j. The notation used in the present paper for the tensor product is not to be confused with the notation used by German authors for the scalar product of two vectors.

or, in operational form:

$$\mathbf{r}' = \{1+(\cos\theta-1)[1-(\mathbf{h}^2)]+\sin\theta\mathbf{h}\times\}\mathbf{r}. \quad (2')$$

We shall call the operator

$$\mathfrak{R} \equiv 1+(\cos\theta-1)[1-(\mathbf{h}^2)]+\sin\theta\mathbf{h}\times \quad (3)$$

rotor, θ the amplitude, and $\mathbf{h}$ the axis of the rotor.[4] We shall now proceed to express $\mathfrak{R}$ in a more concise form. For this purpose we shall consider the powers of an operator of the type $\mathbf{v}\times$, and prove that for an even power we have the identity:[5]

$$(\mathbf{v}\times)^{2m} = (-1)^{m+1}\mathbf{v}^{2m-2}[(\mathbf{v}^2)-v^2] \qquad (m=1, 2, 3\cdots) \quad (4)$$

and for an odd power, the identity:

$$(v\times)^{2n+1} = (-1)^n v^{2n}\mathbf{v}\times \quad (n=0, 1, 2\cdots), \quad (4')$$

where v is the absolute value of $\mathbf{v}$.

Before proceeding to the proof of the above formulae, it will be convenient to establish for later use some formulae for the (functional) products and squares of tensor products, and products of axials and tensor products. If $\mathbf{u}_1, \mathbf{v}_1; \mathbf{u}_2, \mathbf{v}_2; \mathbf{y}$ are any vectors, we shall have by definition (see footnote 3):

$$(\mathbf{u}_1\mathbf{v}_1)(\mathbf{u}_2\mathbf{v}_2)\mathbf{y} = (\mathbf{u}_1\mathbf{v}_1)[\mathbf{u}_2\cdot\mathbf{y}]\mathbf{v}_2 = [\mathbf{u}_2\cdot\mathbf{y}][\mathbf{u}_1\cdot\mathbf{v}_2]\mathbf{v}_1 = [\mathbf{u}_1\cdot\mathbf{v}_2](\mathbf{u}_2\mathbf{v}_1)\mathbf{y},$$

which shows that we must have:

$$(\mathbf{u}_1\mathbf{v}_1)(\mathbf{u}_2\mathbf{v}_2) = [\mathbf{u}_1\cdot\mathbf{v}_2](\mathbf{u}_2\mathbf{v}_1).$$

If in particular we put in the preceding formula $\mathbf{u}_1=\mathbf{v}_1=\mathbf{u}_2=\mathbf{v}_2=\mathbf{w}$ we shall get the identity

$$(\mathbf{w}^2)^2 = w^2(\mathbf{w}^2). \quad (5)$$

For the product of an axial tensor $\mathbf{u}\times$ with a tensor product $(\mathbf{v}_1\mathbf{v}_2)$ applied to any vector $\mathbf{y}$ we shall have:

$$\mathbf{u}\times\cdot(\mathbf{v}_1\mathbf{v}_2)\mathbf{y} = [\mathbf{v}_1\cdot\mathbf{y}][\mathbf{u}\times\mathbf{v}_2],$$

which proves the (functional) identity:

$$\mathbf{u}\times\cdot(\mathbf{v}_1\mathbf{v}_2) = (\mathbf{v}_1\mathbf{u}\times\mathbf{v}_2). \quad (6)$$

Let us now prove Eq. (4) for $m=1$. If $\mathbf{y}$ is any vector, we shall have, on account of a known formula of vector analysis:[6]

$$(\mathbf{v}\times)^2 y = \mathbf{v}\times(\mathbf{v}\times\mathbf{y}) = [\mathbf{v}\cdot\mathbf{y}]y - v^2\mathbf{y} = [(\mathbf{v}^2)-v^2]\mathbf{y}. \quad (7)$$

Assuming now Eq. (4) to hold for a certain value $m=1$ of the index m, we shall prove it true for the value m, with which its general validity will be established. With the above assumption, we shall have, on account of (7):

$$(\mathbf{v}\times)^{2m} = (\mathbf{v}\times)^2(\mathbf{v}\times)^{2m-2} = (-1)^{m-1}v^{2m-2}[(\mathbf{v}^2)-v^2]^2. \quad (8)$$

Expanding the last factor of the second member and on account of (5) we shall have:

$$[(\mathbf{v}^2)-v^2]^2 = (\mathbf{v}^2)^2 - 2v^2(\mathbf{v}^2)+v^4 = -v^2[(\mathbf{v}^2)-v^2].$$

Substituting this value in (8) we get (4). Passing now to the proof of Eq. (4') we observe that it is obviously true for $n=0$. For $n=1$, we shall have, on account of (6),

$$(\mathbf{v}\times)^3 = \mathbf{v}\times(\mathbf{v}\times)^2 = \mathbf{v}\times[(\mathbf{v}^2)-v^2] = -v^2\mathbf{v}\times, \quad (9)$$

---

[4] Using the quaternions:

$\rho \equiv (0, x, y, z)$,
$\rho' \equiv (0, x', y', z')$,
$s \equiv (\cos\frac{1}{2}\theta, \sin\frac{1}{2}\theta\cos\alpha, \sin\frac{1}{2}\theta\cos\beta, \sin\frac{1}{2}\theta\cos\gamma)$.

The formulae (1) can be written under the form (see W. R. Hamilton, reference 1):

$$\rho = s\rho s^{-1}, \quad (1'')$$

so that the operator transforming the quaternion ρ defining the position of the point P into the quaternion ρ' defining the position of the point P' can be represented by $s(\ )s^{-1}$. It might be of interest to recall here that a quaternion of components q_0, q_1, q_2, q_3 is equivalent to the tensor $q_0+\mathbf{q}\times$, where q_0 is the symmetric tensor (multiplier) of components $q_0\delta_{ij}$ and $\mathbf{q}\times$ the axial tensor whole axis has components q_1, q_2, q_3. We see therefore that Eq. (1) is equivalent to the tensor equation:

$$\mathbf{r}'\times = (\cos\tfrac{1}{2}\theta+\sin\tfrac{1}{2}\theta\mathbf{h}\times)\mathbf{r}\times(\cos\tfrac{1}{2}\theta+\sin\tfrac{1}{2}\theta\mathbf{h}\times)^{-1},$$

which establishes a relation between the vectors $\mathbf{r}$ and $\mathbf{r}'$ defining the positions of the points P and P'.

[5] The operator (tensor) $\mathbf{v}\times$ is sometimes (improperly) called axial vector, the usual vectors being in this case referred to as polar vectors. The designations "*axial*" or "antisymmetric tensor" are more appropriate. The term "axial" is used by C. Burali-Forti and R. Marcolongo, *Analisi Vettoriale Generale* (Zanichelli, Bologna, 1929), Vol. I, p. 75. With respect to a Cartesian system of coordinates with respect to which v_i are the components of the components of the tensor, the components of $\mathbf{v}\times$ will be

$$\begin{Vmatrix} 0 & v_3 & -v_2 \\ -v_3 & 0 & v_1 \\ v_2 & -v_1 & 0 \end{Vmatrix}.$$

v will be referred to as the *vector* of the axial tensor.

[6] See, e.g., H. B. Phillips, *Vector Analysis* (John Wiley & Sons, Inc., New York, 1933), p. 17.

so that (4′) is verified also in this case. Assuming it true for a value $n-1$ of the index, we shall prove it to hold for the value n. In fact we shall have, on account of (9),

$$(\mathbf{v}\times)^{2n+1}=(\mathbf{v}\times)^2(\mathbf{v}\times)^{2n-1}$$
$$=(-1)^{n-1}v^{2n-2}(\mathbf{v}\times)^3=(-1)^n v^{2n}\mathbf{v}\times$$

with which Eq. (4′) is proved.

Expanding the operator $\mathfrak{R}$ defined by (3) in series of θ, we obtain:

$$\mathfrak{R}\equiv 1+\sum_{s=1}^{\infty}\frac{(-1)^{s+1}}{(2s)!}\theta^{2s}[(\mathbf{h}^2)-1]+\sum_{s=0}^{\infty}\frac{(-1)^s}{(2s+1)!}\theta^{2s+1}\mathbf{h}\times. \quad (3')$$

Introducing the vector:

$$\boldsymbol{\Theta}=\theta\mathbf{h},$$

we can, taking account of (4), (4′), and the definition of the exponential function, write (3′) under the form:

$$\mathfrak{R}\equiv 1+\sum_{s=1}^{\infty}\frac{(-1)^{s+1}}{(2s)!}\Theta^{2s-2}[(\boldsymbol{\Theta}^2)-\Theta^2]+\sum_{s=0}^{\infty}\frac{(-1)^s}{(2s+1)!}\Theta^{2s}\boldsymbol{\Theta}\times=\sum_{s=0}^{\infty}\frac{1}{s!}(\boldsymbol{\Theta}\times)^s. \quad (10)$$

Equations (1), (1′) can therefore be written in the symbolical form:

$$\mathbf{r}'=\mathfrak{R}\mathbf{r}=e^{\boldsymbol{\Theta}\times}\mathbf{r}=e^{\theta\mathbf{h}\times}\mathbf{r}, \quad (10')$$

where the operator $\mathfrak{R}$ has to be considered defined by Eq. (10). This representation of rotations seems to be simpler and easier to handle than the equivalent quaternion representation (1″). The representation (10) of rotations is already being used extensively under the form $e^{i\theta}$ for two-dimensional rotations, corresponding to rotations of points whose radii vectors are perpendicular to the axis of rotation. The commonly used symbol i is obviously equivalent to the operator $\mathbf{h}\times$, $\mathbf{h}$ being a unit vector perpendicular to the complex plane.

The application of the representation (10′) of rotations to the composition dynamics of rotations and theory of elasticity will be discussed in later papers.

Single- and Double-Stub Impedance Matching

ALEXANDER H. WING AND JULIAN EISENSTEIN
Cruft Laboratory, Harvard University, Cambridge, Massachusetts

(Received May 15, 1944)

Single- and double-stub impedance matching on transmission-line feeders are described. Formulae determining the position and the length of a single matching stub for any load impedance or any observed standing-wave voltage distribution are derived, neglecting losses in the matching sections. Conditions for minimum length of stub and minimum distance between load and stub are specified. For the double-stub arrangement, expressions for the lengths of and distance between stubs are derived for any possible combination of load and distance between stubs. A double-stub tuner with any fixed distance between stubs cannot match all loads to the feeder, and the limits are specified. The optimum location on the feeder of the double-stub tuner is discussed. A graphical method employing a circle diagram for computing the lengths and position of the stubs is explained. The graphical determination of the stub lengths of the double-stub tuner is facilitated by auxiliary circular loci which also indicate the range of admittances over which an impedance match may be effected.

I. SINGLE-STUB MATCHING

IT is possible to match any symmetrical antenna or two-terminal impedance to a transmission line by means of a single open or closed stub of suitable length placed on the transmission-line feeder at the proper point.[1]

[1] E. J. Sterba and C. B. Feldman, Proc. I.R.E. **20**, 1163 (1932).

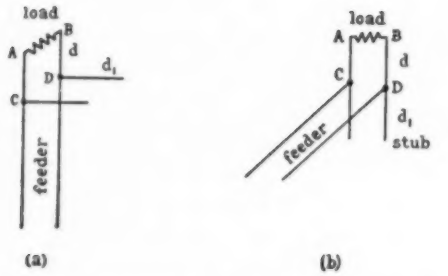

FIG. 1. Illustrating use of an open stub to match a load to a transmission-line feeder.

The method is indicated in Figs. 1 and 2.

The operation of the stub may be explained as follows. When the line is not terminated in its characteristic impedance, "standing waves" exist on the line. Neglecting the losses in the line the impedance looking toward the load is a resistance SR_c at a voltage maximum and a resistance R_c/S at a voltage minimum, where S is the standing-wave ratio $|E_{\max}|/|E_{\min}|$ and R_c is the characteristic resistance of the line. In terms of the characteristic admittance $G_c=1/R_c$, the admittance looking toward the load at a voltage maximum is a conductance G_c/S and at a voltage minimum is a conductance SG_c. Somewhere between these points the conductance is G_c. This is where the stub is located. At this point the admittance looking toward the load has some susceptance. The stub is added in parallel and its length and termination are chosen so that the total susceptance of the parallel combination of stub and section of line connected to the load is zero.

The derivation of formulae for the location and lengths of single and double stubs is facilitated by using the principle of conjugates. If a dissipationless network, Fig. 3, is inserted between an impedance Z_R and a constant-voltage generator whose internal impedance is Z_g, such that maximum power is transferred to Z_R, then at every pair of terminals the impedances looking in opposite directions are conjugates of each other. The proof of this is based on the principle of maximum power transfer. For a constant-voltage generator to deliver maximum power, its load must have an impedance equal to the conjugate of the generator impedance. The same principle applies in reverse. If a constant-voltage generator is delivering maximum power, its load is equal to the conjugate of its internal impedance. From Thevenin's theorem, the circuit to the left of AB, Fig. 3, is equivalent to a generator whose voltage is the open-circuit voltage at the terminals AB and whose internal impedance is such that this generator would deliver maximum power to Z_R. This internal impedance must be the conjugate of Z_R.

The lengths d and d_1 of transmission line, Figs. 1 and 2, form a network transforming Z_R into R_c. Then if a generator whose impedance is R_c is connected to the points CD, Figs. 1 and 2, the conditions of Fig. 3 obtain, neglecting losses in d and d_1. Then if the feeder to the points CD is replaced by R_c, the impedance looking in at AB (Z_R disconnected) is the conjugate of Z_R.

The input impedance of a dissipationless transmission line of length d and characteristic resistance R_c, terminated in an impedance Z_R, is

$$Z=R_c\frac{Z_R+jR_c\tan\beta d}{R_c+jZ_R\tan\beta d} \tag{1}$$

$$=R+jX,$$

where $\beta=2\pi/\lambda=\omega(lc)^{\frac{1}{2}}$ is the phase constant for the line. In terms of admittance,

$$Y=G_c\frac{Y_R+jG_c\tan\beta d}{G_c+jY_R\tan\beta d} \tag{2}$$

$$=G-jB. \tag{3}$$

In terms of the "per unit admittance" or dimensionless ratio

$$y=g-jb=Y/G_c, \tag{4}$$

$$y=\frac{y_R+j\tan\beta d}{1+jy_R\tan\beta d}, \tag{5}$$

where $y_R=g_R-jb_R=Y_R/G_c=R_c/Z_R$.

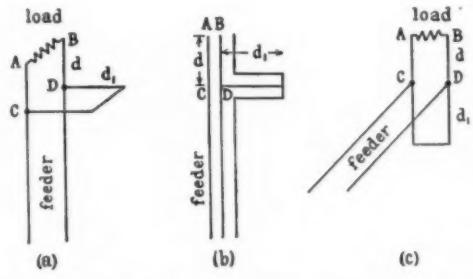

FIG. 2. Closed-stub construction on two-wire and coaxial feeders.

For an open stub, $y_R=0$ and

$$y]_{\text{open}}=j\tan\beta d \tag{6}$$

so that the "per unit" susceptance b of an open stub is

$$b]_{\text{open}}=-\tan\beta d. \tag{7}$$

For a closed stub, y_R is ideally infinite, and

$$y]_{\text{closed}}=-j\cot\beta d \tag{8}$$

so that the "per unit" susceptance of a closed stub is

$$b]_{\text{closed}}=\cot\beta d. \tag{9}$$

With properly chosen lengths d and d_1, Fig. 2, the admittance Y_R of the load is transformed into the admittance G_c, or the per unit admittance of the load $y_R=g_R-jb_R$ is transformed into the per unit admittance $1+j0$. Then from the principle of conjugates the admittance looking into the terminals AB must be the conjugate of Y_R when the feeder is replaced by G_c. Applying (5) to the length of line d, Fig. 2, with AB as the input terminals and the feeder replaced by G_c, the per unit admittance y is the sum of the per unit admittance $1+j0$ (replacing the feeder) and the per unit admittance $-j\cot\beta d_1$ of the closed stub; and the per unit admittance looking into AB is the conjugate of y_R. Hence

$$\frac{(1-j\cot\beta d_1)+j\tan\beta d}{1+j(1-j\cot\beta d_1)\tan\beta d}=g_R+jb_R. \tag{10}$$

Clearing the fraction and equating reals and imaginaries,

$$1=g_R+g_R\cot\beta d_1\tan\beta d-b_R\tan\beta d \tag{11}$$

and

$$-\cot\beta d_1+\tan\beta d=g_R\tan\beta d+b_R+b_R\cot\beta d_1\tan\beta d. \tag{12}$$

Equating the values of $\tan\beta d$ from (11) and (12),

$$\frac{1-g_R}{g_R\cot\beta d_1-b_R}=\tan\beta d=\frac{-\cot\beta d_1-b_R}{g_R+b_R\cot\beta d_1-1} \tag{13}$$

whence

$$\cot^2\beta d_1=\frac{(1-g_R)^2+b_R^2}{g_R}. \tag{14}$$

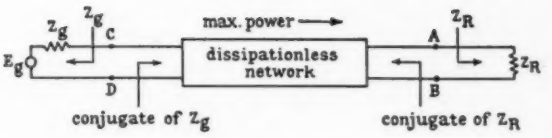

FIG. 3. Diagram illustrating the principle of conjugates in impedance matching.

Then

$$\cot\beta d_1=\left[\frac{(1-g_R)^2+b_R^2}{g_R}\right]^{\frac{1}{2}}, \tag{15}$$

and

$$\tan\beta d=\frac{1-g_R}{g_R\cot\beta d_1-b_R}. \tag{16}$$

} Closed stub

If βd and βd_1 are expressed in degrees,

$$d_1=\lambda\frac{(\beta d_1)\text{ degrees}}{360} \tag{17}$$

and

$$d=\lambda\frac{(\beta d)\text{ degrees}}{360} \tag{18}$$

where λ is the wave-length on the line.

For two-wire line construction of center-to-center distance D, it may be advisable to subtract $D/2$ from d_1 to allow for the inductive reactance of the closing wire, which is approximately equivalent to a line of length $D/2$ terminated by zero impedance. For coaxial construction no such correction is necessary.

For an open stub, Fig. 1, $-\tan\beta d_1$ from (7) replaces $\cot\beta d_1$ from (9) in (10). Then

$$\tan\beta d_1=\left[\frac{(g_R-1)^2+b_R^2}{g_R}\right]^{\frac{1}{2}}, \tag{19}$$

$$\tan\beta d=\frac{g_R-1}{g_R\tan\beta d_1+b_R}. \tag{20}$$

} Open stub

If stubs less than $\lambda/4$ in length are used, so that $\cot\beta d_1$ and $\tan\beta d_1$ in (15) and (19) are positive, a closed stub can be placed nearer the load than any other stub when $g_R<1$ and an open stub can be placed nearer the load than any other stub when $g_R>1$.

At a voltage maximum the line in effect is terminated by a resistance SR_c or a conductance G_c/S for which $g=1/S$ and $b=0$. Then if d is

measured from the position of a voltage maximum, (15), (16), (19), (20) become

$$\cot \beta d_1 = \pm \frac{S-1}{\sqrt{S}}, \quad \left.\begin{matrix} \text{closed stub} \\ d \text{ measured} \\ \text{from } E_{max} \end{matrix}\right\} \tag{21}$$

$$\tan \beta d = \pm \sqrt{S}, \tag{22}$$

and

$$\tan \beta d_1 = \pm \frac{S-1}{\sqrt{S}}, \quad \left.\begin{matrix} \text{open stub} \\ d \text{ measured} \\ \text{from } E_{max} \end{matrix}\right\} \tag{23}$$

$$\tan \beta d = \mp \sqrt{S}. \tag{24}$$

At a voltage minimum, the feeder in effect is terminated by a resistance R_c/S or a conductance SG_c for which $g=S$ and $b=0$. Then

$$\cot \beta d_1 = \pm \frac{S-1}{\sqrt{S}}, \quad \left.\begin{matrix} \text{closed stub} \\ d \text{ measured} \\ \text{from } E_{min} \end{matrix}\right\} \tag{25}$$

$$\tan \beta d = \mp \frac{1}{\sqrt{S}}, \tag{26}$$

and

$$\tan \beta d_1 = \pm \frac{S-1}{\sqrt{S}}, \quad \left.\begin{matrix} \text{open stub} \\ d \text{ measured} \\ \text{from } E_{min} \end{matrix}\right\} \tag{27}$$

$$\tan \beta d = \pm \frac{1}{\sqrt{S}}. \tag{28}$$

The distance d is measured from the position of E_{max} or E_{min} in the direction away from the load.

From (21), (23), or (25), (27), the closed and open stubs are of equal lengths when $(S-1)/\sqrt{S}=1$ or when $S=2.62$. For standing-wave ratios greater than 2.62, a closed stub is shorter than any other stub that can be used; and for standing-wave ratios less than 2.62 an open stub is shorter than any other stub that can be used.

For a load impedance Z_R,

$$S = \frac{|Z_R+R_c|+|Z_R-R_c|}{|Z_R+R_c|-|Z_R-R_c|} \tag{29}$$

or in terms of $y_R = Y_R/G_c = R_c/Z_R$,

$$S = \frac{|y_R+1|+|y_R-1|}{|y_R+1|-|y_R-1|}. \tag{30}$$

II. DOUBLE-STUB MATCHING

Although the single stub is extremely simple in its application, there are some disadvantages. It is not always convenient to provide an adjustment in the position of the stub, especially when coaxial cable is used. An open stub may not be lengthened easily. To overcome these difficulties two closed stubs of adjustable length but fixed position may be used, Fig. 4. The load admittance involves two variables g_R and b_R. To match these to the feeder, two adjustments are required. For the single stub the adjustments are the position and the length of the stub. For the double stub the position of and the spacing between the stubs are fixed in any given installation, and the two adjustments are the lengths of the two stubs. A given spacing will not accommodate all loads, but a spacing can be chosen suitable to the range of impedances or variations in load or frequency which might be encountered in a situation where these do not vary too widely. A spacing of $\lambda/2$ is not useful since such a length for d, Fig. 4, provides no impedance transformation.

From (9) the per unit susceptance of a closed stub of length d is $\cot \beta d$. If the susceptance of the stub d_2, Fig. 4, is added to the susceptance of the load, (10) becomes

$$\frac{(1-j \cot \beta d_1)+j \tan \beta d}{1+j(1-\cot \beta d_1) \tan \beta d} = g_R + j(b_R + \cot \beta d_2) \tag{31}$$

and (15) and (16) become

$$\cot \beta d_1 = \left[\frac{(1-g_R)^2+(b_R+\cot \beta d_2)^2}{g_R}\right]^{\frac{1}{2}}, \tag{32}$$

$$\tan \beta d = \frac{1-g_R}{g_R \cot \beta d_1 - (b_R+\cot \beta d_2)}. \tag{33}$$

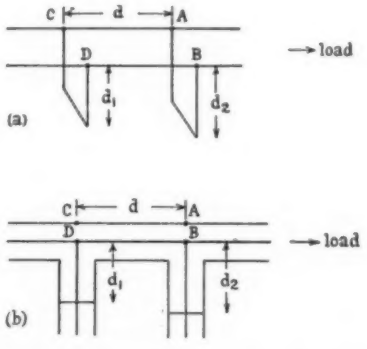

FIG. 4. Double-stub matching arrangement for (a) two-wire line, (b) coaxial line.

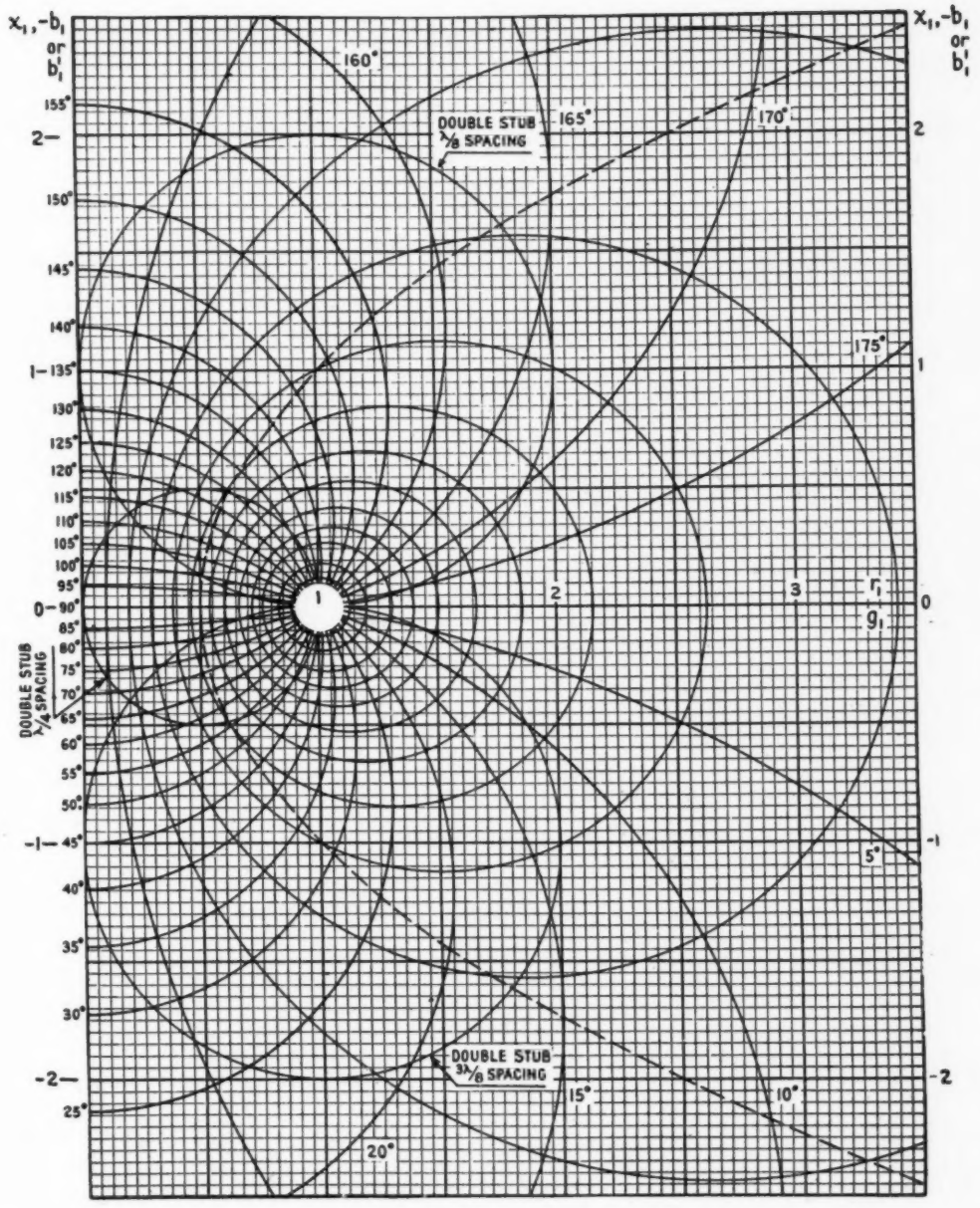

FIG. 5. Circle diagram with double-stub loci.

Since the spacing d is usually chosen arbitrarily, more useful formulae are those for d_1 and d_2 in terms of d and the per unit admittance of the load. From (32) and (33),

$$\cot \beta d_1 = \pm \frac{1}{(g_R)^{\frac{1}{2}}} (\cot^2 \beta d - g_R + 1)^{\frac{1}{2}} - \cot \beta d, \quad (34)$$

$$\cot \beta d_2 = \pm (g_R)^{\frac{1}{2}} (\cot^2 \beta d - g_R + 1)^{\frac{1}{2}} - \cot \beta d - b_R. \quad (35)$$

If the + sign is taken in (34) it must also be taken in (35).

For (34) and (35) to be real requires that

$$\cot^2 \beta d - g_R + 1 \geqslant 1$$

or

$$\cot^2 \beta d \geqslant g_R - 1.$$

Hence for a given spacing d the greatest per unit

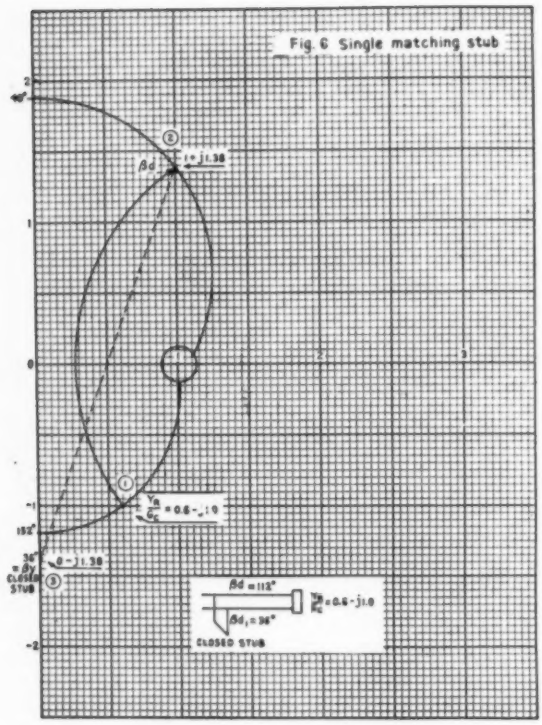

FIG. 6. Single matching stub.

conductance that can be matched to the feeder is

$$g_R]_{\max} = 1 + \cot^2 \beta d. \tag{36}$$

The susceptance of the load imposes no limitation since it is in parallel with the susceptance of d_2 which is adjustable to yield the susceptance required by (35). Except when g_R has the maximum allowable value, the choice of the + or − sign in (34) and (35) determines one of two possible combinations of d_1 and d_2 which will effect the impedance match.

Since at a voltage maximum the line in effect is terminated by a per unit conductance $1/S$ which is less than 1, a double-stub arrangement with any useful distance between stubs may always be used if the stub nearer the load is placed at a voltage maximum.

For $d = \lambda/4$, $\beta d = \pi/2$ or 90°, and (34) and (35) become

$$\left.\begin{aligned} \cot \beta d_1 &= \pm \frac{1}{(g_R)^{\frac{1}{2}}}(1-g_R)^{\frac{1}{2}} \\ \cot \beta d_2 &= \pm (g_R)^{\frac{1}{2}}(1-g_R)^{\frac{1}{2}} - b_R \end{aligned}\right\} d = \frac{\lambda}{4}. \tag{37, 38}$$

The per unit conductance looking toward the load at the junction of the stub d_2 must be equal to or less than 1.

For $d = 3\lambda/8$, $\beta d = 3\pi/4$ or 135°, and (34) and (35) become

$$\left.\begin{aligned} \cot \beta d_1 &= \pm \frac{1}{(g_R)^{\frac{1}{2}}}(2-g_R)^{\frac{1}{2}} + 1 \\ \cot \beta d_2 &= \pm (g_R)^{\frac{1}{2}}(2-g_R)^{\frac{1}{2}} + 1 - b_R \end{aligned}\right\} d = \frac{3\lambda}{8}. \tag{39, 40}$$

The per unit conductance looking toward the load at the junction of the stub d_2 must be equal to or less than 2.

III. CIRCLE DIAGRAM

The angles βd, βd_1, and βd_2 may be obtained graphically from a circle diagram,[2, 3] Fig. 5. For the dissipationless line the circles of constant attenuation (αl of reference 2, or A_s of reference 3) for the general case become circles of constant standing-wave ratio, the ratio being equal to the coordinate of the intersection with the axis of reals to the right of the point 1,0. The circles of constant phase have the same significance for the dissipationless line as for the general case including dissipation on the line.

For purposes of stub matching, neglecting attenuation in the line, the circles of constant standing-wave ratio may be constructed simply by drawing circles with centers on the axis of reals and passing through the points $(S, 0)$ and $(1/S, 0)$ where S is the standing-wave ratio. These are the circles surrounding the point 1,0 in Fig. 5. In Fig. 5 these circles have been drawn for particular values of the attenuation function of the general case,[2, 3] but the values of the attenuation functions have not been marked on the diagram.

The circles of constant phase pass through the point 1,0 and intersect the axis of imaginaries at the coordinate $-\cot \theta$ where $\theta = \beta d$. The center is at the point $(0, -\cot 2\theta)$ and the radius is $|\csc 2\theta|$.

The ratio $Y/G_c = g - jb$ is plotted with g along the axis of reals and $-b$ along the axis of

[2] J. C. Slater, *Microwave Transmission* (McGraw-Hill Book Company, Inc., New York, 1942), Chapter I.
[3] Ronold King, J. App. Phys. **14**, 577–600 (1943).

imaginaries. This is done because admittance, conductance, and susceptance have been defined[4] as $Y=G-jB$, whereas impedance is defined[4] as $Z=R+jX$, so that G replaces R and $-B$ replaces X when the diagram is used for admittances rather than impedances.

The input admittance of a line of length d terminated in an admittance Y_R may be graphically determined as follows. Enter the chart at the point whose horizontal coordinate is g_R and whose vertical coordinate is $-b_R$ where $Y_R/G_c = g_R+j(-b_R)$. Follow the circle of constant standing-wave ratio (interpolation may be necessary) clockwise through an angle βd as indicated by the circles of constant phase. The coordinates of this second point are the g and $-b$ of the input per unit admittance Y/G_c.

The per unit admittance of a closed stub of length d may be found on the left-hand margin as the coordinate of the intersection of the circle of constant phase angle equal to βd with the axis of imaginaries. For example, the ratio Y/G_c for a $\lambda/12$ stub whose $\beta d=30°$ is $-j\,1.73$.

The diagram will always yield values βd for a *closed* stub. If βd is greater than $\pi/2$ or 90° for a closed stub, a quarter-wave-length may be removed and an *open* stub of the remaining length may be used instead.

As an example of the use of the chart for calculating the stub length for a single stub, let $Y_R/G_c=0.6-j\,1.0$ for the load connected to the feeder. Enter the chart at point 1, Fig. 6, at 0.6 unit to the right of the origin and 1.0 unit below the origin. The circle of constant phase for this point is 40°. Follow the circle of constant standing-wave ratio clockwise to the vertical line passing through the point 1,0. This line is the locus of all points whose per unit conductance is 1, corresponding to admittances whose conductance is G_c. The intersection has the coordinates 1, 1.38 and the phase-angle is 152°. Then the angle βd corresponding to the length d of Fig. 2 is 152°–40°=112°. The per unit admittance looking toward the load at the points *CD*, Fig. 2, is $1+j\,1.38$. A stub whose $Y/G_c=-j\,1.38$ is required. On the left-hand margin the angle corresponding to -1.38 is 36°. Then $\beta d_1=36°$ for a closed stub. If $\lambda=100$ cm, $d=(112°/360°)100=31.1$ cm and $d_1=(36°/360°)\times 100=10$ cm.

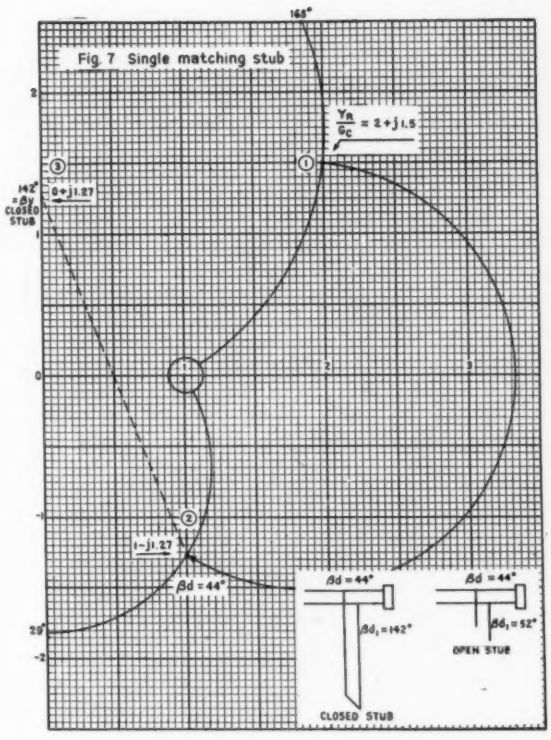

FIG. 7. Single matching stub.

As an example indicating an open stub, let $Y_R/G_c=2+j\,1.5$. Enter the chart at $2+j\,1.5$, point 1 of Fig. 7. The phase-angle is 165°. Follow the circle of constant standing-wave ratio clockwise to the vertical line passing through 1,0. The intersection is at $1-j\,1.27$, point 2 of Fig. 7. The phase angle is 29°. The required βd is 15°+29° or 44°. The required stub has a per unit admittance of $+j\,1.27$ or an angle βd_1 of 142°. Then βd_1 is 142° for a closed stub or 142°−90° for an open stub.

The circle diagram may be used also to determine the lengths of the stubs in the double-stub tuner, in terms of βd_2 and βd_1. A cut-and-try process may be followed, in which the object is to find the angles βd_2 and βd_1 which for a given βd will make the total per unit admittance at *CD*, Fig. 4, equal to $1+j0$. The cut-and-try may be eliminated by the use of auxiliary circles such as those marked for the $\lambda/8$, $\lambda/4$, and $3\lambda/8$ spacings, Fig. 5.

[4] American Standard Definitions of Electrical Terms, ASA C42—1941, American Institute of Electrical Engineers.

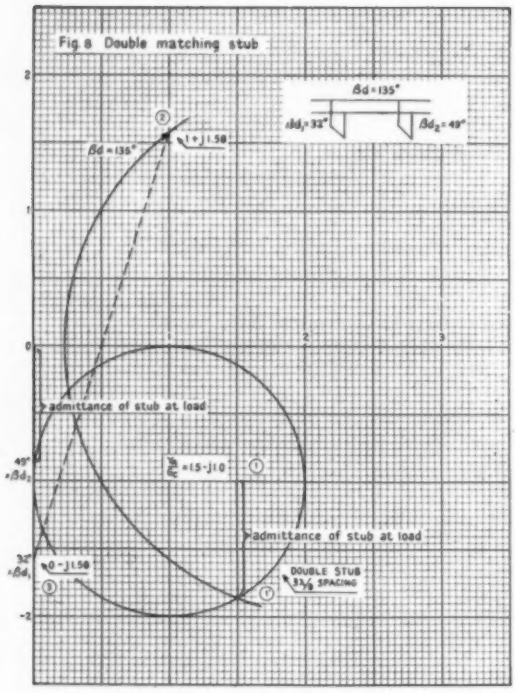

FIG. 8. Double matching stub.

IV. AUXILIARY LOCI

The admittances of the load and stub d_2 are transformed by the section of line d to an admittance whose per unit conductance is 1. The locus of the per unit admittances $g-jb$ which will be so transformed is

$$\left(g-\frac{1}{2\sin^2\beta d}\right)^2+(b+\cot\beta d)^2=\left(\frac{1}{2\sin^2\beta d}\right)^2, \quad (41)$$

which is a circle of radius $1/(2\sin^2\beta d)$ with center at $g=1/(2\sin^2\beta d)$ and $-b=\cot\beta d$. The locus of the centers is the parabola $b^2=2g-1$ of which the point 1,0 is the focus. The locus circle for any d is tangent to the axis of imaginaries, and passes through the point 1,0. The locus circles for d equal to $\lambda/8$, $\lambda/4$ and $3\lambda/8$ are shown in Fig. 5.

As an example of the use of the chart for double stubs, let $Y_R/G_c=1.5+j\,1.0$ be the per unit admittance of the load connected to AB, Fig. 4, and let $d=3\lambda/8$. The first step is to add an admittance in the form of a closed stub of length d_2 so that the combined per unit admittance falls on the locus marked "Double stub, $3\lambda/8$ spacing," Fig. 5. Let this be done by dropping vertically downward from point 1, Fig. 8, at $1.5-j\,1.0$ to point 1′ at $1.5-j\,1.87$. The per unit admittance added is $-j\,0.87$, which corresponds to a closed stub 49° long so that $\beta d_2=49°$. From this point the solution is the same as for the single stub with $\beta d=135°$. Point 2, Fig. 8, has the coordinates $1+j\,1.58$, so that the per unit admittance of the stub d_1 must be $-j\,1.58$. Therefore $\beta d=32°$ as would be indicated on the left-hand margin of Fig. 5.

If the per unit conductance of the load does not fall within the range covered by the locus circle, a transforming section of line must be employed between the load and the stub d_2, such that at the location of the stub d_2 the conductance looking toward the load falls within the proper range. For example, if the spacing between stubs is $3\lambda/8$, a load admittance whose per unit conductance is greater than 2 must be transformed into an admittance having a per unit conductance equal to or less than 2, since the area within the $3\lambda/8$ locus circle extends over a range limited by $0<g\leq 2$.

Letters to the Editor

Rate of Rise of Water in Capillary Tubes

GERALD PICKETT
Portland Cement Association, Chicago, Illinois
June 2, 1944

THIS is in regard to the paper "Rate of rise of water in capillary tubes" by William A. Rense.[1]

The writer disagrees with the conclusion reached by the author that the rise of water in capillary tubes illustrated in his Fig. 2 produced turbulent flow. Under the conditions of the experiment described, the maximum value of Reynolds' number—that occurring at the very instant of insertion of the tube—would not be more than about 200, and at the time when the author considers that turbulence has ceased the value would be about 3. Yet, it is well known that turbulent flow does not exist in tubes under conditions for which the Reynolds' number, $\rho va/\mu$, is much less than about 900.

The author's conclusion that the flow was turbulent during most of the rise rests, apparently, on his success in fitting most of the experimental data with his Eq. (5) and on his inability to account for the results without assuming turbulent flow.

Nevertheless, if all the forces acting on the water are properly taken into account, the experimental results can be accounted for without assuming turbulent flow. As a matter of fact, the capillary forces that force the water up the tube do not appear in any of the author's equations.

From a consideration of Newton's laws of motion and all of the more important forces acting on the water in the tube, the following differential equation is obtained:

$$\frac{2\sigma\cos\theta}{a}\pi a^2-\rho g z\pi a^2-\frac{8\mu}{a^2}z\frac{dz}{dt}\pi a^2=\frac{d}{dt}\left(\rho\pi a^2 z\frac{dz}{dt}\right). \qquad (A)$$

where

σ is the surface tension of the water,
θ is the angle that the surface of the water makes with the tube,
a is the radius of the tube,
ρ is the density of the water, assumed to be constant,
g is the gravitational constant, and
μ is the viscosity of the water.

The first term in Eq. (A) is the capillary pull; the second term is the gravitational pull; the third term is the viscous force; and the last term is the inertia force or the time-rate-of-change of momentum. Cos θ is practically unity for water and glass under static conditions but might be somewhat less than unity when the rate of rise is very rapid, especially under atmospheric conditions, since some finite time would be required for removal of the adsorbed gases.

Equation (A) may be reduced to

$$\frac{2\sigma\cos\theta}{a}-\rho g z-\frac{8\mu}{a^2}z\frac{dz}{dt}-\rho\left(\frac{dz}{dt}\right)^2-\rho z\frac{d^2z}{dt^2}=0. \qquad (B)$$

Unfortunately, Eq. (B) does not have a simple solution; but if cos θ is assumed to be unity, the following equation is an asymptotical solution for small values of t:

$$z^2=\frac{\rho^2a^4}{32\mu^2}\left(\frac{2\sigma}{\rho a}-gz\right)\left(\frac{8\mu}{\rho a^2}t-1+\exp\left(-8\mu t/\rho a^2\right)\right). \qquad (C)$$

Equation (C) is a quadratic equation for z for a given value of t.

In addition the following finite-difference equation is applicable for all values of t except $t=0$.

$$\left(\frac{2\rho}{(\Delta t)^2}+\frac{8\mu}{a^2\Delta t}\right)z_n^2+\left[\rho g+\frac{\overset{z}{\rho_{n-2}}}{(\Delta t)^2}-\left(\frac{8\mu}{a^2\Delta t}+\frac{4\rho}{(\Delta t)^2}\right)z_{n-1}\right]z_n+\frac{\overset{2}{z_{n-1}}}{(\Delta t)^2}=\frac{2\sigma}{a}. \qquad (D)$$

Equation (D) is a quadratic equation for a particular value of z in terms of its values z_{n-1} and z_{n-2} at times Δt and $2\Delta t$ earlier, respectively. By making the time intervals Δt in Eq. (D) sufficiently small and performing step-by-step integration, one may obtain a solution to any desired accuracy. The best procedure appears to be to use Eq. (C) for relatively small values of t and Eq. (D) with step-by-step integration for larger values.

The writer has taken values of σ, ρ, and μ for water at room temperature and a value for the tube radius a such as to give the maximum rise indicated by the author's curve and has performed the operations indicated above. The result is in excellent agreement with the indicated experimental values.

The conclusion is that the rise of water in a capillary tube is in agreement with a theory that takes into account surface tension, viscosity, and density of the fluid, and the corresponding capillary, viscous, gravitation, and inertia forces. Turbulent flow cannot play a part because the Reynolds' number is far too low.

[1] William A. Rense, J. App. Phys. **15**, 436 (1944).

Dark Field Illumination in Electron Microscopy

GABOR B. LEVY
Schenley Research Institute, Inc., Lawrenceburg, Indiana
April 22, 1944

DARK field illumination is frequently used in microscopy and a number of devices are available to achieve this end. In electron microscopy similar use is not made of dark field illumination, although it was demonstrated feasible several years ago.[1]

With the RCA type B electron microscope,[2] which is in general use in this country, it was found that dark field illumination can be obtained simply as follows:

After the field has been selected and focused in the usual manner, the beam is moved away from the projector aperture by means of the objective lens adjustment screws. This movement is continued until the main beam glances off the aperture of the projector lens. The intermediate image port permits visual observation of this process. The field is then moved back into position by means of the specimen control mechanism and a dark field picture of the field appears on the final screen.

The adjustment is rather critical and strongly influenced by the illumination (condenser setting). Nevertheless, with some practice, dark field and light field illumination can be changed within a period of one minute.

Figure 2 illustrates the characteristics of the dark field illumination thus obtained. The object was metal smoke

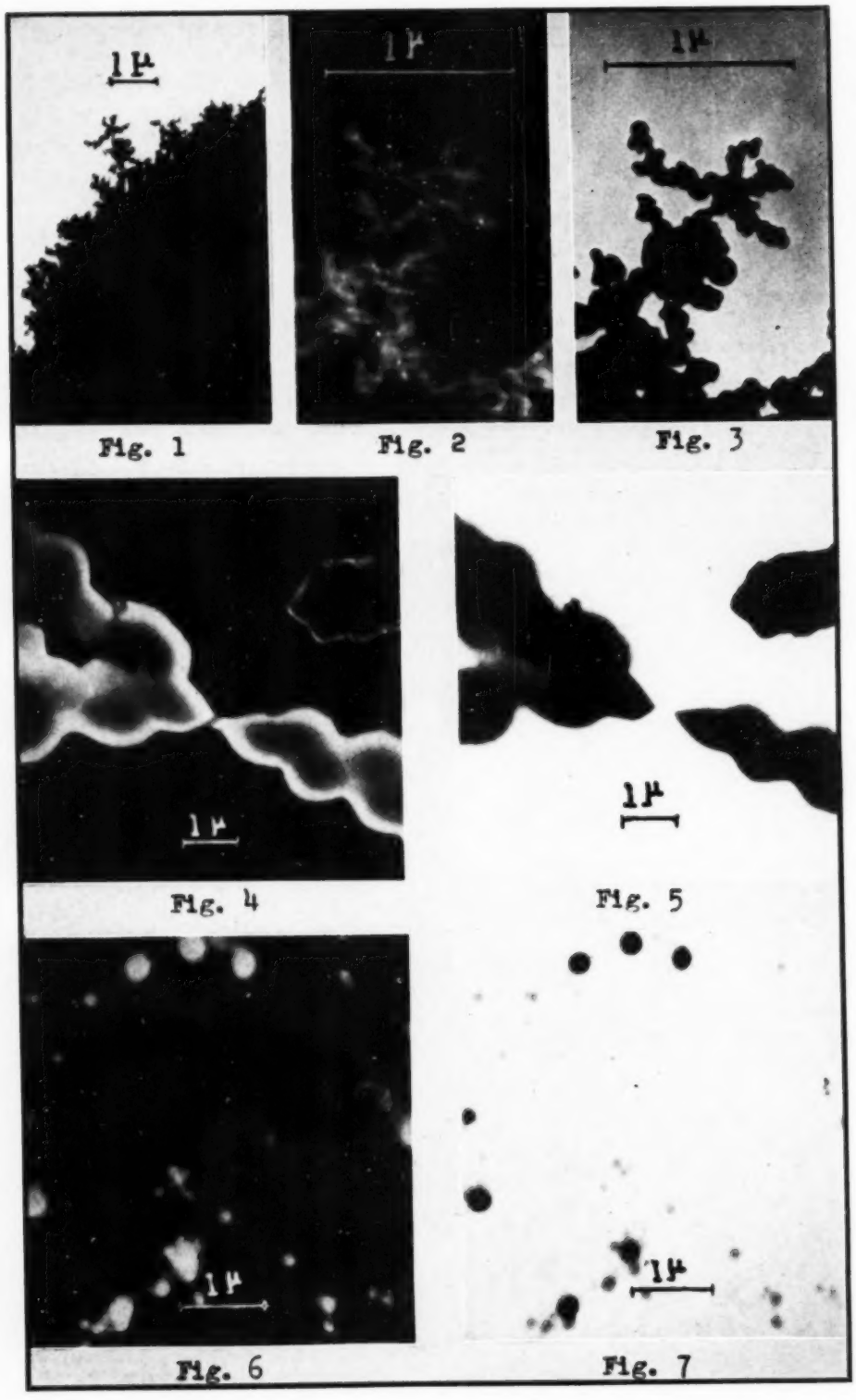

FIGS. 1–7. Photographs showing the characteristics of the dark field illumination.

and Figs. 1 and 3 show the same specimen under light field illumination.

When the use of a supporting film is necessary, a true dark field cannot be obtained, due to the electron scattering on the film itself. Instead, a field with grayish background is observed. Nevertheless, very useful observations can be made under these conditions. For example, in Fig. 4 (*Streptococcus lactis*) the connecting membrane between individual micro-organisms can be made visible. Figure 5 shows the same field under ordinary illumination.

Very small colloidal particles can also be made visible as can be seen in Figs. 6 and 7, representing dark and light field micrographs, respectively, of diluted goats' milk. Here, particles which are hardly visible under ordinary illumination are clearly discernible in the dark field.

Considering these advantages of dark field illumination and the ease with which it can be obtained, in the manner described above, it is hoped that this type of illumination will find wide application in the field of electron microscopy.

The writer gratefully acknowledges the interest and encouragement of Dr. A. J. Liebmann and M. Rosenblatt and the assistance of J. Ostrow and E. P. Oliveto.

[1] M. von Ardenne, *Elektronen-Uebermikroskopie* (J. Springer, Berlin, 1940) and earlier references on p. 37.

[2] *Electron Microscope Type "EMB-4,"* RCA Victor Division of Radio Corporation of America, instruction book IB 39006. *Note:* For dark field illumination, objective aperture as described on pages 52–55 has to be used.

Viscosity of Water

J. R. Coe, Jr., and T. B. Godfrey
National Bureau of Standards, Washington, D. C.
May 27, 1944

SOME time before the entry of the United States into the war, the authors suspended work upon an absolute determination of the viscosity of water at the National Bureau of Standards, in order to engage in research of a temporarily more urgent nature. When our experiments were interrupted, values of the viscosity of water at several temperatures had been obtained. These values are based upon considerably less data than we had hoped to obtain before the publication of results. However, since the date when we may resume our observations is indefinite, and since some who know of the work have urged that we make a provisional communication, we submit the following values, which in our opinion, are the most accurate available.

Absolute viscosity of water at 20°C: 1.002 centipoise.

Viscosity of water relative to its viscosity at 20°C:

Temp. °C	η/η_{20}
25	0.8885
30	.7960
40	.6518.

Our values were calculated from observations made with an apparatus which is substantially the apparatus previously described [1] by one of us. Some changes, principally in the method of measuring pressure, have been made. The positions of the mercury surfaces in the differential manometer were determined by means of electrical contacts, instead of by a volumetric method as originally contemplated. Some additional details of the apparatus and procedure are briefly noted below.

TABLE I. Viscosity of water relative to its viscosity at 20°C, η/η_{20}, including, for comparison, values obtained by others.

Temp. °C	Compilers' values: Bingham 1918[a]	Dorsey 1929[b]	Cragoe 1943[c]	Hosking 1909[d]	Experimenters' values: White & Twining 1913[e]	Geddes 1933[f]	Coe & Godfrey 1941[g]	Swindells 1942[h]
−9.30	2.571	—	2.528	—	2.531			
−8.48	2.479	—	2.445	—	2.440			
−7.23	2.350	—	2.326	—	2.324			
−6.20	2.252	—	2.234	—	2.234			
−4.70	2.121	—	2.110	—	2.106			
−2.10	1.922	—	1.919	—	1.916			
0	1.7832	1.7784	1.7829	1.7821	—			
5	1.5112	1.5056	1.5140	1.5129	—			
10	1.3012	1.2984	1.3035	1.3027	—			
15	1.1347	1.1348	1.1358	1.1352	—			
20	1.0000	1.0000	1.0000	1.0000	(1.0000)	1.0000	1.0000	1.0000
25	0.8893	0.8872	0.8885	0.8873	(0.8885)	0.8885	0.8885	0.8885
30	.7967	7933	.7959	.7952	—	.7947	.7960	—
40	.6527	.6480	.6518	.6531	—	.6519	.6518	.6513
50	.5457	.5445	.5460	.5467	—	—	—	.5456
60	.4665	.4658	.4659	.4662	—	.4660	—	.4657

[a] Values defined by $1/\eta = 2.1482\{(t-8.435)+[8078.4+(t-8.435)^2]^{\frac{1}{2}}\}-130$. Bingham, Bull. Bur. Stand. **14**, 59 (1918). *Fluidity and Plasticity* (McGraw-Hill Book Company, Inc., New York, 1922).

[b] Dorsey, *International Critical Tables* (1929), Volume III, p. 10.

[c] Values defined by

$$\log\frac{\eta}{\eta_{20}} = \frac{1.2348(20-t)-0.001467(t-20)^2}{t+96}.$$

Cragoe, unpublished compilation made at the National Bureau of Standards on the properties of certain aqueous solutions, released for distribution but classified as restricted, with respect only to solutions.

[d] Hosking, Phil. Mag. [6] **18**, 260 (1909).

[e] Values given by $\frac{\eta\ (\text{reported})}{0.8905}\left(\frac{\eta_{25}}{\eta_{20}}=0.8885\right)$; since $\eta_{25}=0.8950$ was assumed in calibration. White and Twining, Am. Chem. J. **50**, 380 (1913).

[f] Geddes, J. Am. Chem. Soc. **55**, 4832 (1933).

[g] J. R. Coe, Jr., and T. B. Godfrey, unpublished measurements obtained at the National Bureau of Standards and briefly described here.

[h] Swindells, unpublished measurements obtained at the National Bureau of Standards using two types of viscometers (Bingham and Ostwald).

Capillary: KPG (Jena); approximately 48 cm long, 0.5-mm ID; ends cut off square; optically flat surfaces at ends, 15 mm in diameter; measurements made with both directions of flow at 20°, in only one direction at other temperatures; mean radius at 20°C:

$r = 0.251621$ mm by determining the mass of mercury required to fill the capillary.

$r = 0.251624$ mm by measuring the electrical resistance of the capillary when filled with mercury.

Rates of flow: From 0.07 to 0.26 cm³/sec.; injector driven by synchronous motor with power from a generator whose frequency was controlled and known to within a few parts in a million.

End correction: In the expression

$$\eta = \frac{\pi r^4 p}{8Q(l+cr)} - \frac{m\rho Q}{8\pi(l+cr)},$$

where η = viscosity; r = radius of capillary; p = pressure drop between reservoirs in which the capillary terminates; Q = volume of liquid per unit of time; l = length of capillary; ρ = density of liquid; m and c = dimensionless constants;

TABLE II. Absolute viscosity of water in centipoises (comparison with measurements of Thorpe and Rodger).

Temp. °C	Correction term[a]	Thorpe & Rodger's values with $m=1.00$	$m=1.12$	$m=1.18$	Calculated values[b]
22.02	0.00370	0.9550	0.9546	0.9543	0.9544
30.72	.00447	.7860	.7855	.7852	.7855
39.32	.00527	.6622	.6616	.6613	.6614
47.03	.00605	.5760	.5754	.5750	.5755
55.53	.00690	.5010	.5002	.4998	.5002
64.01	.00777	.4414	.4405	.4400	.4401

[a] Values quoted from Thorpe and Rodger, Phil. Trans. **A185**, 397 (1894), for the last term in (η) equation.
[b] Calculated from equation given in reference *c* of Table I with $\eta_{20}=1.002$.

the value of m was experimentally determined, but the value of c was not independently determined. Measurements with a shorter length of capillary in order to obtain a value for c were planned, but the work was interrupted before this was done. For c, a value of 0.6, rounded off from the value of 0.573 given by Barr,[2] was used. Values of m ranging from 1.151 to 1.185 were obtained. (See Table I.)

For determination of absolute viscosity, it is essential that the radius and length of the capillary be determined with high accuracy. The work of Thorpe and Rodger is outstanding in this respect. They also employed many refinements which were unusual at that time. One major weakness in their work was the failure to determine the coefficient m experimentally. They assumed $m=1.00$ in calculating absolute viscosities. The values given below are the mean values obtained from their measurements with two directions of flow and using: (1) $m=1.00$ as assumed by them; (2) $m=1.12$, a value formerly assumed extensively; and (3) $m=1.18$, corresponding to the highest value obtained in our work. In spite of this uncertainty, the use of any reasonable value of m makes their measurements in agreement within 0.1 percent in general with the results obtained at the National Bureau of Standards in the range 20° to 60°C, as indicated by comparison with the values in the last column which were calculated with $\eta_{20}=1.002$. (See Table II.)

Our work was initiated by the Society of Rheology and in its earlier stages was partly financed by the Chemical Foundation. We wish to express our gratitude to these organizations.

[1] J. R. Coe, Jr., Physics **4**, 274 (1933).
[2] Barr, *A Monograph on Viscometry* (Oxford University Press, London, 1931), p. 28.

Etymology of the Word Microradiograph

S. E. MADDIGAN
Chase Brass & Copper Company, Waterbury, Connecticut
May 29, 1944

IN the May issue of *Journal of Applied Physics*,[1] Miss E. L. Garvin of the Eastman Kodak Company drew attention to the seemingly illogical choice of certain engineering and scientific terms, particularly the word microradiograph which has been used in publications by me and several other investigators to designate an enlargement of a radiograph with a high magnification factor of, say, 100 times. Similar comments have recently been made by L. V. Chilton[2] and also in a previous note by Miss Garvin.[3]

While I am in complete agreement with Miss Garvin regarding the desirability of a logical standardization of terms, I believe that, before abandonment, the word microradiograph requires further consideration both as regards the experimental process involved, and also as regards etymological associations.

Reference to pages 1552–4 of Webster's *New International Dictionary*, second edition, reveals that the prefix "micro" may have the connotation of either enlargement or reduction in the recording process. In a great many cases it implies the recording on an enlarged scale of minute quantities, for example, micronometer, microphonograph, micromotoscope, etc. Microphotograph is defined as "a microscopically small photograph." One finds the word micrograph defined as "a graphic reproduction of an object as seen through a microscope. When a photograph, it is a photomicrograph." By general usage in the field of metal investigations, micrograph or photomicrograph is understood to mean an enlarged reproduction of the metal *surface*, and from this standpoint the name electron micrograph fits in logically with photomicrograph, since the electron microscope actually does produce an enlarged record of the metal surface.

In the case of microradiograph, Miss Garvin has failed entirely to penetrate behind the word structure and visualize the experimental procedure involved. According to the same dictionary a radiograph "depends on the differential absorption of rays transmitted through the media." The microradiograph certainly fulfills this definition, and on the other hand is not a record of the metal surface but rather a three-dimensional picture of the metal interior. The true value of the microradiograph depends upon the three-dimensional properties and also upon the differential absorption of the x-rays. Thus we have essentially a radiograph rather than a micrograph. The microradiograph itself is an enlargement of the original radiograph, and the experimental process is logically brought out by attaching a prefix to the word radiograph. The prefix "micro" is quite proper for the purpose of designating an enlargement, and therefore the word microradiograph seems to the writer to be quite logical, and at the same time quite clear in describing the experimental procedure involved.

The name radiomicrograph or, better, x-ray micrograph, should be reserved for quite another type of record. Certain French investigators, notably J. J. Trillat,[4] have described a procedure for recording the surface structure of the metal sample "by reflection" of x-rays. In this case the photographic record produced is quite analogous to the record obtained by the use of visible light and the optical microscope.

Miss Garvin's note appears to be an effort to reserve the word microradiograph for microfilm records such as those mentioned by her on chest radiographs recorded on microfilm for military medical records. The question regarding which field should have claim to the term should be based both on prior usage, and on volume of usage in the literature.

[1] E. L. Garvin, J. App. Phys. **15**, 455 (1944).
[2] L. V. Chilton, J. Sci. Inst. **21**, 33 (1944).
[3] E. L. Garvin, Metal Progress **45** (March, 1944).
[4] J. J. Trillat, Comptes rendus (Dec. 1941); *ibid.* (Jan. 1942).

Rapid Determinations of Elastic Constants of Glass and Other Transparent Substances

W. T. Szymanowski
The University of Pittsburgh, Pittsburgh, Pennsylvania
May 18, 1944

THE rapid and reliable determination of the elastic constants of glass becomes increasingly important as well in research as in production. Existing static and dynamic methods are cumbersome and long, so that intelligent research in the field of the best composition of glass for definite purposes is very often rendered more difficult because of lack of a method permitting a quick check of expected results.

On the other hand, also in the field of production there is need of a constant and reliable check of the quality of the products, especially in mass production.

Supersonic diffraction methods are offering the greatest possibilities for such a quick and reliable determination of elastic constants. Among them the method developed by Schaefer and Bergman,[1] the theory of which was given by Fues and Ludloff,[2] has given the most promising results. The practical application, however, of this method is difficult because of the necessity of using a very small circular aperture, which produces a comparatively weak diffraction pattern. The quick finding of the resonance point for such a pattern is rather troublesome and the pattern can be only photographed and then evaluated. The method described in the following avoids the above difficulties and permits thus a rapid determination of the elastic constants.

A strong monochromatic source of light illuminates with polarized light an ordinary adjustable slit. After passing the slit the beam of light is made slightly convergent by a lens, and goes through the investigated transparent sample. The sample is set on a piezoquartz, the electrodes of which are connected to an oscillator of variable frequency. After passing through the sample and a crossed Nicol the light forms a magnified image of the slit which is viewed by a microscope with a filar micrometer eyepiece.

The piezoquartz, which is excited in one of its overtones, sets the sample into strong longitudinal resonance vibrations, which are diffracting the beam of light. The diffraction pattern, as viewed in the microscope, forms then in the first order a line on each side of the central image of the slit. The sample is, however, set at the same time into transverse vibrations giving rise to another diffraction pattern superimposed over the longitudinal one. This is formed also by two lines equidistant from the central image. The mutual distance, however, of these lines is less than two times the mutual distance of the longitudinal diffraction lines.

The measurement of the distance between the two parallel lines, as well in the longitudinal, as in the transverse diffraction pattern can be easily and rapidly performed and repeated by means of the traveling wires of the micrometer eyepiece. These distances are the only experimental data, besides the density ρ of the sample, and the resonant frequency ν, necessary for the determination of the Poisson ratio σ, the shear modulus μ, and Young's modulus E, because:

$$\sigma=\frac{1-2(d_l/d_t)^2}{2-2(d_l/d_t)^2}, \quad \mu=\frac{\nu^2k^2}{(d_t/2)^2}$$

and

$$E=2\mu(1+\sigma),$$

where d_l = distance of the 2 parallel lines in the longitudinal diffraction pattern, d_t = distance of the 2 parallel lines in the transverse diffraction pattern, k = apparatus constant obtained by calibration with a grating having a known grating constant.

The resonant frequency is best measured by beats, or with an accurate wavemeter.

Since the elastic wave-length is very small in comparison with the size of the sample, its shape and to a certain extent its size have no effect on the measurement of the elastic constants. As a permanent record a photograph of the diffraction patterns can be easily made.

The error in the determination of the absolute value of the elastic constants is estimated to be around 1 percent, but could be still greatly reduced by refinements in the method. However, differences in samples amounting to a few tenths of a percent can be easily detected.

By this method the following elastic constants were determined for a sample of soft glass:

$$\mu=3203 \text{ kg/mm}^2,$$
$$E=7889 \text{ kg/mm}^2,$$
$$\sigma=0.2315,$$

which values are checking well with accepted values for such a kind of glass.

Without any further trouble the method can be applied to any transparent substance. For instance, Lucite showed also well-defined diffraction patterns.

Experiments are in progress to extend the method to opaque substances and anisotropic bodies.

A detailed account will be published at a later date.

[1] Schaefer and Bergman, Sitz. Ber. Berlin Akad., p. 155 (1934); *ibid.*, p. 192 (1934); *ibid.*, p. 222 (1935).
[2] Fues and Ludloff, Sitz. Ber. Berlin Akad., p. 248 (1935).

Recent Applications of Physics

Prepared by CLARK GOODMAN, Associate Editor

Material to be included in this section should be submitted to Dr. Clark Goodman, Massachusetts Institute of Technology, Cambridge 39, Massachusetts.

Thickness Control with X-Rays

In his acceptance address upon receipt of the Franklin Medal, Dr. W. D. Coolidge revealed that white-hot sheet steel, at temperatures as high as 2000°F, and moving at a speed of 20 m.p.h. as it emerges from a rolling mill, can have its thickness accurately measured by x-rays. A beam of x-rays is produced by a tube and collimator located below the sheet. The intensity of the transmitted radiation is measured by an ionization chamber or equivalent device. Since this intensity is related to the thickness by the usual exponential law, the instrument can be calibrated to read directly in terms of the thickness of the sheet. If desired, the output of the device

can be arranged to control the mill so as to maintain automatically an essentially constant thickness of sheet steel.

Production of Piezoelectric Crystals On December 7, 1941, this country's annual production of quartz crystals could be counted by the thousand—now the output has boomed to an eight-digit figure. This enormous expansion in production has been made possible by the application of a number of physical techniques. Polarized light, index of refraction, and interference studies are used in the inspection, grading, and classification of the highly irregular raw quartz. Accurate orientation of the crystals must be made in order that they may be wafered or cut in certain preferred directions with respect to the optic axis. The application of rapid routine x-ray diffraction methods, using a Geiger-Müller tube amplifier for measuring the x-ray intensities, not only has expedited this operation but has increased its accuracy. Diamond saws, some made by sintering an alloy containing diamond dust, are used for the delicate operation of slicing the crystals.

In order to select the useful portion of the wafer, it must be etched, some form of fluoride solution being commonly used. Optical examination reveals twinning and imperfections. The selected portions are cut out and lapped to the desired thickness. Periodic frequency checks are made during the hand finishing process until sufficient quartz has been removed so that the crystal oscillates at the proper frequency. One type of frequency measuring device utilizes two crystal oscillators: one a standard and the other a test oscillator. The beat between the two is measured with a direct-reading frequency-meter counter or saturation circuit. However, the most elegant method is a cathode-ray oscilloscope with proper sweep frequency circuits which spread the desired spectrum of frequencies over the screen.

After aging, the plates may be coated with non-corrosive metals such as gold, silver, or aluminum. Gold is conveniently applied by sputtering. These metallic coatings provide electrical contact and a sensitive means of frequency control. Because of the diverse nature of the temperatures and climates where these oscillators may be used, each crystal is subjected to a test procedure which determines its frequency and activity stability throughout a broad range of temperatures. Those crystals which fail to meet the rigid specifications are either reclaimed by making necessary modifications or are discarded.

After the war, quartz will undoubtedly find applications for frequency control in all types of radio equipment, in navigating instruments, in train block-signal controls, in the elimination of radio interference from induction and dielectric furnaces, in picture transmissions, smoke recorders, teletype, weather forecasting instruments, and innumerable other peacetime activities. The North American Philips Company, Inc., is largely responsible for these increased production methods. Further information on this subject can be obtained from their booklet entitled "How quartz crystals are manufactured," copies of which are available from the North American Philips Company, Inc., 100 East 42 Street, New York 17, New York.

Tricky Techniques RCA engineers have developed an electronic method for conserving paint in the spraying of the metal shells of vacuum tubes. A direct-contact blower maintains a continuous spray of paint as long as there are no shells missing on the conveyor. If only one shell is absent, the time constant of the electronic circuit is so arranged that the spray is not interrupted. However, if two or more shells are missing, the solenoid-operated valve in the spray line is tripped by a gas-filled tetrode with an adjustable resistance and capacitance in its grid circuit.

High Speed Radiography High speed photography has found many applications in industry, journalism, and scientific research. Using ordinary light, this method naturally is limited to the external behavior or appearance of the subject. More recently this technique has been extended to the x-ray region. C. M. Slack and L. F. Ehrke, Westinghouse research engineers, have developed a cold-cathode x-ray tube that makes radiographs with exposures down to a microsecond at wavelengths of 0.04A or greater. The latest tube operates at a peak of 300,000 volts, and currents of from 1000 to 2000 amperes are reached during the discharge. The energetic pulse results from the abrupt discharge of a group of condensers through a spark gap in series with the tube. The breakdown of the spark gap is controlled by a thyratron circuit feeding into an induction coil, the secondary voltage of the induction coil being superposed on the initial potential across the condensers.

At present high speed radiography is restricted almost exclusively to ballistics research. It makes possible studies of the action of bullets in motion within gun barrels and when they hit targets of armor plate or other materials. The Army has two of these machines at Frankford Arsenal in Philadelphia and two at the Ballistics Research Laboratories of the Army Ordnance Proving Grounds in Aberdeen, Maryland. Two mobile units are placed side by side, so that two pictures of a single bullet can be taken at different stages of its flight.

Metal-Plated Plastics The application of plastics for war purposes is broadened by the electrolytic deposition of a thin coating of metal. A conductive and adherent bond coat is sprayed on, after which almost any metal can be deposited. The most common metals used are copper, silver, gold, cadmium, lead, tin, and zinc. Masking with Scotch tape, rubber, or lacquer allows certain areas to remain bare and hence nonconducting.

Plating extends the properties of plastics to make them suitable alternatives for critical metals. Aluminum and magnesium can be replaced in aircraft for electrical and radio shielding. Electrical units combining the properties of a conductor and insulator in one integral unit are possible. The plating has good heat and electrical conducting properties and has excellent shielding characteristics at high frequencies. Further information can be obtained from the Metaplast Corporation, 205 West 19 Street, New York City.